



universität
wien

DISSERTATION

Titel der Dissertation

Entanglement beyond two qubits:
geometry and entanglement witnesses

Verfasser

Mag. Philipp Krammer

angestrebter akademischer Grad

Doktor der Naturwissenschaften
(Dr. rer. nat.)

Wien, im Juli 2009

Studienkennzahl lt. Studienblatt: A 091 411

Dissertationsgebiet lt. Studienblatt: Physik

Betreuer: Ao. Univ.-Prof. Dr. Reinhold A. Bertlmann

Acknowledgment

The work presented in this thesis would not have been possible without the support of many people. I would like to especially thank:

Above all my supervisor Reinhold A. Bertlmann, for his continuous professional and personal support. His optimistic and fortifying encouragements kept me on the track and enabled me to rethink my sometimes pessimistic attitudes.

The University of Vienna and the CoQuS doctoral program for providing the financial coverage.

Katharina Durstberger and Beatrix C. Hiesmayr for giving me a warm welcome into the world of research.

Marcus Huber for encouraging me on scientific collaborations and inviting me to parties.

Peter Mellecker for his patience.

My family for their unconditional support and encouragement.

My friends for spending their time with me so that I could renew my energies.

List of publications

Journal publications

- Reinhold A. Bertlmann, Katharina Durstberger, Beatrix C. Hiesmayr, and Philipp Krammer
Optimal entanglement witnesses for qubits and qutrits
Phys. Rev. A **72**, 052331 (2005)
- Reinhold A. Bertlmann and Philipp Krammer
Bloch vectors for qudits
J. Phys. A: Math. Theor. **41**, 235303 (2008)
- Reinhold A. Bertlmann and Philipp Krammer
Geometric entanglement witnesses and bound entanglement
Phys. Rev. A **77**, 024303 (2008)
- Reinhold A. Bertlmann and Philipp Krammer
Bound entanglement in the set of Bell-state mixtures of two qutrits
Phys. Rev. A **78**, 014303 (2008)
- Beatrix C. Hiesmayr, Florian Hipp, Marcus Huber, Philipp Krammer, and Christoph Spengler
A simplex of bound entangled multipartite qubit states
Phys. Rev. A **78**, 042327 (2008)
- Philipp Krammer
Characterizing entanglement with geometric entanglement witnesses
J. Phys. A: Math. Theor. **42**, 065305 (2009)
- Reinhold A. Bertlmann and Philipp Krammer
Entanglement witnesses and geometry of entanglement of two-qutrit states
Ann. Phys. **324**, 1388 (2009)
- Beatrix C. Hiesmayr, Marcus Huber, and Philipp Krammer
Two computable sets of multipartite entanglement measures
Phys. Rev. A **79**, 062308 (2009)

E-prints and submissions

- Reinhold A. Bertlmann and Philipp Krammer
Bloch vectors for qudits and geometry of entanglement
e-print arXiv:0706.1743
- Philipp Krammer, Hermann Kampermann, Dagmar Bruß, Reinhold A. Bertlmann, Leong C. Kwek, and Chiara Macchiavello
Multipartite entanglement witnesses via structure factors
e-print arXiv:0904.3860 (submitted)

Theses

- Philipp Krammer
Quantum Entanglement: Detection, Classification, and Quantification
Diploma Thesis, University of Vienna, Austria (2005)

Contents

0. Introduction	1
1. Basic mathematical framework	5
1.1. Vector states and operators	5
1.2. Density operators	8
1.3. Bipartite systems, entanglement, and separability	9
1.3.1. Vector states	9
1.3.2. Density operators	11
1.4. Bound entanglement	13
2. Bloch decompositions beyond qubits	15
2.1. Introduction	15
2.2. Bloch decompositions for qubits	16
2.3. Bloch decompositions for qudits	17
2.4. The generalized Gell-Mann operator basis	18
2.4.1. Definition and examples	18
2.4.2. Decomposing the standard operators with the GGB	21
2.5. The polarization operator basis	22
2.5.1. Definition and examples	22
2.5.2. Decomposing the standard operators with the POB	24
2.6. The Weyl operator basis	25
2.6.1. Definition and example	25
2.6.2. Decomposing the standard operators with the WOB	26
2.7. Bloch decompositions for bipartite systems	27
2.7.1. Bloch decompositions of the maximally entangled two-qudit state	28
2.8. Summary and conclusion	31
3. Geometric entanglement detection	33
3.1. Introduction	33
3.2. Vector states	34
3.3. Density operators	35
3.3.1. The PPT criterion	36
3.3.2. The realignment criterion	37
3.3.3. Entanglement witnesses	38
3.4. Bloch decompositions and entanglement witnesses	39
3.5. Geometric entanglement witnesses	42

3.5.1. Definitions and general methods	42
3.5.2. Entanglement properties of a family of two-qutrit states	47
3.6. Decomposition of entanglement witnesses for experimental application	56
3.7. Summary and conclusion	58
4. Geometric quantification of entanglement	61
4.1. Introduction	61
4.2. The Hilbert-Schmidt measure and geometric entanglement witnesses	62
4.3. Hilbert-Schmidt measure for the isotropic two-qudit states	64
4.4. Hilbert-Schmidt measure for two-parameter families of states	66
4.4.1. Two-qubit states	66
4.4.2. Two-qutrit states	71
4.5. Summary and conclusion	74
5. Structural multipartite entanglement witnesses	77
5.1. Introduction	77
5.2. Multipartite generalization of the entanglement definition	78
5.3. A construction of multi-qubit entanglement witnesses	79
5.3.1. Construction with structure factors	79
5.3.2. Construction with symmetric Bell states	86
5.4. Summary and conclusion	91
6. Conclusion and outlook	93
A. Appendix	95
A.1. Proof of the GGB orthogonality conditions	95
A.2. Derivation of term B in the GGB decomposition of the maximally entangled two-qudit state	97
A.3. Proof of orthonormality of the WOB	98

0. Introduction

Quantum entanglement is a keyword that has become more and more famous and fancy over the last years. But why? The notion itself is rather old, even as old as the introduction of the mathematical formalism of quantum physics. Erwin Schrödinger introduced the term “Verschränkung” in 1935 [113], when he realized that some states allow correlated measurement results, and that one can have maximal information about the state of the whole system, but less information about its parts. The term “system” is used to abstract from a concrete physical realization, in quantum physics it usually comprises one, two, some, or even many particles. In the same year, Einstein, Podolsky, and Rosen (EPR) claimed that quantum theory is incomplete [47], since in their opinion it lacked so-called *elements of reality*, i.e. parameters that determine measurement outcomes if the notion of *locality* is to be maintained. Locality assumes that no information can be transmitted faster than the speed of light, according to Einstein’s theory of special relativity, and was, in EPR’s opinion, unquestionable. The quantum states that allow this so-called *EPR paradox* are entangled states. However, in 1964, John S. Bell showed that the existence of these parameters, called *local hidden variables*, based on the notions of *reality* and *locality*, was not compatible with quantum theory. This actuality is called *Bell’s theorem*, which claims a violation of the so-called *Bell inequalities* by quantum theory. The violation becomes evident for entangled states only. Moreover, Bell inequalities were put into an experimentally testable form by Clauser, Horne, Shimony and Holt (CHSH) [37] in 1969, and a first experimental test that supported Bell’s theorem was done by Aspect, Grangier and Roger in 1982 [3].

Not until the 1990’s it became clear that entanglement is also a resource in quantum information theory, especially for quantum communication protocols, e.g. quantum dense coding, quantum teleportation, and quantum cryptography. For overviews, see, e.g., Refs. [29, 97, 26] and references therein. In these protocols quantum entanglement is the ingredient that distinguishes quantum from classical procedures and provides advantages for security issues or the amount of data transfer. Nowadays entanglement theory is a growing research field.

The fundamental questions of entanglement theory are: Given an arbitrary quantum state,

- is it entangled or not?
- if it is entangled, how much is it entangled?
- if it is entangled, can it be used to perform the usual quantum communication protocols?

- if it is entangled, does it violate some type of Bell inequality?

Although the mathematical definition of entanglement is simple (see Sec. 1.3), each of the above questions has not yet been answered in general, i.e. for an arbitrary state of a system that comprises an arbitrary number of subsystems. Much has been achieved, however, and many of the above questions can be answered for pure states or lower dimensional systems, or for particular families of states; for reviews of entanglement theory, see, e.g., Refs. [65, 30, 120, 69, 54].

The aim of this thesis is to present new methods for entanglement detection and quantification. The methods used are predominantly those of standard analytical linear algebra. The greater part of the thesis presents entanglement detection methods, in particular, geometric constructions of entanglement witnesses (called *geometric entanglement witnesses*). A mathematical formalism that supports these methods is supplied by *Bloch decompositions*, to which also a chapter is dedicated and is used throughout the whole thesis. These decompositions are presented for arbitrary dimensions, where properties of the well-known case of two dimensions are generalized to higher dimensions. Moreover, it is demonstrated how to geometrically quantify entanglement with geometric entanglement witnesses. Entanglement witnesses are also the subject of the last part, where we extend the Hilbert space to more than two subsystems and construct entanglement witnesses on a more “physical” ground. All of the presented results are illustrated by relevant examples, and related literature is cited throughout the whole text. The articles that the thesis is based upon are cited in the introduction of each chapter.

What makes entanglement theory a fascinating field of research? It is on the one hand a challenge to contribute to a subject that has so many open problems, regardless of the fact that the underlying mathematical structure is rather simple, as it is mere linear algebra. On the other hand, the development of quantum information theory and applications has become rapidly increasing and exciting in recent years, since it allows extensions of classical information tasks with quantum ones. With the ongoing progress in computation technologies, quantum information processing will become inevitable and necessary in the near future.

The thesis is organized as follows:

In Chapter 1 we start with the mathematical basics of quantum theory that will be frequently used in the course of the thesis, and the definition of entanglement is presented.

In Chapter 2 we investigate the formalism of *Bloch decompositions*, i.e. the decomposition of operators into suitable bases of orthogonal operators, for arbitrary dimensions. Three particular bases are presented, and we derive a method to decompose any density operator via the decomposition of so-called *standard operators*, which are given and proven in Lemma 2.1, Lemma 2.2, and Lemma 2.3. As an example we determine the decomposition of the isotropic two-qudit state into these bases.

In Chapter 3 we briefly review entanglement detection criteria relevant for the later presented detection methods. We derive approaches to identify operators

as entanglement witnesses using Bloch decompositions, given in Corollary 3.2 and Lemma 3.1. Moreover, we give the definitions of geometric operators and *geometric entanglement witnesses* and present a method to detect entangled and bound entangled states, and to identify separable states by *shifting* geometric operators (Proposition 3.1). We illustrate and apply the introduced procedures on a three-parameter family of two-qutrit states, where we determine the regions of entangled, bound entangled, and separable states. In the last section we briefly show a possible decomposition of entanglement witnesses for three-dimensional subsystems into measurable quantities, such that this decomposition should allow an experimental application.

In Chapter 4 we show how to use geometric entanglement witnesses in the context of entanglement quantification. In detail, we determine the *Hilbert-Schmidt measure* of entanglement, which is a special kind of geometric entanglement measure, for the isotropic two-qudit states and two-parameter families of two-qubit and two-qutrit states.

In Chapter 5 we present a construction of multipartite entanglement witnesses using so-called *structure factors*, which contain two-point correlations only and can be tested in experiments (Definition 5.7). These *structural entanglement witnesses* can be either used in photon experiments where expectation values can be obtained by locally measuring the involved operators, or in calculations and/or experiments on spin chains, where the structure factor provides a quantity that can be obtained in scattering experiments. We furthermore show which states are detected by the structural witnesses, among them *Dicke states* and non-symmetric versions of Dicke states with changed phases of the constituting terms, and give an alternative construction of particular structural witnesses with symmetric Bell states of qubit pairs.

We conclude and take an outlook on further possible research in Chapter 6. The bibliography is listed alphabetically. Identical authors of different references are cited only once, and are abbreviated with a line in the following references.

1. Basic mathematical framework

1.1. Vector states and operators

We consider quantum systems described by a Hilbert space of finite dimension, i.e., the corresponding physical quantities have discrete measurement outcomes of a limited number. The physical realization of such systems can be diverse, e.g., particles with a particular spin quantum number s (half integer or integer), or photons of particular polarization (horizontal or vertical), or atoms that can be in particular discrete quantum states.

One way to describe such systems mathematically is via vector states $|\psi\rangle$ that are elements of the vector space \mathbb{C}^d , where d is the dimension of the system, i.e. the number of possible measurement outcomes. The vector space \mathbb{C}^d is a Hilbert space of dimension d , denoted as \mathcal{H}^d , with a scalar product $\langle\phi|\psi\rangle \in \mathbb{C}$ for $|\psi\rangle, |\phi\rangle \in \mathbb{C}^d$ and $\langle\phi|$ is the Hermitian conjugate of $|\phi\rangle$. It is the familiar scalar product of complex vectors in \mathbb{C}^d . A norm is given by $\|\psi\| = \langle\psi|\psi\rangle^{1/2}$, and usually vector states are normalized by $\|\psi\| = 1$. A basis $\{|\phi_i\rangle\}$ that spans the Hilbert space consists of d vector states. Usually the basis states are chosen mutually orthogonal, $\langle\phi_i|\phi_j\rangle = \delta_{ij}$, and any vector state $|\psi\rangle$ can be decomposed into the basis by

$$|\psi\rangle = \sum_i c_i |\phi_i\rangle, \quad (1.1)$$

with coefficients $c_i = \langle\psi|\phi_i\rangle \in \mathbb{C}$ and $i = 0, \dots, d-1$ or, equivalently, $i = 1, \dots, d$. Via unitary matrices U ($U^\dagger U = \mathbb{1}$) we can transform one orthogonal basis $\{|\phi_i\rangle\}$ into another orthogonal basis $\{|\tilde{\phi}_i\rangle\}$,

$$|\tilde{\phi}\rangle = \sum_j u_{ij} |\phi_j\rangle, \quad (1.2)$$

where u_{ij} are the matrix elements of a unitary matrix U , i.e. the entry in the i -th column and j -th row. The fact that quantum states correspond to elements of a vector space mirrors the physical features that distinguishes them from classical states - like the *superposition* of quantum states, given in Eq. 1.1. From a historical point of view, the regarded Hilbert space is the discrete finite dimensional analogue of the continuous infinite dimensional Hilbert space L^2 . In this case the vector states are quadratically integrable functions $\psi \in L^2$, the “wave functions” that Erwin Schrödinger introduced at the beginning of the 20th century and marked the beginning of the mathematical formalism of quantum physics.

An operator O acts on vector states and assigns another vector state to the vector state it acts upon, $O|\psi\rangle = |\phi\rangle$. The adjoint operator O^\dagger to the operator

O is defined via the scalar product

$$\langle \phi | O | \psi \rangle = \langle \psi | O^\dagger | \phi \rangle^*, \quad (1.3)$$

where “*” denotes complex conjugation. If $A = A^\dagger$, then A is called Hermitian (or selfadjoint, the two notations are equivalent for finite dimensional Hilbert spaces) and an *observable* since the physical meaning becomes evident: The operator corresponds to a measurement and its eigenvalues λ_i correspond to possible measurement outcomes, they are real for Hermitian operators and given by the eigenvalue equation

$$A|\lambda_i\rangle = \lambda_i|\lambda_i\rangle. \quad (1.4)$$

The eigenvectors $|\lambda_i\rangle$ form an orthogonal basis of the Hilbert space and thus can be used to decompose any vector states like in Eq. (1.1).¹ In quantum information theory one abstracts and simplifies notation and refers to a “standard” basis $\{|i\rangle\}$ that replaces the eigenvectors of realizations in physical systems. According to this notation a vector state can be decomposed into the standard basis as

$$|\psi\rangle = \sum_i c_i |i\rangle. \quad (1.5)$$

The notation of the vector states as vectors of \mathbb{C}^d is obtained by just calculating the coefficients $c_j = \langle j | \psi \rangle$,

$$|\psi\rangle = \begin{pmatrix} c_0 \\ c_1 \\ \vdots \\ c_{d-1} \end{pmatrix}. \quad (1.6)$$

Following this notation the basis states $|i\rangle$ simply have one entry 1 at the i -th position 0 at all other positions. Another important quantity is the expectation value of an observable (the average measurement outcome) for a vector state $|\psi\rangle$, given by

$$\langle O \rangle_\psi = \langle \psi | O | \psi \rangle. \quad (1.7)$$

Remark on terminology. A vector state that is an element of the two dimensional Hilbert space \mathcal{H}^2 is called “qubit” in quantum information terminology. The term is the quantum analogue of the familiar expression *bit*, which is the classical minimum information quantity that can take only two values, 0 and 1. In quantum theory, the Hilbert space \mathcal{H}^2 has the two standard basis states $|0\rangle$ and $|1\rangle$, and, unlike to classical information theory, a qubit $|\psi\rangle$ cannot only be in these two basis states but also in a superposition, $|\psi\rangle = c_0|0\rangle + c_1|1\rangle$. For higher dimensional systems one extends the terminology and calls a vector state of \mathcal{H}^3 *qutrit*, and a vector state of a Hilbert space \mathcal{H}^d of arbitrary dimension d “qudit”.

¹Note that for degenerate eigenvalues we can have different eigenvectors to the same eigenvalue, in which case this should be accounted for in the notation $|\lambda_i\rangle$.

Just as vector states can be expressed as vectors, operators can be expressed as matrices by constructing the entries with any orthogonal basis, usually the standard basis,

$$(O)_{ij} = \langle i|O|j\rangle, \quad (1.8)$$

where the adjoint operator can be readily obtained by taking the transpose and complex conjugate of the matrix,

$$(O^\dagger)_{ij} = (O)_{ji}^* = \langle j|O|i\rangle^*. \quad (1.9)$$

Operators also form a Hilbert space, called *Hilbert-Schmidt space* \mathcal{A} , with an inner product

$$\langle A, B \rangle := \text{Tr} A^\dagger B, \quad A, B \in \mathcal{A}. \quad (1.10)$$

Using this definition of the inner product the Hilbert-Schmidt norm is given by

$$\|A\| = \sqrt{\langle A, A \rangle} = \sqrt{\text{Tr} A^\dagger A}, \quad (1.11)$$

and the Hilbert-Schmidt distance is defined by the norm as

$$d(A, B) = \|A - B\|. \quad (1.12)$$

The trace operation is defined by the matrix elements,

$$\text{Tr} O = \sum_i (O)_{ii} = \sum_i \langle \phi_i | O | \phi_i \rangle, \quad (1.13)$$

with any orthogonal basis of vector states $\{|\phi_i\rangle\}$, e.g. the standard basis or the basis out of the eigenvectors of the operator, in which case we can also write the trace as the sum of the eigenvalues λ_i of the operator,

$$\text{Tr} O = \sum_i \lambda_i. \quad (1.14)$$

The trace operation is independent of the choice of the basis, since

$$\begin{aligned} \sum_i \langle \tilde{\phi}_i | O | \tilde{\phi}_i \rangle &= \sum_{i,j,k} \langle \phi_j | u_{ij}^* O u_{ik} | \phi_k \rangle = \sum_{i,j,k} u_{ij}^* u_{ik} \langle \phi_j | O | \phi_k \rangle \\ &= \sum_{j,k} (U^\dagger U)_{jk} \langle \phi_j | O | \phi_k \rangle = \sum_{j,k} \delta_{jk} \langle \phi_j | O | \phi_k \rangle = \sum_j \langle \phi_j | O | \phi_j \rangle, \end{aligned} \quad (1.15)$$

where we used Eq. (1.2) for the transformation between two different bases.

As convenient as the description of quantum states with vector states might seem at first sight, unfortunately it is often not quite adequate to describe the properties of quantum systems. In experiments vector states cannot be prepared perfectly and it cannot be avoided that the system interacts with the environment. Therefore the concept of vector states has to be extended to the concept of *density operators*, where we can differentiate between *pure states* that are equivalent to the vector states considered before, and *mixed states*, that take the mentioned imperfections and interactions into account.

1.2. Density operators

Definition 1.1. A quantum state (or just “state”) is an operator $\rho \in \mathcal{A}$ that has the following properties:

$$\rho^\dagger = \rho, \quad (1.16)$$

$$\text{Tr}\rho = 1, \quad (1.17)$$

$$\rho \geq 0, \quad (1.18)$$

where property (1.18) means that ρ is positive semidefinite², i.e. it has no negative eigenvalues.

Another frequently used term for an operator that satisfies the above properties is *density operator* or *density matrix*. Any state ρ also satisfies $\text{Tr}\rho^2 \leq 1$. If $\text{Tr}\rho^2 = 1$ we call the state *pure*, if $\text{Tr}\rho^2 < 1$ we call it *mixed*. The value of $\text{Tr}\rho^2$ is a measure for the *mixedness* of the state that varies between $1/d$ for the maximally mixed state $1/d\mathbb{1}$ and 1 for pure states. The origin of the classification into pure and mixed states lies in the notation of a state as a decomposition into projectors onto vector states,

$$\rho = \sum_i p_i |\psi_i\rangle\langle\psi_i|, \quad p_i \geq 0, \quad \sum_i p_i = 1, \quad (1.19)$$

which physically describes an ensemble (or, equivalently, a classical mixture) of vector states $|\psi\rangle$, where each vector state occurs with probability p_i . If we have only one term in the decomposition, $\rho = |\psi\rangle\langle\psi|$, then ρ is just the projector onto the vector state $|\psi\rangle$, and is therefore called “pure”, and we have $\text{Tr}\rho^2 = 1$. Consequently the state is called “mixed” if we have more than one term in the decomposition, and in this case $\text{Tr}\rho^2 < 1$. It is important to notice that in the case of mixed states a decomposition of ρ (1.19) is not unique, in general infinitely many decompositions of vector states that result in the same density operator ρ exist.

Note that in this general mathematical description of quantum states the states are elements of the Hilbert-Schmidt space of operators that act upon the Hilbert space of vector states. The expectation value of an operator O for a state ρ is defined by the Hilbert-Schmidt inner product (1.10),

$$\langle O \rangle_\rho := \text{Tr}\rho O. \quad (1.20)$$

For pure states $\rho_p = |\psi\rangle\langle\psi|$ we have $\text{Tr}\rho_p O = \langle\psi|O|\psi\rangle$, since we can take the trace using an orthogonal basis where $|\psi\rangle$ is one of the basis vectors. Hence it is evident that the density operator formalism is equivalent to the vector state formalism in the handling of pure states. Vector states thus are fully equivalent to

²In this work usually omit the word “semidefinite”, where by “positive” we implicitly mean “positive semidefinite”.

pure states, and one sometimes mixes notation, where it is clear from the context if $|\psi\rangle$ or $|\psi\rangle\langle\psi|$ is meant.

Evidently we can also express a state ρ as a matrix, just like any operator (see Eq. (1.8)). Usually one uses the standard basis, obtaining the matrix elements

$$\rho_{ij} = \langle i|\rho|j\rangle. \quad (1.21)$$

From the density matrix elements we can easily reconstruct the density operator,

$$\rho = \sum_{i,j} \rho_{ij} |i\rangle\langle j|. \quad (1.22)$$

1.3. Bipartite systems, entanglement, and separability

Quantum systems can be composite systems of many subsystems, e.g. a system of many particles. The suitable mathematical description of such systems is straightforward; one considers a Hilbert space that comprises the Hilbert spaces of N subsystems:

$$\mathcal{H}^D = \mathcal{H}^{d_1} \otimes \mathcal{H}^{d_2} \otimes \dots \otimes \mathcal{H}^{d_N}, \quad \text{where } D = d_1 d_2 \dots d_N. \quad (1.23)$$

In the case of few subsystems, one also uses a notation by labeling the Hilbert spaces of the subsystems alphabetically, e.g. in the case of two subsystems, $\mathcal{H}_A \otimes \mathcal{H}_B$, with dimension $d_A \times d_B$. In the language of quantum communication, one calls the two subsystems “parties” and usually names them “Alice” and “Bob”. For the sake of clarity and shortness we will in the following definitions consider bipartite systems. The greater part of this thesis deals with bipartite systems. In Chapter 5, however, we also consider multipartite systems, where we briefly generalize the definitions of this section.

1.3.1. Vector states

The notation of the composite Hilbert space (1.23) using the tensor multiplication originates in the definition of the tensor product of vector states of the two subsystems, which is defined via the scalar product,

$$\langle \phi_A \otimes \phi_B | \psi_A \otimes \psi_B \rangle = \langle \phi_A | \psi_A \rangle \langle \phi_B | \psi_B \rangle. \quad (1.24)$$

Here we used the notation $|\psi_A \otimes \psi_B\rangle = |\psi_A\rangle \otimes |\psi_B\rangle$. A vector state $|\psi_p\rangle \in \mathcal{H}_A \otimes \mathcal{H}_B$ that can be written in the form

$$|\psi_p\rangle = |\psi_A\rangle \otimes |\psi_B\rangle \quad (1.25)$$

is called *product vector state*.

Operators of bipartite systems are elements of the Hilbert-Schmidt space $\mathcal{A}^D = \mathcal{A}_A \otimes \mathcal{A}_B$ and act on the Hilbert space $\mathcal{H}_A \otimes \mathcal{H}_B$. A tensor product of operators is defined via their action on product vector states,

$$(A \otimes B)|\psi_A \otimes \psi_B\rangle = A|\psi_A\rangle \otimes B|\psi_B\rangle, \quad A, B \in \mathcal{A}^D. \quad (1.26)$$

Operators O that can be written as $O = A \otimes B$ are called *local*, since their effect can be reduced to the action on the states of the two subsystems. Operators that cannot be put into the form $A \otimes B$ are called *global*, they have effects on the whole state that cannot be reduced to the subsystems. The expression of an operator $C \in \mathcal{A}^D$ as a $D \times D$ matrix can be obtained with any orthogonal basis of the whole system, see Eq. (1.8), but a reasonable choice if one is interested in local properties is the *standard product basis*, which is a basis of D product vector states $|i\rangle \otimes |j\rangle$, shortly written as $\{|ij\rangle\}$, where $|i\rangle$ are the vector states of the standard basis for Alice's subsystem, and $|j\rangle$ are Bob's:

$$(C)_{ijkl} = \langle ij|C|kl\rangle. \quad (1.27)$$

A product vector state is also called *uncorrelated*, since expectation values of local operators can be written as a single factor,

$$\langle \psi_A \otimes \psi_B | A \otimes B | \psi_A \otimes \psi_B \rangle = \langle \psi_A | A | \psi_A \rangle \langle \psi_B | B | \psi_B \rangle. \quad (1.28)$$

Interestingly, and unique for quantum theory, there exist states that cannot be written in the form of Eq. (1.25).

Definition 1.2. A vector state $|\psi\rangle \in \mathcal{H}^D$ that is not a product vector state, i.e. that cannot be written in the form of Eq. (1.25), is called *entangled*.

Example. As an example of an entangled state consider the famous Bell singlet state that is an element of $\mathcal{H}^2 \otimes \mathcal{H}^2$,

$$|\psi^-\rangle = \frac{1}{\sqrt{2}} (|01\rangle - |10\rangle), \quad (1.29)$$

where $|ij\rangle$ is the short notation of $|i\rangle \otimes |j\rangle$. It is entangled since it cannot be written as a single product term, for details concerning entanglement detection for vector states see Sec. 3.2.

Entangled states are *correlated* because obviously expectation values of local operators cannot be written as a single factor like it can be done for uncorrelated vector states in Eq. (1.28). One calls a bipartite state of dimension 2×2 shortly a *two-qubit state*, of dimension 3×3 *two-qudit state*, and of arbitrary dimensions $d \times d$ *two-qudit state*.

1.3.2. Density operators

In contrast to the vector states, density operators of bipartite systems are elements of the Hilbert-Schmidt space, $\mathcal{A}^D = \mathcal{A}_A \otimes \mathcal{A}_B$ on the Hilbert space $\mathcal{H}^D = \mathcal{H}_A \otimes \mathcal{H}_B$ that satisfy the defining properties (1.16) - (1.18). The definition of entanglement for density operators is conceptually different than that for vector states, since unentangled states need not be uncorrelated, there also exist so-called *classically correlated* states. A state ρ of the whole system can be easily expressed as a matrix like in Eq. (1.27), where usually we use the standard product basis,

$$(\rho)_{ikjl} = \langle ik | \rho | jl \rangle. \quad (1.30)$$

If the density matrix elements are known, the density operator can be simply obtained by the decomposition

$$\rho = \sum_{i,j,k,l} \rho_{ikjl} |ik\rangle \langle jl| = \sum_{i,j,k,l} \rho_{ikjl} |i\rangle \langle j| \otimes |k\rangle \langle l|. \quad (1.31)$$

A product state is a state of the whole system that can be written as $\sigma_p = \rho^A \otimes \rho^B$. It is uncorrelated, since we have a single factor for the expectation value of local operators,

$$\text{Tr} \rho^A \otimes \rho^B A \otimes B = \text{Tr} \rho^A A \text{Tr} \rho^B B. \quad (1.32)$$

One can also classically prepare states that involve correlations [138]. Consider, e.g., a state preparation device that can be switched to a number n of different settings, where a setting i occurs with a certain probability p_i , and if a setting i occurs, then the party j prepares a particular state $\rho_i^{(j)}$, such that the prepared mixed state σ is in total a mixture of product states,

$$\sigma = \sum_i p_i \rho_i^A \otimes \rho_i^B, \quad p_i \geq 0, \quad \sum_i p_i = 1. \quad (1.33)$$

In Ref. [138] this preparation procedure is described in detail, and a state that can be written in the form of (1.33) is called *classically correlated*. Unlike the product state, it contains correlations if $\max\{i\} \geq 2$, since the expectation value of local observables now no longer factorizes,

$$\text{Tr} \sigma A \otimes B = \sum_i p_i \text{Tr} \rho_i^A A \text{Tr} \rho_i^B B. \quad (1.34)$$

Nevertheless, it is not entangled since the correlations are due to the statistical “classical” mixture only. In the recent literature one calls a state (1.33) *separable* to emphasize the counterpart to an entangled state, which is defined in the following:

Definition 1.3. A state $\rho \in \mathcal{A}^D$ that is not a separable state, i.e. that cannot be written in the form of Eq. (1.33), is called *entangled*.

Remark 1.1. Note that a separable state σ (1.33) can always be written as a mixture of pure product states, because the mixed states ρ_A^i and ρ_B^i describe ensembles of pure states (see Eq. (1.19)):

$$\sigma = \sum_i \tilde{p}_i |\psi_i^A\rangle\langle\psi_i^A| \otimes |\psi_i^B\rangle\langle\psi_i^B|, \quad \tilde{p}_i \geq 0, \quad \sum_i \tilde{p}_i = 1. \quad (1.35)$$

Despite the clear and simple definition of entanglement, there is in general no straightforward and generally applicable method (called *operational* method) to decide for a given density operator if it can be written in a form (1.33). Only in the case of pure states ($\text{Tr}\rho^2 = 1$), which is equivalent to the vector state case, and for mixed states in dimensions 2×2 and 2×3 , one can always easily decide if the state is entangled or not. Concrete criteria for the detection of entanglement will be presented in Sec. 3.3.

Reduced density operators. An important concept of composite quantum systems are reduced density operators and, in connection to them, partial traces.

Definition 1.4. We define the reduced density operators ρ^A and ρ^B to a state (density operator) ρ of the whole system as

$$\rho^A := \text{Tr}_B \rho, \quad \rho^B := \text{Tr}_A \rho, \quad (1.36)$$

where the partial traces are given by

$$\begin{aligned} \text{Tr}_B \rho &:= \sum_{i,j} \sum_b \langle i \otimes b | \rho | j \otimes b \rangle |i\rangle\langle j|, \\ \text{Tr}_A \rho &:= \sum_{i,j} \sum_a \langle a \otimes i | \rho | a \otimes j \rangle |i\rangle\langle j|. \end{aligned} \quad (1.37)$$

Note that the matrix elements of the reduced density matrices are then simply given by

$$(\rho^A)_{ij} = (\text{Tr}_B \rho)_{ij} = \sum_b \langle i \otimes b | \rho | j \otimes b \rangle, \quad (1.38)$$

and equally for Bob's reduced density operator.

The reduced density operators describe the states that Alice and Bob locally have at their hands. It is important to notice that they can be mixed even if the whole state is pure, in which case the whole state has to be an entangled pure state, see Sec. 3.2. The motivation for Definition 1.4 is that the partial trace operation is the only operation that guarantees a consistent measurement statistics (see Ref. [97]), i.e.

$$\text{Tr} \rho^A A = \text{Tr} \rho A \otimes \mathbb{1}. \quad (1.39)$$

1.4. Bound entanglement

Apart from being separable or entangled, quantum states have another classifying property: the *distillability*. The concept of distillation can be briefly described as a procedure in which the two parties, Alice and Bob, are in possession of a certain entangled mixed state, and they would like to transform it into a maximally entangled pure state by statistical local operations and classical communication. A statistical local operation is a quantum operation that each party can perform only on her/his part of the state and leads to a particular outcome that occurs with some probability (for details on quantum operations see, e.g., Refs. [97, 69]). Classical communication allows the parties to inform each other about intentions and outcomes via classical channels (e.g. via telephone). Distillation protocols are protocols that give a series of operations that have to be performed on many identical copies of the same entangled mixed state, such that in the end one ends up with fewer more entangled states. In the limit of infinitely many copies of the input state (and thus also infinitely many iterations of the protocol), one obtains a maximally entangled pure state. The first distillation protocol was given by Bennett, Brassard, Popescu, Schumacher, and Smolin in Ref. [15] and is therefore called BBPSSW protocol. Note that distillation is also referred to as “purification” for obvious reasons. Extensions of this protocol can be found in Ref. [17]. The quantification of entanglement, i.e. the precise meaning of saying “more entangled” is done via the *fraction* with respect to some maximally entangled pure state. If, e.g., we want to distill the Bell singlet state $|\psi^-\rangle$ out of the input states ρ , we observe the singlet fraction $\langle\psi^-|\rho|\psi^-\rangle$ that should increase after an application of the protocol.

We say that an entangled state is *distillable*, if there exists a protocol such that we can distill a maximally entangled pure state out of it. Interestingly, mixed entangled states for which this is not the case, i.e. which are not distillable, exist. Such states are called *bound entangled* [105]. But which states are bound entangled? The following two theorems help in answering this question, which we state without proofs; these are given in the corresponding references.

Theorem 1.1 ([63, 65]). *Any two-qubit entangled state is distillable.*

Theorem 1.2 ([64, 65]). *All bipartite PPT entangled states (states that remain positive under partial transposition) are bound entangled.*

The partial transposition and the corresponding entanglement criterion will be explained in more detail in Sec. 3.3.1.

The first evidence for bound entangled states was given in Ref. [67], where the first PPT entangled states were constructed. Many references including examples and construction procedures for bound entangled states followed, see e.g. Refs. [16, 41, 68, 32, 71, 23, 22, 83]. Bound entanglement in multipartite systems is investigated, e.g., in Refs. [45, 43, 115, 58].

2. Bloch decompositions beyond qubits

2.1. Introduction

Bloch decompositions are an alternative representation of operators and states to the usual matrix notation. Since the space of operators is a Hilbert space - the so-called Hilbert-Schmidt space - there exist bases of operators which can be used to decompose any operator that is an element of Hilbert-Schmidt space. For two-dimensional Hilbert-Schmidt spaces (qubits) we have the well known decomposition into Pauli operators, where an operator can be characterized in general by four parameters, and a state by three parameters. These three parameters are the coefficients of the Bloch decomposition into the Pauli operators (the coefficient of the identity operator is fixed), and form a real vector, the so-called *Bloch vector* [27, 97]. Any density operator is uniquely characterized by a Bloch vector, and all Bloch vectors are contained in the *Bloch ball*, where pure states lie on the surface and mixed states inside. For higher dimensions there exist various operator bases apt for decomposing operators and states, we discuss three possible choices: the *generalized Gell-Mann operator basis*, the *polarization operator basis*, and the *Weyl operator basis*. Different to the qubit case, not all possible vectors of in general complex numbers can be assigned to states, and the geometry of the Bloch vectors is rather complicated (see Refs. [80, 92, 86] for analytical and numerical calculations in this respect). The aim of this chapter is, however, a more practical one: Since for high dimensions the matrix notation of operators and states can become quite unhandy, Bloch decompositions offer a relief in computational effort. They also turn out to be adequate for identifying operators as entanglement witnesses (see Sec. (3.5)). We present a method to decompose an arbitrary operator into one of the bases by using decompositions of the so-called *standard operators* (see Lemma 2.1, Lemma 2.2, and Lemma 2.3) and demonstrate the application for the maximally entangled two-qudit state.

The chapter is organized as follows: In Sec. 2.2 we shortly review the Bloch vector concept for qubits, and in Sec. 2.3 we give the general properties of an operator basis for qudits. In Secs. 2.4, 2.5, and 2.6 we define the three bases that can be used as generalizations of the Pauli operator basis, the generalized Gell-Mann operator basis, the polarization operator basis, and the Weyl operator basis. Various examples for concrete dimensions are given. We present a method to decompose operators and states of general dimension into the operator bases by using decompositions of the standard operators, given in Lemma 2.1, Lemma 2.2,

and Lemma 2.3. In Sec. 2.7 we show how to extend Bloch decompositions to bipartite systems. We illustrate the method to find the Bloch decomposition by determining the decomposition of the maximally entangled two-qudit state for the three bases. We conclude in Sec. 2.8.

This chapter is based on Ref. [21]:

- Reinhold A. Bertlmann and Philipp Krammer
Bloch vectors for qudits
 J. Phys. A: Math. Theor. **41**, 235303 (2008)

2.2. Bloch decompositions for qubits

Let us start with a simple introduction into the subject, the case of a two-dimensional Hilbert space. In this case we have two standard basis vectors, $|0\rangle$ and $|1\rangle$, so that the matrix form of any operator O is a 4×4 matrix with entries $\rho_{ij} = \langle i|O|j\rangle$. A convenient choice of a basis of operators are the identity operator $\mathbb{1}_2$ and the Pauli operators $\{\sigma^i\} = \{\sigma^x, \sigma^y, \sigma^z\}$. In this way an operator O can be decomposed as

$$O = a\mathbb{1}_2 + \vec{c} \cdot \vec{\sigma}, \quad a, c_i \in \mathbb{C}, \quad (2.1)$$

where $\vec{c} \cdot \vec{\sigma} = \sum_{i=1}^3 c_i \sigma^i$. The coefficients are given by $a = 1/2 \text{Tr}O$, $c_i = 1/2 \text{Tr}O\sigma_i$. A state ρ has to meet the requirements (1.16) - (1.18). Therefore we decompose it as

$$\rho = \frac{1}{2} (\mathbb{1}_2 + \vec{n} \cdot \vec{\sigma}), \quad n_i \in \mathbb{R}, \quad |\vec{n}|^2 \leq 1, \quad (2.2)$$

with $|\vec{n}|^2 := \sum_i n_i^2$. The Pauli operators are traceless ($\text{Tr}\sigma_i = 0$) and orthogonal to each other in the sense of the Hilbert-Schmidt inner product

$$\text{Tr}\sigma_i\sigma_j = 2\delta_{ij}, \quad (2.3)$$

and therefore one can easily find the Bloch coefficients n_i of the decomposition (2.2) via $n_i = \text{Tr}\rho\sigma_i$. The vector \vec{n} is called *Bloch vector*, it has only real entries since the Pauli operators and states ρ are Hermitian operators. Additionally in the qubit case, the state properties $\text{Tr}\rho = 1$ and $\rho \geq 0$ are equivalent to $\text{Tr}\rho = 1$ and $\det \rho \geq 0$. For any Bloch decomposition (2.2) we find

$$\det \rho = \frac{1}{4} (1 - |\vec{n}|^2) \geq 0, \quad (2.4)$$

and thus any three-dimensional Bloch vector \vec{n} with $|\vec{n}|^2 \leq 1$ and real entries corresponds to a state ρ , and can be seen as an alternative representation of the density matrix. Geometrically, the Bloch vectors are points in a three-dimensional vector space that lie inside a ball given by $|\vec{n}|^2 \leq 1$, and the pure states lie on the surface of the ball, $|\vec{n}|^2 = 1$, which follows immediately from condition $\text{Tr}\rho^2 = 1$.

Also expectation values of observables O can be conveniently expressed with the Bloch decompositions (2.1) and (2.2),

$$\text{Tr}\rho O = a + \vec{c} \cdot \vec{n}. \quad (2.5)$$

2.3. Bloch decompositions for qudits

In order to generalize the Bloch vector concept of qubits to arbitrary dimensional Hilbert spaces, we have to identify the properties of a suitable basis into which the operators can be decomposed. Such a basis of the Hilbert-Schmidt space on a Hilbert space of dimension d should inherit the following properties from the qubit case:

- i) The basis includes the identity operator $\mathbb{1}_d$ and $d^2 - 1$ operators $\{A_i\}$ which are traceless, i.e.

$$\mathrm{Tr} A_i = 0. \quad (2.6)$$

- ii) The operators $\{A_i\}$ are orthogonal,

$$\mathrm{Tr} A_i^\dagger A_j = N_A \delta_{ij} \quad \text{with} \quad N_A \in \mathbb{R}. \quad (2.7)$$

Hence with a basis $\{\mathbb{1}_d, A_i\}$ that satisfies the properties (2.6) and (2.7) we can decompose an operator O as

$$O = a\mathbb{1}_d + \vec{c} \cdot \vec{A}, \quad (2.8)$$

where $\vec{c} \cdot \vec{A} = \sum_{i=1}^{d^2-1} c_i A_i$ and the coefficients are given by

$$a = \frac{1}{d} \mathrm{Tr} O, \quad c_i = \frac{1}{N_A} \mathrm{Tr} O A_i^\dagger, \quad a, c_i \in \mathbb{C}. \quad (2.9)$$

We decompose a state ρ as

$$\rho = \frac{1}{d} \left(\mathbb{1}_d + \sqrt{\frac{d(d-1)}{N_A}} \sum_{i=1}^{d^2-1} \vec{n} \cdot \vec{A} \right), \quad n_i \in \mathbb{C}, \quad (2.10)$$

where $|\vec{n}|^2 = \sum_i n_i^* n_i \leq 1$. This decomposition implies $\mathrm{Tr} \rho = 1$ and $\mathrm{Tr} \rho^2 \leq 1$. Alternatively to $\mathrm{Tr} \rho^2$ we can use $|\vec{n}|^2$ as a measure of the purity of ρ instead of $\mathrm{Tr} \rho^2$, where the relation is

$$|\vec{n}|^2 = \frac{d \mathrm{Tr} \rho^2 - 1}{d - 1}, \quad (2.11)$$

and the measure varies between 0 (for the maximally mixed state) and 1 (for pure states).

Any vector $\vec{n} \in \mathbb{C}^{d^2-1}$ with $|\vec{n}|^2 \leq 1$ for which $\rho^\dagger = \rho$ and $\rho \geq 0$ in the decomposition (2.10) is called *Bloch vector*. The components of the Bloch vector are given by

$$n_i = \sqrt{\frac{d}{N_A(d-1)}} \mathrm{Tr} \rho A_i^\dagger. \quad (2.12)$$

Remark 2.1. For qubits the basis of Pauli operators is unitary *and* Hermitian. It seems that these two properties cannot be satisfied simultaneously for bases of higher dimensions. If a basis consists of non-Hermitian operators, then in general the coefficients are complex numbers. The most significant difference to the qubit case is, however, that a vector $\vec{n} \in \mathbb{C}^{d^2-1}$ with $|\vec{n}|^2 \leq 1$ that implies $\rho^\dagger = \rho$ in the decomposition (2.10) does not necessarily imply $\rho \geq 0$. The imposed map is not bijective: all qudit states $\rho \in \mathcal{A}^d$ can be mapped onto vectors $\vec{n} \in \mathbb{C}^{d^2-1}$ with $|\vec{n}|^2 \leq 1$, but not all vectors $|\vec{n}|^2 \leq 1$ can be mapped onto states ρ . Nevertheless, it is always true that pure states lie on the surface of the hyperball $|\vec{n}|^2 \leq 1$ ($|\vec{n}|^2 = 1$) and the mixed ones inside ($|\vec{n}|^2 < 1$).

The geometric character of the space of Bloch vectors in higher dimensions turns out to be quite complex (see Refs. [80, 86, 76, 81, 92] for details). In the next sections we will present concrete operator bases appropriate for Bloch decompositions.

2.4. The generalized Gell-Mann operator basis

2.4.1. Definition and examples

The generalized Gell-Mann operators (GGO) are higher-dimensional extensions of the Pauli operators (for qubits) and the Gell-Mann operators (for qutrits), they are the standard generators of the group $SU(N)$ of all complex unitary $N \times N$ matrices with determinant 1 (in our case $N = d$). They are defined as three different types of operators (see, e.g., Refs. [80, 106]). The matrix expression of the GGO is then simply derived by determining the matrix elements in the standard basis (1.8).

Definition 2.1. The generalized Gell-Mann operators are defined as

i) $\frac{d(d-1)}{2}$ symmetric GGO:

$$\Lambda_s^{jk} = |j\rangle\langle k| + |k\rangle\langle j|, \quad 1 \leq j < k \leq d, \quad (2.13)$$

ii) $\frac{d(d-1)}{2}$ antisymmetric GGO:

$$\Lambda_a^{jk} = -i|j\rangle\langle k| + i|k\rangle\langle j|, \quad 1 \leq j < k \leq d, \quad (2.14)$$

iii) $(d-1)$ diagonal GGO:

$$\Lambda^l = \sqrt{\frac{2}{l(l+1)}} \left(\sum_{j=1}^l |j\rangle\langle j| - l|l+1\rangle\langle l+1| \right), \quad 1 \leq l \leq d-1. \quad (2.15)$$

In total we have $d^2 - 1$ GGO; it follows from the definitions that all GGO are Hermitian and traceless. They are also orthogonal,

$$\text{Tr}\Lambda_i\Lambda_j = 2\delta_{ij}, \quad (2.16)$$

where we shortly write Λ_i for anyone of the GGO, and, together with the identity operator $\mathbb{1}_d$ they form a basis of the operator space, the generalized Gell-Mann operator basis (GGB). It takes some lines to proof the orthogonality of the GGB which is done in Appendix A.1.

Examples. For $d = 3$ the GGO are the familiar Gell-Mann operators, which have the following matrix form (where we altered the usual notation to the previously introduced one that considers the three different types):

i) three symmetric Gell-Mann matrices:

$$\lambda_s^{12} = \begin{pmatrix} 0 & 1 & 0 \\ 1 & 0 & 0 \\ 0 & 0 & 0 \end{pmatrix}, \quad \lambda_s^{13} = \begin{pmatrix} 0 & 0 & 1 \\ 0 & 0 & 0 \\ 1 & 0 & 0 \end{pmatrix}, \quad \lambda_s^{23} = \begin{pmatrix} 0 & 0 & 0 \\ 0 & 0 & 1 \\ 0 & 1 & 0 \end{pmatrix}, \quad (2.17)$$

ii) three antisymmetric Gell-Mann matrices:

$$\lambda_a^{12} = \begin{pmatrix} 0 & -i & 0 \\ i & 0 & 0 \\ 0 & 0 & 0 \end{pmatrix}, \quad \lambda_a^{13} = \begin{pmatrix} 0 & 0 & -i \\ 0 & 0 & 0 \\ i & 0 & 0 \end{pmatrix}, \quad \lambda_a^{23} = \begin{pmatrix} 0 & 0 & 0 \\ 0 & 0 & -i \\ 0 & i & 0 \end{pmatrix}, \quad (2.18)$$

ii) two diagonal Gell-Mann matrices:

$$\lambda^1 = \begin{pmatrix} 1 & 0 & 0 \\ 0 & -1 & 0 \\ 0 & 0 & 0 \end{pmatrix}, \quad \lambda^2 = \frac{1}{\sqrt{3}} \begin{pmatrix} 1 & 0 & 0 \\ 0 & 1 & 0 \\ 0 & 0 & -2 \end{pmatrix}. \quad (2.19)$$

The matrix form of the GGO - which we call generalized Gell-Mann matrices (GGM) - for $d = 4$ shows the generalization procedure:

i) 6 symmetric GGM:

$$\Lambda_s^{12} = \begin{pmatrix} 0 & 1 & 0 & 0 \\ 1 & 0 & 0 & 0 \\ 0 & 0 & 0 & 0 \\ 0 & 0 & 0 & 0 \end{pmatrix}, \quad \Lambda_s^{13} = \begin{pmatrix} 0 & 0 & 1 & 0 \\ 0 & 0 & 0 & 0 \\ 1 & 0 & 0 & 0 \\ 0 & 0 & 0 & 0 \end{pmatrix},$$

$$\Lambda_s^{14} = \begin{pmatrix} 0 & 0 & 0 & 1 \\ 0 & 0 & 0 & 0 \\ 0 & 0 & 0 & 0 \\ 1 & 0 & 0 & 0 \end{pmatrix}, \quad \Lambda_s^{23} = \begin{pmatrix} 0 & 0 & 0 & 0 \\ 0 & 0 & 1 & 0 \\ 0 & 1 & 0 & 0 \\ 0 & 0 & 0 & 0 \end{pmatrix},$$

$$\Lambda_s^{24} = \begin{pmatrix} 0 & 0 & 0 & 0 \\ 0 & 0 & 0 & 1 \\ 0 & 0 & 0 & 0 \\ 0 & 1 & 0 & 0 \end{pmatrix}, \quad \Lambda_s^{34} = \begin{pmatrix} 0 & 0 & 0 & 0 \\ 0 & 0 & 0 & 0 \\ 0 & 0 & 0 & 1 \\ 0 & 0 & 1 & 0 \end{pmatrix}, \quad (2.20)$$

ii) 6 antisymmetric GGM:

$$\begin{aligned} \Lambda_a^{12} &= \begin{pmatrix} 0 & -i & 0 & 0 \\ i & 0 & 0 & 0 \\ 0 & 0 & 0 & 0 \\ 0 & 0 & 0 & 0 \end{pmatrix}, & \Lambda_a^{13} &= \begin{pmatrix} 0 & 0 & -i & 0 \\ 0 & 0 & 0 & 0 \\ i & 0 & 0 & 0 \\ 0 & 0 & 0 & 0 \end{pmatrix}, \\ \Lambda_a^{14} &= \begin{pmatrix} 0 & 0 & 0 & -i \\ 0 & 0 & 0 & 0 \\ 0 & 0 & 0 & 0 \\ i & 0 & 0 & 0 \end{pmatrix}, & \Lambda_a^{23} &= \begin{pmatrix} 0 & 0 & 0 & 0 \\ 0 & 0 & -i & 0 \\ 0 & i & 0 & 0 \\ 0 & 0 & 0 & 0 \end{pmatrix}, \\ \Lambda_a^{24} &= \begin{pmatrix} 0 & 0 & 0 & 0 \\ 0 & 0 & 0 & -i \\ 0 & 0 & 0 & 0 \\ 0 & i & 0 & 0 \end{pmatrix}, & \Lambda_a^{34} &= \begin{pmatrix} 0 & 0 & 0 & 0 \\ 0 & 0 & 0 & 0 \\ 0 & 0 & 0 & -i \\ 0 & 0 & i & 0 \end{pmatrix}, \end{aligned} \quad (2.21)$$

iii) 3 diagonal GGM:

$$\begin{aligned} \Lambda^1 &= \begin{pmatrix} 1 & 0 & 0 & 0 \\ 0 & -1 & 0 & 0 \\ 0 & 0 & 0 & 0 \\ 0 & 0 & 0 & 0 \end{pmatrix}, & \Lambda^2 &= \frac{1}{\sqrt{3}} \begin{pmatrix} 1 & 0 & 0 & 0 \\ 0 & 1 & 0 & 0 \\ 0 & 0 & -2 & 0 \\ 0 & 0 & 0 & 0 \end{pmatrix}, \\ \Lambda^3 &= \frac{1}{\sqrt{6}} \begin{pmatrix} 1 & 0 & 0 & 0 \\ 0 & 1 & 0 & 0 \\ 0 & 0 & 1 & 0 \\ 0 & 0 & 0 & -3 \end{pmatrix}. \end{aligned} \quad (2.22)$$

Using the GGB we obtain, in general, the following Bloch vector expansion of a density matrix:

$$\rho = \frac{1}{d} \left(\mathbb{1} + \sqrt{\frac{d(d-1)}{2}} \vec{n} \cdot \vec{\Lambda} \right), \quad (2.23)$$

with the Bloch vector $\vec{n} = (\{n_s^{jk}\}, \{n_a^{jk}\}, \{n^l\})$, where the components are ordered and for the indices we have the restrictions $1 \leq j < k \leq d$ and $1 \leq l \leq d-1$, and $\vec{\Lambda}$ is a vector of all GGO. For example, for qutrits the Bloch vector components are $\vec{n} = (n_s^{12}, n_s^{13}, n_s^{23}, n_a^{12}, n_a^{13}, n_a^{23}, n^1, n^2)$ corresponding to the Gell-Mann matrices (2.17), (2.18), (2.19). The components are given by

$$n_i = \sqrt{\frac{d}{2(d-1)}} \text{Tr} \rho \Lambda_i, \quad n_i \in \mathbb{R}, \quad (2.24)$$

where we use the short notation of Eq. (2.16) again. The coefficients n_i are real because the GGO are Hermitian. All Bloch vectors lie within a hyperball of radius $|\vec{n}|^2 \leq 1$. As mentioned in Remark 2.1, the allowed range of \vec{n} is restricted concerning its correspondence to states. For the GGB the set of all Bloch vectors has an interesting geometric structure which has been calculated analytically for the case of qutrits by studying two-dimensional planes in the eight-dimensional Bloch space [80] or numerically by considering three-dimensional cross-sections [92].

2.4.2. Decomposing the standard operators with the GGB

The simplest operator basis of \mathcal{A}^d is given by the operators

$$|j\rangle\langle k|, \quad \text{with } j, k = 1, \dots, d, \quad (2.25)$$

which we call *standard operators*. They form an orthogonal basis and a decomposition of an operator O into this basis is merely a decomposition into the matrix elements of O in the standard basis $\{|i\rangle\}$ (see Eq. (1.8)),

$$O = \sum_{jk} (O)_{jk} |j\rangle\langle k|. \quad (2.26)$$

This is not a Bloch decomposition since the standard operators do not satisfy the desired property of tracelessness (2.6). The matrix notation of the standard operators are just $d \times d$ matrices that have only one entry 1 and the other entries 0. Hence if we know the Bloch decomposition of the standard operators into any suitable operator basis, we can find the Bloch decomposition of any operator.

Lemma 2.1. *The Bloch decompositions of the standard operators (2.25) in the generalized Gell-Mann operator basis are given by*

$$|j\rangle\langle k| = \begin{cases} \frac{1}{2} (\Lambda_s^{jk} + i\Lambda_a^{jk}) & \text{for } j < k \\ \frac{1}{2} (\Lambda_s^{kj} - i\Lambda_a^{kj}) & \text{for } j > k \\ -\sqrt{\frac{j-1}{2j}} \Lambda^{j-1} + \sum_{n=0}^{d-j-1} \frac{1}{\sqrt{2(j+n)(j+n+1)}} \Lambda^{j+n} + \frac{1}{d} \mathbb{1} & \text{for } j = k. \end{cases} \quad (2.27)$$

Proof. The first two cases can be easily verified using Eqs. (2.13) and (2.14).

To show the last case we first set up a recurrence relation for $|l\rangle\langle l|$, which we obtain by eliminating the term $\sum_{j=1}^{l-1} |j\rangle\langle j|$ in the two expressions (2.15) for Λ^l and Λ^{l-1} ,

$$|l\rangle\langle l| = -\sqrt{\frac{l-1}{2l}} \Lambda^{l-1} + \sqrt{\frac{l+1}{2l}} \Lambda^l + |l+1\rangle\langle l+1|, \quad (2.28)$$

and we consider the case $l+1 = d$,

$$|d-1\rangle\langle d-1| = -\sqrt{\frac{d-2}{2(d-1)}} \Lambda^{d-2} + \sqrt{\frac{d}{2(d-1)}} \Lambda^{d-1} + |d\rangle\langle d|. \quad (2.29)$$

From Λ^{d-1} given by Eq. (2.15),

$$\Lambda^{d-1} = \sqrt{\frac{2}{(d-1)d}} \left(\sum_{j=1}^{d-1} |j\rangle\langle j| - (d-1)|d\rangle\langle d| \right), \quad (2.30)$$

we get the Bloch decomposition of $|d\rangle\langle d|$,

$$|d\rangle\langle d| = \frac{1}{d} \left(-\sqrt{\frac{(d-1)d}{2}} \Lambda^{d-1} + \mathbb{1}_d \right), \quad (2.31)$$

where we have applied $\sum_{j=1}^{d-1} |j\rangle\langle j| = \mathbb{1}_d - |d\rangle\langle d|$.

Inserting now decomposition (2.31) into relation (2.29) we gain the Bloch vector expansion for $|d-1\rangle\langle d-1|$ and recurrence relation (2.28) provides $|d-2\rangle\langle d-2|$ and so forth. Thus finally we find (via mathematical induction)

$$\begin{aligned} |d-n\rangle\langle d-n| &= -\sqrt{\frac{d-n-1}{2(d-n)}} \Lambda^{d-n-1} \\ &+ \sum_{k=0}^{n-1} \frac{1}{\sqrt{2(d-n+k+1)(d-n+k)}} \Lambda^{d-n+k} + \frac{1}{d} \mathbb{1}, \end{aligned} \quad (2.32)$$

the relation we had to prove, where $d-n=j$. □

2.5. The polarization operator basis

2.5.1. Definition and examples

Definition 2.2. The polarization operators of the Hilbert-Schmidt space \mathcal{A}^d are defined as the following d^2 operators [127, 86]:

$$T_{LM} = \sqrt{\frac{2L+1}{2s+1}} \sum_{k,l=1}^d C_{sm_l, LM}^{sm_k} |k\rangle\langle l|. \quad (2.33)$$

The used indices have the properties

$$\begin{aligned} s &= \frac{d-1}{2}, \\ L &= 0, 1, \dots, 2s, \\ M &= -L, -L+1, \dots, L-1, L, \\ m_1 &= s, m_2 = s-1, \dots, m_d = -s. \end{aligned} \quad (2.34)$$

The coefficients $C_{sm_l, LM}^{sm_k}$ are identified with the usual Clebsch-Gordan coefficients $C_{j_1 m_1, j_2 m_2}^{j m}$ of the angular momentum theory and are displayed explicitly in tables, e.g., in Ref. [127].

For $L = M = 0$ the polarization operator is proportional to the identity operator [127, 86],

$$T_{00} = \frac{1}{\sqrt{d}} \mathbb{1}. \quad (2.35)$$

It is shown in Ref. [86] that all polarization operators (except T_{00}) are traceless, in general *not* Hermitian, and that orthogonality relation (2.7) is satisfied,

$$\text{Tr } T_{L_1 M_1}^\dagger T_{L_2 M_2} = \delta_{L_1 L_2} \delta_{M_1 M_2}. \quad (2.36)$$

Therefore the d^2 polarization operators (2.33) form an orthogonal operator basis suitable for Bloch decompositions - the polarization operator basis (POB) - of the Hilbert-Schmidt space \mathcal{A}^d .

Examples. For qubit states ($d = 2$) the POB is given by the following operators in matrix form ($s = 1/2; L = 0, 1; M = -1, 0, 1$):

$$\begin{aligned} T_{00} &= \frac{1}{\sqrt{2}} \begin{pmatrix} 1 & 0 \\ 0 & 1 \end{pmatrix}, & T_{11} &= - \begin{pmatrix} 0 & 1 \\ 0 & 0 \end{pmatrix}, \\ T_{10} &= \frac{1}{\sqrt{2}} \begin{pmatrix} 1 & 0 \\ 0 & -1 \end{pmatrix}, & T_{1-1} &= \begin{pmatrix} 0 & 0 \\ 1 & 0 \end{pmatrix}. \end{aligned} \quad (2.37)$$

For the next higher dimension, $d = 3$ ($s = 1$), the case of qutrits, we get 9 polarization operators T_{LM} with $L = 0, 1, 2$ in the matrix form

$$\begin{aligned} T_{11} &= -\frac{1}{\sqrt{2}} \begin{pmatrix} 0 & 1 & 0 \\ 0 & 0 & 1 \\ 0 & 0 & 0 \end{pmatrix}, & T_{10} &= \frac{1}{\sqrt{2}} \begin{pmatrix} 1 & 0 & 0 \\ 0 & 0 & 0 \\ 0 & 0 & -1 \end{pmatrix}, \\ T_{1-1} &= \frac{1}{\sqrt{2}} \begin{pmatrix} 0 & 0 & 0 \\ 1 & 0 & 0 \\ 0 & 1 & 0 \end{pmatrix}, & T_{22} &= \begin{pmatrix} 0 & 0 & 1 \\ 0 & 0 & 0 \\ 0 & 0 & 0 \end{pmatrix}, \\ T_{21} &= \frac{1}{\sqrt{2}} \begin{pmatrix} 0 & -1 & 0 \\ 0 & 0 & 1 \\ 0 & 0 & 0 \end{pmatrix}, & T_{20} &= \frac{1}{\sqrt{6}} \begin{pmatrix} 1 & 0 & 0 \\ 0 & -2 & 0 \\ 0 & 0 & 1 \end{pmatrix}, \\ T_{2-1} &= \frac{1}{\sqrt{2}} \begin{pmatrix} 0 & 0 & 0 \\ 1 & 0 & 0 \\ 0 & -1 & 0 \end{pmatrix}, & T_{2-2} &= \begin{pmatrix} 0 & 0 & 0 \\ 0 & 0 & 0 \\ 1 & 0 & 0 \end{pmatrix}. \end{aligned} \quad (2.38)$$

The decomposition of any density matrix into a Bloch vector by using the POB has, in general, the following form:

$$\rho = \frac{1}{d} \left(\mathbb{1}_d + \sqrt{d(d-1)} \sum_{L=1}^{2s} \sum_{M=-L}^L n_{LM} T_{LM} \right) = \frac{1}{d} \left(\mathbb{1}_d + \sqrt{d(d-1)} \vec{n} \cdot \vec{T} \right), \quad (2.39)$$

with the Bloch vector $\vec{n} = (n_{1-1}, n_{10}, n_{11}, n_{2-2}, n_{2-1}, n_{20}, \dots, n_{LM})$, where the components are given by

$$n_{LM} = \sqrt{\frac{d}{d-1}} \operatorname{Tr} \rho T_{LM}^\dagger, \quad n_{LM} \in \mathbb{C}. \quad (2.40)$$

In general, the components n_{LM} are complex numbers, since the polarization operators T_{LM} are not Hermitian. Again all Bloch vectors lie within a hyperball $|\vec{n}|^2 \leq 1$. For qubits the decomposition with the POB (2.37) is equivalent to the standard description of Bloch vectors with Pauli matrices. In higher dimensions, however, the structure of the allowed range of \vec{n} (due to the positivity requirement $\rho \geq 0$) is quite complicated, as can be seen already for $d = 3$ (for details see Ref. [86]).

2.5.2. Decomposing the standard operators with the POB

Lemma 2.2 ([127]). *The standard operators (2.25) can be decomposed into the POB as*

$$|i\rangle\langle j| = \sum_L \sum_M \sqrt{\frac{2L+1}{2s+1}} C_{sm_j, LM}^{sm_i} T_{LM}. \quad (2.41)$$

Note that \sum_M is actually fixed by the condition $m_j + M = m_i$.¹

Proof. Inserting definition (2.33) on the right-hand side (RHS) of equation (2.41) we find

$$\begin{aligned} \text{RHS} &= \sum_{k,l} \left(\sum_L \frac{2L+1}{2s+1} C_{sm_j, LM}^{sm_i} C_{sm_l, LM}^{sm_k} \right) |k\rangle\langle l| = \\ &= \sum_{k,l} \delta_{jl} \delta_{ik} |k\rangle\langle l| \\ &= |i\rangle\langle j|, \end{aligned} \quad (2.42)$$

where we used the sum rule for Clebsch–Gordan coefficients [127]

$$\sum_{c,\gamma} \frac{2c+1}{2b+1} C_{a\alpha, c\gamma}^{b\beta} C_{a\alpha', c\gamma}^{b\beta'} = \delta_{\alpha\alpha'} \delta_{\beta\beta'}. \quad (2.43)$$

□

¹Relation (2.41) is given in Ref. [127] without proof.

2.6. The Weyl operator basis

2.6.1. Definition and example

Finally, we want to discuss a basis of operators in \mathcal{A}^d that consists of the following d^2 operators:

$$U_{nm} = \sum_{k=0}^{d-1} e^{\frac{2\pi i}{d} kn} |k\rangle \langle (k+m) \bmod d|, \quad n, m = 0, 1, \dots, d-1. \quad (2.44)$$

The operators in notation (2.44) have been introduced in the context of quantum teleportation of qudit states [13] and are often called *Weyl operators* in the literature (see, e.g., Ref. [96]). They have been introduced in classical theories of discrete phase space. The d^2 operators (2.44) are unitary, traceless (except for U_{00}), and orthogonal,

$$\text{Tr } U_{nm}^\dagger U_{l_j} = d \delta_{nl} \delta_{mj}, \quad (2.45)$$

and thus form an appropriate Bloch basis (a proof is presented in Appendix A.3, see also Refs. [49, 101]) – the Weyl operator basis (WOB). They can be used to create a basis of d^2 maximally entangled qudit states [96, 139, 134], see also Sec. 3.5.2.

The operator U_{00} represents the identity $U_{00} = \mathbb{1}_d$, where Eq. (2.44) reduces to the completeness relation $\sum_{k=0}^{d-1} |k\rangle \langle k| = \mathbb{1}_d$.

Example. As an example let us consider qutrits, $d = 3$. In this case the Weyl operators (2.44) have the matrix form

$$\begin{aligned} U_{01} &= \begin{pmatrix} 0 & 1 & 0 \\ 0 & 0 & 1 \\ 1 & 0 & 0 \end{pmatrix}, & U_{02} &= \begin{pmatrix} 0 & 0 & 1 \\ 1 & 0 & 0 \\ 0 & 1 & 0 \end{pmatrix}, \\ U_{10} &= \begin{pmatrix} 1 & 0 & 0 \\ 0 & e^{2\pi i/3} & 0 \\ 0 & 0 & e^{-2\pi i/3} \end{pmatrix}, & U_{11} &= \begin{pmatrix} 0 & 1 & 0 \\ 0 & 0 & e^{2\pi i/3} \\ e^{-2\pi i/3} & 0 & 0 \end{pmatrix}, \\ U_{12} &= \begin{pmatrix} 0 & 0 & 1 \\ e^{2\pi i/3} & 0 & 0 \\ 0 & e^{-2\pi i/3} & 0 \end{pmatrix}, & U_{20} &= \begin{pmatrix} 1 & 0 & 0 \\ 0 & e^{-2\pi i/3} & 0 \\ 0 & 0 & e^{2\pi i/3} \end{pmatrix}, \\ U_{21} &= \begin{pmatrix} 0 & 1 & 0 \\ 0 & 0 & e^{-2\pi i/3} \\ e^{2\pi i/3} & 0 & 0 \end{pmatrix}, & U_{22} &= \begin{pmatrix} 0 & 0 & 1 \\ e^{-2\pi i/3} & 0 & 0 \\ 0 & e^{2\pi i/3} & 0 \end{pmatrix}. \end{aligned} \quad (2.46)$$

Using the WOB we can find the Bloch decomposition of a density operator,

$$\rho = \frac{1}{d} \left(\mathbb{1}_d + \sqrt{(d-1)} \sum_{l,m=0}^{d-1} n_{lm} U_{lm} \right) = \frac{1}{d} \left(\mathbb{1}_d + \sqrt{(d-1)} \vec{n} \cdot \vec{U} \right), \quad (2.47)$$

where $n_{00} = 0$. The components of the Bloch vector $\vec{n} = (\{n_{lm}\})$ are ordered and given by

$$n_{lm} = \frac{1}{\sqrt{(d-1)}} \text{Tr} \rho U_{lm}^\dagger, \quad n_{lm} \in \mathbb{C}. \quad (2.48)$$

In general, the components n_{lm} are complex numbers, since the Weyl operators are not Hermitian. The complex conjugates satisfy the relation $n_{lm}^* = e^{-\frac{2\pi i}{d} lm} n_{-l-m}$,² which follows easily from definition (2.44) together with the hermiticity of ρ .

All Bloch vectors lie within a hyperball $|\vec{n}| \leq 1$. For example, for qutrits the Bloch vector is expressed by $\vec{n} = (n_{01}, n_{02}, n_{10}, n_{11}, n_{12}, n_{20}, n_{21}, n_{22})$ and for all dimensions $d > 2$ the detailed structure of the geometry of Bloch vectors is not known yet.

2.6.2. Decomposing the standard operators with the WOB

Lemma 2.3. *The standard operators (2.25) can be decomposed with the WOB as*

$$|j\rangle\langle k| = \frac{1}{d} \sum_{l=0}^{d-1} e^{-\frac{2\pi i}{d} lj} U_{l(k-j) \bmod d}. \quad (2.49)$$

Proof. For the proof we need the equivalence

$$\sum_{n=0}^{d-1} e^{\frac{2\pi i}{d} nx} = \begin{cases} d & \text{if } x = 0 \\ 0 & \text{if } x \neq 0 \end{cases}, \quad x \in \mathbb{Z}. \quad (2.50)$$

We insert the definition of the Weyl operators (2.44) on the right hand side (RHS) of Eq. (2.49), use Eq. (2.50) and get

$$\begin{aligned} \text{RHS} &= \frac{1}{d} \sum_{l,r=0}^{d-1} e^{\frac{2\pi i}{d} l(r-j)} |r\rangle\langle (r+k-j) \bmod d| \\ &= |j\rangle\langle k| + \frac{1}{d} \sum_{r \neq j, r=0}^{d-1} \sum_{l=0}^{d-1} e^{\frac{2\pi i}{d} l(r-j)} |r\rangle\langle (r+k-j) \bmod d| \\ &= |j\rangle\langle k|. \end{aligned} \quad (2.51)$$

□

Remark 2.2. Note that in two dimensions the WOB as well as the GGB coincides with the Pauli matrix basis and the POB represents a rotated Pauli basis (where $\sigma_{\pm} = \frac{1}{2}(\sigma_1 \pm i\sigma_2)$), in particular we have

$$\{U_{00}, U_{01}, U_{10}, U_{11}\} = \{\mathbb{1}, \sigma_1, \sigma_3, i\sigma_2\}, \quad (2.52)$$

$$\{\mathbb{1}, \lambda_s^{12}, \lambda_a^{12}, \lambda^1\} = \{\mathbb{1}, \sigma_1, \sigma_2, \sigma_3\}, \quad (2.53)$$

$$\{T_{00}, T_{11}, T_{10}, T_{1-1}\} = \left\{ \frac{1}{\sqrt{2}} \mathbb{1}, -\sigma_+, \frac{1}{\sqrt{2}} \sigma_3, \sigma_- \right\}. \quad (2.54)$$

²Negative indices are taken *mod d*.

2.7. Bloch decompositions for bipartite systems

Of course Bloch decompositions of operators and states are possible for composite systems as well. However, we restrict ourselves to the case of two subsystems, since the generalized Bloch decompositions for more parties are lengthy and rather inconvenient, but nevertheless straightforward to obtain from the general equations in the bipartite case.

We consider a Hilbert space of a bipartite system, $\mathcal{H}^D = \mathcal{H}^{d_A} \otimes \mathcal{H}^{d_B}$. Useful definitions are given in Sec. 1.3. Let $\{\mathbb{1}, A_i\}$ and $\{\mathbb{1}, B_i\}$ be bases for Alice and Bob, respectively, that satisfy the properties (2.6) and (2.7), then any operator $O \in \mathcal{A}^D$ can be decomposed into a basis of $(d^2)^2$ operators as

$$O = e \mathbb{1}_{d_A} \otimes \mathbb{1}_{d_B} + \sum_{i=0}^{d_A-1} a_i A_i \otimes \mathbb{1}_{d_B} + \sum_{j=0}^{d_B-1} b_j \mathbb{1}_{d_A} \otimes B_j + \sum_{i,j} c_{ij} A_i \otimes B_j, \quad (2.55)$$

$e, a_i, b_i, c_{ij} \in \mathbb{C}.$

Any bipartite state $\rho \in \mathcal{A}^D$ can be decomposed in the way of Eq. (2.55), with $e = 1/d^2$ (introduced in [48] for two-qubit systems). A bipartite product state $\sigma_p := \rho_A \otimes \rho_B$ on \mathcal{H}^D of dimension $d_A \times d_B$ can be written as

$$\begin{aligned} \sigma_p = \frac{1}{d^2} & \left(\mathbb{1}_{d_A} \otimes \mathbb{1}_{d_B} + \sum_{i=0}^{d_A-1} f_A n_i A_i \otimes \mathbb{1}_d + \sum_{j=0}^{d_B-1} f_B m_j \mathbb{1}_d \otimes B_j \right. \\ & \left. + \sum_{i,j} f_A f_B n_i m_j A_i \otimes B_j \right), \quad n_{nm}, m_{lk} \in \mathbb{C}, |\vec{n}| \leq 1, |\vec{m}| \leq 1, \\ f_A := & \sqrt{\frac{d_A(d_A-1)}{N_A}}, \quad f_B := \sqrt{\frac{d_B(d_B-1)}{N_B}}, \end{aligned} \quad (2.56)$$

where the state is pure if and only if $|\vec{n}| = |\vec{m}| = 1$. To obtain the Bloch decomposition (2.56), we simply perform the tensor product of two Bloch decompositions of the one-partite states (2.10) of each party.

Singular value optimization (SVO). For a given operator O and same dimensions of the subsystems $d_A = d_B =: d$, one can always find an orthogonal basis in which the coefficient matrix $C^{cor} = (c_{ij})$, called *correlation coefficient matrix*, is diagonal: Given an operator decomposition (2.55), we have to perform a singular value decomposition of C ,

$$S = UC^{cor}V^\dagger, \quad (2.57)$$

where U and V are unitary matrices with entries u_{ij} and v_{ij} and S is the resulting diagonal matrix with the d^2 diagonal real positive singular values s_i of C^{cor} as diagonal entries. The new operators of the basis $\{\mathbb{1}_d, D_i\}$ are then given by a linear combination of the old operators,

$$D_i^A = \sum_j u_{ij}^* A_j, \quad D_i^B = \sum_j v_{ij} B_j, \quad (2.58)$$

which satisfies the same orthogonality condition, $\text{Tr} D_i^A D_j^A = N_A \delta_{ij}$ (and equivalently for D_i^B). So we can rewrite Eq. (2.55) as

$$O = e \mathbb{1}_d \otimes \mathbb{1}_d + \sum_{i=0}^{d-1} r_i D_i^A \otimes \mathbb{1}_d + \sum_{j=0}^{d-1} t_j \mathbb{1}_d \otimes D_j^B + \sum_{i,j} s_i D_i^A \otimes D_j^B, \quad (2.59)$$

where $r_i = \sum_j a_j u_{ij}$, $t_j = \sum_k b_k v_{jk}^*$ and $s_i = \sum_{j,l} u_{ij} c_{jl} v_{il}^*$. We call the decomposed operator that is written in the optimized way of Eq. (2.59) ‘‘singular value optimized’’ (SVO). Of course a product state can then also be decomposed in terms of the new basis,

$$\begin{aligned} \sigma_p = & \frac{1}{d^2} \left(\mathbb{1}_d \otimes \mathbb{1}_d + \sum_{i=0}^{d_A-1} f_A \bar{n}_i D_i^A \otimes \mathbb{1}_d + \sum_{j=0}^{d_B-1} f_B \bar{m}_j \mathbb{1}_d \otimes D_j^B \right. \\ & \left. + \sum_{i,j} f_A f_B \bar{n}_i \bar{m}_j D_i^A \otimes D_j^B \right), \quad \bar{n}_i, \bar{m}_j \in \mathbb{C}, \quad |\bar{n}| \leq 1, \quad |\bar{m}| \leq 1. \end{aligned} \quad (2.60)$$

Remark 2.3. Note that the SVO bases $\{\mathbb{1}, D_i^A\}$ and $\{\mathbb{1}, D_i^B\}$ depend on the decomposed operator, in general they do not imply a real positive diagonal correlation coefficient matrix for other operators or states.

2.7.1. Bloch decompositions of the maximally entangled two-qudit state

The usual method to find the Bloch decomposition of an operator or state is via the trace methods of Eqs. (2.9) and (2.12). However, if the operator or state does not have a concrete expression in a certain dimension of the Hilbert space, but the dimension is left as a variable, it might get inconvenient and unclear to perform these trace methods. The method via the standard operators is then easier to apply: We just have to insert the Bloch decompositions of the standard operators into the standard operator decomposition of the operator (2.26) and get the desired Bloch decomposition of the operator. The standard operator decompositions for the considered three operator bases are provided in Lemma 2.1, Lemma 2.2, and Lemma 2.3.

The maximally entangled two-qudit vector state is given by

$$|\phi_+^d\rangle = \frac{1}{\sqrt{d}} \sum_j |j\rangle \otimes |j\rangle, \quad (2.61)$$

where the sum runs from $j = 0, \dots, d-1$ or from $j = 1, \dots, d$, respectively. The terminology ‘‘maximally entangled’’ is explained in Sec. 3.2.

The corresponding two-qudit state, i.e. the density operator to the vector state (2.61), can be written in terms of standard operators as

$$|\phi_+^d\rangle \langle \phi_+^d| = \frac{1}{d} \sum_{j,k=1}^d |j\rangle \langle k| \otimes |j\rangle \langle k|. \quad (2.62)$$

We can use this expression to insert the standard operator decompositions in the three bases, the GGB, the POB, and the WOB.

Expansion into GGB. For the generalized Gell-Mann matrix basis, it is convenient to split the state $|\phi_+^d\rangle\langle\phi_+^d|$ into two parts,

$$|\phi_+^d\rangle\langle\phi_+^d| = A + B, \quad (2.63)$$

where A and B are defined by

$$A = \frac{1}{d} \sum_{j < k} |j\rangle\langle k| \otimes |j\rangle\langle k| + \frac{1}{d} \sum_{j < k} |k\rangle\langle j| \otimes |k\rangle\langle j|, \quad (2.64)$$

$$B = \frac{1}{d} \sum_j |j\rangle\langle j| \otimes |j\rangle\langle j|, \quad (2.65)$$

and to calculate the two terms separately.

For term A we use the standard operator decomposition of Lemma 2.1 for the case $j \neq k$ and get

$$\begin{aligned} A &= \frac{1}{4d} \left[\sum_{j < k} (\Lambda_s^{jk} + i\Lambda_a^{jk}) \otimes (\Lambda_s^{jk} + i\Lambda_a^{jk}) + \sum_{j < k} (\Lambda_s^{jk} - i\Lambda_a^{jk}) \otimes (\Lambda_s^{jk} - i\Lambda_a^{jk}) \right] \\ &= \frac{1}{2d} \sum_{i < j} (\Lambda_s^{jk} \otimes \Lambda_s^{jk} - \Lambda_a^{jk} \otimes \Lambda_a^{jk}). \end{aligned} \quad (2.66)$$

The calculations for the GGB decomposition of term B are a bit more involved and are presented in Appendix A.2. We obtain

$$B = \frac{1}{2d} \sum_{m=1}^{d-1} \Lambda^m \otimes \Lambda^m + \frac{1}{d^2} \mathbb{1}_d \otimes \mathbb{1}_d. \quad (2.67)$$

Thus all together for the state $|\phi_+^d\rangle\langle\phi_+^d|$ we find the GGB Bloch decomposition

$$|\phi_+^d\rangle\langle\phi_+^d| = \frac{1}{d^2} \mathbb{1}_d \otimes \mathbb{1}_d + \frac{1}{2d} \Lambda, \quad (2.68)$$

where we defined

$$\Lambda = \sum_{i < j} \Lambda_s^{jk} \otimes \Lambda_s^{jk} - \sum_{i < j} \Lambda_a^{jk} \otimes \Lambda_a^{jk} + \sum_{m=1}^{d-1} \Lambda^m \otimes \Lambda^m. \quad (2.69)$$

Expansion into POB. To find the Bloch decomposition of $|\phi_+^d\rangle\langle\phi_+^d|$ in the polarization operator basis we use the standard operator decomposition of Lemma 2.2 and the sum rule for the Clebsch-Gordan coefficients [127]

$$\sum_{\alpha, \gamma} C_{a\alpha, b\beta}^{c\gamma} C_{a\alpha, b'\beta'}^{c\gamma} = \frac{2c+1}{2b+1} \delta_{bb'} \delta_{\beta\beta'}. \quad (2.70)$$

2. Bloch decompositions beyond qubits

We obtain

$$\begin{aligned}
|\phi_+^d\rangle\langle\phi_+^d| &= \frac{1}{d} \sum_{i,j=1}^d |i\rangle\langle j| \otimes |i\rangle\langle j| \\
&= \frac{1}{d} \sum_{L,L'} \frac{\sqrt{(2L+1)(2L'+1)}}{2s+1} \left(\sum_{i,j} C_{sm_j,LM}^{sm_i} C_{sm_j,L'M}^{sm_i} \right) T_{LM} \otimes T_{L'M} \\
&= \frac{1}{d} \sum_{L,L'} \frac{\sqrt{(2L+1)(2L'+1)}}{2L+1} \delta_{L,L'} T_{LM} \otimes T_{L'M} \\
&= \frac{1}{d} \sum_L T_{LM} \otimes T_{LM}. \tag{2.71}
\end{aligned}$$

We separate the term with the identity operator (recall Eq. (2.35)) in correspondence with Eq. (2.55), which yields

$$|\phi_+^d\rangle\langle\phi_+^d| = \frac{1}{d^2} \mathbb{1} \otimes \mathbb{1} + \frac{1}{d} T, \tag{2.72}$$

with

$$T := \sum_{L,M \neq 0,0} T_{LM} \otimes T_{LM}. \tag{2.73}$$

Expansion into WOB. Finally we obtain the WOB expansion of $|\phi_+^d\rangle\langle\phi_+^d|$ with the WOB standard operator decomposition of Lemma 2.3 (see also Ref. [96] for an alternative derivation),

$$\begin{aligned}
|\phi_+^d\rangle\langle\phi_+^d| &= \frac{1}{d} \sum_{j,k=1}^d |j\rangle\langle k| \otimes |j\rangle\langle k| \\
&= \frac{1}{d^3} \sum_{j,k=0}^{d-1} \sum_{l,l'=0}^{d-1} e^{-\frac{2\pi i}{d} j(l+l')} U_{l(k-j) \bmod d} \otimes U_{l'(k-j) \bmod d} \\
&= \frac{1}{d^3} \sum_{m,k=0}^{d-1} \sum_{l,l'=0}^{d-1} e^{-\frac{2\pi i}{d} (k-m)(l+l')} U_{lm} \otimes U_{l'm} \\
&= \frac{1}{d^2} \left(\sum_m U_{0m} \otimes U_{0m} + \sum_m \sum_{l,l'; l+l'=d} U_{lm} \otimes U_{l'm} \right) \\
&\quad + \frac{1}{d^3} \sum_m \sum_{l,l'; l,l' \neq 0,0; l+l' \neq d} \left(\sum_k e^{-\frac{2\pi i}{d} (k-m)(l+l')} \right) U_{lm} \otimes U_{l'm}. \tag{2.74}
\end{aligned}$$

The last term in Eq. (2.74) vanishes due to relation (2.50). Identifying $U_{00} = \mathbb{1}_d$ and using a comfortable notation with negative values of the index l , which have to be considered as *mod d*, we gain the WOB Bloch decomposition

$$|\phi_+^d\rangle\langle\phi_+^d| = \frac{1}{d^2} \mathbb{1} \otimes \mathbb{1} + \frac{1}{d^2} U, \quad (l, m) \neq (0, 0), \tag{2.75}$$

where

$$U := \sum_{l,m=0}^{d-1} U_{lm} \otimes U_{-lm}, \quad (l, m) \neq (0, 0). \quad (2.76)$$

2.8. Summary and conclusion

In this chapter we present three operator bases that are appropriate for Bloch decompositions of operators and states, the *generalized Gell-Mann operator basis* (GGB), the *polarization operator basis* (POB), and the *Weyl operator basis* (WOB). We give a method to derive a decomposition of arbitrary operators and states for general dimensions via the decomposition of standard operators, which we explicitly provide for the three bases. By the example of the decomposition of the maximally entangled two-qudit states we illustrate the application of the method.

By investigating the three presented bases we conclude that there is no unique way to generalize the Pauli operator basis for qubits. The main reason is the fact that the Pauli operators are both unitary *and* Hermitian, whereas there does not seem to be an operator basis for higher dimensions that reveals these two properties at once. Hence for different intentions different operator bases should be used. The generalized Gell-Mann operators are Hermitian, and thus useful with respect to experimental applications, as Hermitian operators are observables (see also Sec. 3.6). They are, however, not unitary. The polarization operators are neither Hermitian nor unitary, but calculations of decompositions can be performed quicker than with the generalized Gell-Mann operators, if the relations for the Clebsch-Gordan coefficients are known, respectively. The Weyl operators are not Hermitian but unitary, which has the advantage that one can use them to construct a basis of maximally entangled vector states, and then easily find decompositions of mixtures of these states (see Sec. 3.5.2 in this context). The disadvantage of non-Hermiticity is, however, that the decomposition coefficients (and hence also the Bloch vectors) are in general complex numbers, and thus a direct geometrical interpretation cannot be done in the same straightforward way as in the qubit case.

In the presented example of the decomposition of the maximally entangled two-qudit state, the result could be obtained quicker and easier with the POB and the WOB, whereas the calculations were lengthy for the GGB, due to the rather complicated definition of the diagonal generalized Gell-Mann operators. On the whole the definition of the POB and the WOB is more compact and better arranged than that of the GGB, which simplifies application for these two bases. In the literature, however, the predominantly used basis is the GGB.

3. Geometric entanglement detection

3.1. Introduction

In this chapter we present geometric methods to detect entanglement. In particular, we construct *geometric entanglement witnesses* that bear the advantage that the corresponding hyperplanes in Hilbert-Schmidt space can be directly related to a Euclidean geometry representation. First constructions of this kind were introduced in Refs. [102, 25]. The mathematical application is simplified by the Bloch decompositions of operators and states that we have provided in Chapter 2 and are extended here to identify operators as entanglement witnesses (see Corollary 3.2 and Lemma 3.1). We show how to use geometric entanglement witnesses to detect PPT entangled (bound entangled) states and how to identify separable states by using optimal geometric entanglement witnesses. This is attained by shifting the witnesses along parameterized lines of states (see Proposition 3.1). Two main methods are explained in detail: the *outside-in* shift and the *inside-out* shift. The outside-in shift is used for detecting (bound) entangled states, whereas with the inside-out shift we can construct the shape of the set of separable states for convex families of states.

Additionally, we use the decomposition into the generalized Gell-Mann matrices basis to derive a further decomposition into measurable observables constructed with spin-1 operators. This decomposition is intended to simplify experimental application of entanglement witnesses for two-qutrit states. An example for the optimal witness detecting the entangled isotropic two-qutrit states is presented.

The chapter is organized as follows: In Sec. 3.2 we briefly discuss entanglement detection for vector states. In Sec. 3.3 we review three important entanglement criteria for mixed states: the PPT criterion [100, 62], the realignment criterion [109, 34], and the entanglement witness criterion [62, 119]. In Sec. 3.4 we formulate Corollary 3.2 and Lemma 3.1 for the identification of operators as entanglement witnesses using Bloch decompositions. In Sec. 3.5 we define geometric operators and the related geometrical entanglement witnesses and present the mentioned outside-in and inside-out shift methods. Furthermore we give an application example of these two methods for a three-parameter family of two-qutrit states, for which we determine the entanglement properties (i.e. the regions of NPT entangled, PPT entangled, and separable states). Finally, in Sec. 3.6 we show how to decompose entanglement witnesses into observables constructed with spin-1 operators and give an example of the witness for the isotropic two-qutrit

states. In Sec. 3.7 final conclusions are drawn.

The chapter is mainly based on Refs. [23, 22, 83, 24]:

- Reinhold A. Bertlmann and Philipp Krammer
Geometric entanglement witnesses and bound entanglement
Phys. Rev. A **77**, 024303 (2008)
- Reinhold A. Bertlmann and Philipp Krammer
Bound entanglement in the set of Bell-state mixtures of two qutrits
Phys. Rev. A **78**, 014303 (2008)
- Philipp Krammer
Characterizing entanglement with geometric entanglement witnesses
J. Phys. A: Math. Theor. **42**, 065305 (2009)
- Reinhold A. Bertlmann and Philipp Krammer
Entanglement witnesses and geometry of entanglement of two-qutrit states
Ann. Phys. **324**, 1388 (2009)

3.2. Vector states

For a vector state $|\psi\rangle$ or, equivalently, the corresponding density operator $|\psi\rangle\langle\psi|$, we can easily and operationally decide whether it is entangled or not, for an arbitrary dimension of the Hilbert space. In Definition 1.2 we defined an entangled vector state as a vector state that cannot be written as a product vector state $|\psi_A\rangle \otimes |\psi_B\rangle$. Given a vector state $|\psi\rangle$ this might not always be possible to decide at first sight, since it could be given by several product terms, and in general it is not trivial to find the particular basis in which we can write it as only one product term. Consider in this respect, e.g., the vector state

$$|\tilde{\psi}\rangle = \frac{1}{2} (|00\rangle - |11\rangle + |10\rangle - |01\rangle) . \quad (3.1)$$

It can be written as

$$|\tilde{\psi}\rangle = |+\rangle \otimes |-\rangle , \quad (3.2)$$

with $|+\rangle = 1/\sqrt{2}(|0\rangle + |1\rangle)$ and $|-\rangle = 1/\sqrt{2}(|0\rangle - |1\rangle)$, but this is maybe not straightforward to see from Eq. 3.1.

We can take, however, advantage of the density operator formalism: The corresponding pure density operator to a vector state $|\psi\rangle$ is the projector $|\psi\rangle\langle\psi|$. For a product vector state the reduced density operators ρ^A and ρ^B are the pure states $|\psi^A\rangle\langle\psi^A|$ and $|\psi^B\rangle\langle\psi^B|$. Thus we can state the following theorem:

Theorem 3.1. *The state $|\psi\rangle\langle\psi|$ is entangled if and only if the reduced density operators are pure states.*

Confirming the purity of one reduced density operator is enough, as the reduced density operator for the other subsystem has to be pure as well, since the whole state is a pure state. Remember that a state ρ is pure if and only if it has the property $\text{Tr}\rho = 1$, or, equivalently, $\rho^2 = \rho$, or $R(\rho) = 1$, where $R(\rho)$ is the rank of the density matrix, i.e. the number of its non-vanishing eigenvalues. Furthermore, we call a vector state *maximally entangled* if the reduced density matrix of the lower dimensional system is the maximally mixed state $1/\min\{d_A, d_B\}\mathbb{1}$. It is “maximally” entangled because the reduced density matrix is “maximally” far away from being pure. A consistent method to quantify the entanglement of pure states is provided by the *entropy measure* of entanglement and is given in Refs. [17, 14].

Examples. As an example let us first consider the vector state $|\tilde{\psi}\rangle$ of Eq. (3.1). The reduced density operator ρ^A (see Definition 1.4) of $|\tilde{\psi}\rangle\langle\tilde{\psi}|$ is

$$\rho^A = \frac{1}{2} (|0\rangle\langle 0| + |1\rangle\langle 1| + |1\rangle\langle 0| + |0\rangle\langle 1|) , \quad (3.3)$$

which is a pure state and hence $|\tilde{\psi}\rangle$ is not entangled.

In a second example we want to determine the entanglement properties of the two-qubit Bell state $|\psi^-\rangle$ (1.29). It has the reduced density operators

$$\rho_A = \rho_B = \frac{1}{2} (|0\rangle\langle 0| + |1\rangle\langle 1|) = \frac{1}{2}\mathbb{1}_2 , \quad (3.4)$$

which is the maximally mixed state. Therefore $|\psi^-\rangle$ is entangled, in particular it is also maximally entangled.

3.3. Density operators

The definition of entangled density operators (states) is given in Definition 5.2. It implies that in order to find out whether a given state is entangled or separable, we have to know if it can be written in the form of a separable state (1.33). This mathematical problem is known as the separability problem. So far no general solution has been found, apart from the case of pure states, where the separable states are uncorrelated pure product states; a method for entanglement detection in this case is given in the previous section. In the case of mixed states ρ (with $\text{Tr}\rho^2 < 1$) there is no *operational* method to detect the entanglement of any state on an *arbitrary dimensional* Hilbert space. This problem is known as the *separability problem*.

In order to classify existing criteria for separability or entanglement, the following terminology is used: We say a criterion is *necessary* for separability if it is satisfied by any separable state. Therefore a violation of a necessary separability criterion detects the entanglement of a state with certainty and hence it implies a *sufficient* entanglement criterion (when negating the involved condition). States

that satisfy the necessary separability criterion can be separable or entangled. A sufficient separability criterion on the other hand guarantees that a state is separable for sure if it satisfies the criterion, but can be entangled or separable if the criterion is violated (and so implies a necessary criterion for entanglement). Therefore only a necessary *and* sufficient criterion for separability can give a definite answer for any state: If it is violated, the state is entangled, if it is satisfied, the state is separable¹. Apart from the classification into necessary and sufficient criteria, we classify the criteria according to their employability as *operational* and *non-operational* [30]. An operational criterion gives a “recipe” that has to be performed on the state in question in order to decide if it satisfies the criterion or not, and can be applied to any state. A non-operational criterion, on the other hand, is characterized by a lack of a general recipe, it provides a mathematical necessity, it is in general difficult to find out if it is satisfied by a given state, but *in principle* possible.

The criteria presented in the forthcoming sections help in detecting the entanglement of mixed states. Of course, they can be also used for entanglement detection of pure states, as they can be applied for all density operators.

We call an entanglement criterion C1 *stronger* than a criterion C2, if C1 detects all the entangled states that C2 detects, and even more than those states. C2 is then called *weaker* than C1. Two or more entanglement criteria are called *equal*, if they detect the same entangled states. If they detect different sets of entangled states that do not coincide, but might have overlaps, then the criteria are neither stronger nor weaker with respect to each other.

3.3.1. The PPT criterion

A simple and strong entanglement criterion is the *PPT criterion* [100, 62]. To understand it, we first need to introduce the partial transposition. The transposition T is just the standard matrix transposition, i.e. a map that maps a matrix onto its transpose. Applied on a one-partite state ρ it is defined as

$$\rho^T := T(\rho) = \sum_{i,j} \rho_{ij} (|i\rangle\langle j|)^T = \sum_{i,j} \rho_{ij} |j\rangle\langle i|. \quad (3.5)$$

The matrix elements are given by

$$\langle i|\rho^T|j\rangle = \langle j|\rho|i\rangle. \quad (3.6)$$

Definition 3.1. The partial transposition $\mathbb{1} \otimes T$ of a bipartite state is defined as

$$\rho^\Gamma := (\mathbb{1} \otimes T)(\rho) = \sum_{i,j,k,l} \rho_{ikjl} |i\rangle\langle j| \otimes (|k\rangle\langle l|)^T = \sum_{i,j,k,l} \rho_{ikjl} |i\rangle\langle j| \otimes |l\rangle\langle k|, \quad (3.7)$$

and the matrix elements are given by

$$\langle ik|\rho^\Gamma|jl\rangle = \langle il|\rho|jk\rangle. \quad (3.8)$$

¹Or: If we consider the corresponding necessary and sufficient entanglement criterion, then of course the state is entangled if it satisfies the criterion and separable if it violates it.

The partial transposition therefore is a map where only one subsystem applies transposition, while the other one does not. Here it is irrelevant if Alice or Bob applies the transposition, it could also be defined as $T \otimes \mathbb{1}$. With Definition 3.1 at hand, the following useful theorem can be formulated:

Theorem 3.2 (PPT criterion [100]). *A separable state σ (1.33) stays positive under partial transposition (PPT).*

Proof. Applying the partial transposition on a separable state (1.33), we get $\sigma^\Gamma = \sum_i p_i \rho_i^A \otimes (\rho_i^B)^T$. The transposition of the states ρ_i^B does not affect the positivity condition, $(\rho_i^B)^T \geq 0$. Thus the whole separable state is still a positive operator after partial transposition. \square

Remark 3.1. In Ref. [62] the PPT criterion was proven to be a necessary and sufficient separability criterion for states of 2×2 and 2×3 dimensional systems.

For states on Hilbert spaces of this low dimensions, e.g. two qubits, we can always decide if it is entangled or separable – hence for these cases the separability problem is solved. In Ref. [100] Peres provided the necessary PPT criterion, that of course is valid for bipartite systems of arbitrary dimension, and the sufficiency for low dimensions was added by the Horodeckis in Ref. [62]. The criterion is therefore also referred to as the Peres-Horodecki criterion.

States that are positive under partial transposition are called PPT states, states that are negative under partial transposition are called NPT states. All NPT states are entangled, PPT states can be separable or entangled. As already stated in Sec. 1.4, entangled PPT states are *bound entangled*, i.e. not distillable. Thus one can find bound entangled states with criteria that are stronger than the PPT criterion. It is still an open question if there exist bound entangled NPT states, although there are strong implications that such states exist [44, 42].

3.3.2. The realignment criterion

An entanglement criterion that has structural similarities to the PPT criterion is the *realignment criterion* (or *greatest cross norm criterion*) [110, 109, 111, 34]. First, we have to define the definition of the realignment operation on a density operator [34, 69]:

Definition 3.2. The realignment map R of a bipartite state ρ is defined as

$$\rho_R := R(\rho) = \sum_{i,j,k,l} \rho_{ikjl} (|i\rangle\langle j| \otimes |k\rangle\langle l|)_R = \sum_{i,j,k,l} \rho_{ikjl} |i\rangle\langle k| \otimes |j\rangle\langle l|, \quad (3.9)$$

and the matrix elements are given by

$$\langle ik|\rho_R|jl\rangle = \langle ij|\rho|kl\rangle. \quad (3.10)$$

The realignment criterion is formulated as follows (in this form it can be found in Ref. [69], it was introduced and proven in Ref. [109] as a computable criterion and formulated and proven in terms of matrix operations in [34]):

Theorem 3.3 (Realignment criterion [109, 34]). *For a separable state σ the sum of the singular values s_i of the realigned operator σ_R has to be smaller or equal to 1,*

$$\sum_i s_i = \text{Tr} \sqrt{\sigma_R^\dagger \sigma_R} \leq 1. \quad (3.11)$$

Thus, if a state ρ violates the criterion, it has to be entangled, but both separable and entangled states can satisfy it. The realignment criterion is neither weaker nor stronger than the PPT criterion, meaning that it detects some entangled states that the PPT criterion does not, and vice versa. Thus an application of both criteria is easy to perform and allows a detection of many entangled states, both free and bound entangled, but they do not constitute a necessary and sufficient criterion together, since there exist PPT entangled states that are not detected by the realignment criterion [34].

3.3.3. Entanglement witnesses

Entanglement witnesses provide a simple and useful necessary and sufficient entanglement criterion. It is, however, nonoperational.

Theorem 3.4 (Entanglement Witness Criterion (EWC) [62, 119, 120]). *A state $\rho \in \mathcal{A}^D$ is entangled if and only if there exists a Hermitian operator W such that*

$$\text{Tr} \rho W = \langle \rho, W \rangle < 0 \text{ and} \quad (3.12)$$

$$\text{Tr} \sigma W = \langle \sigma, W \rangle \geq 0 \quad \forall \sigma \in \mathcal{S}, \quad (3.13)$$

where \mathcal{S} is the set of all separable states. An operator W that satisfies the above conditions is called “entanglement witness”.

We call inequality (3.12) “entanglement condition” and inequality (3.13) “separability condition”. If for a witness W_{opt} a separable state $\tilde{\sigma}$ exists for which $\text{Tr} \tilde{\sigma} W_{\text{opt}} = 0$, then W_{opt} is called an *optimal* entanglement witness.² It is closest to the set of separable states and thus detects more entangled states than not optimal witnesses.

The EWC is a consequence of the Hahn-Banach theorem of functional analysis. It geometrically corresponds to the fact that an element of a Banach space can always be separated by a hyperplane from a convex and compact subset that does not contain the element (see, e.g., Ref. [107] for details on the Hahn-Banach theorem). This geometrical connection is illustrated in Fig. 3.1.

²An alternative definition of optimal entanglement witnesses that is similar to the one presented here but mathematically more elaborate can be found in [88].

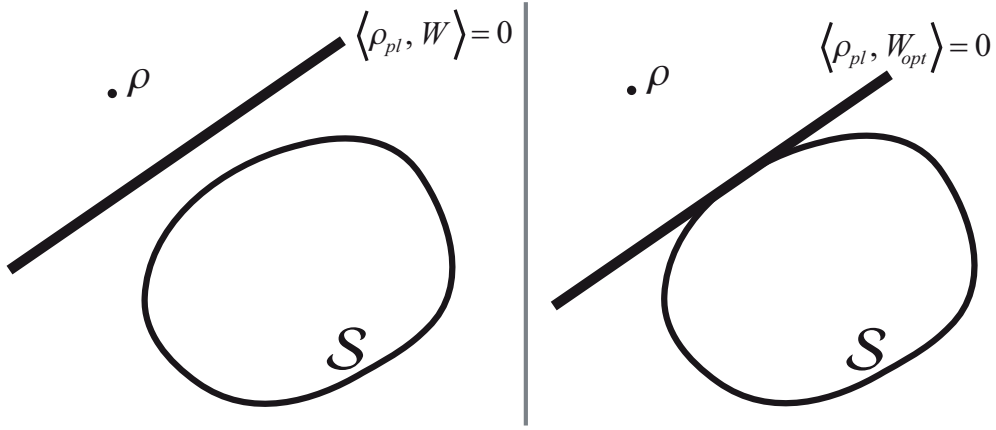


Figure 3.1.: Graphic illustration of the EWC. The left picture displays a non-optimal, the right picture an optimal entanglement witness as a hyperplane that includes the states ρ_{pl} and separates the entangled state ρ from the set of separable states \mathcal{S} .

Although it is intuitive and simple, the EWC is not easy to implement given an arbitrary state ρ , since in general it is difficult to find a suitable witness that satisfies Eq. (3.13), and even more difficult to state that there does not exist any witness for this state, which would imply separability. Nevertheless the criterion plays an important role in the theoretical understanding of entanglement, and has the advantage that a witness W corresponds to a physical observable that can be implemented in experiments, and therefore allows a detection of entanglement without performing a full tomography of the state [52, 53, 28, 7, 2, 114]. Various construction methods of entanglement witnesses can be found, e.g., in Refs. [88, 89, 31, 75, 72, 74, 35]. In Sec. 3.5 a geometric construction of entanglement witnesses is investigated in detail.

3.4. Bloch decompositions and entanglement witnesses

The cumbersome task in the application of entanglement witnesses is the verification of the separability condition (3.13). In this context it turns out to be helpful to consider Bloch decompositions of operators, as introduced in Sec. 2.3. First, let us reformulate and, for our purposes, simplify the separability condition (3.13) of the EWC (Theorem 3.4):

Corollary 3.1. *An operator $C \in \mathcal{A}^D$ satisfies $\text{Tr}\sigma C \geq 0 \forall \sigma \in \mathcal{S}$ if and only if $\text{Tr}\sigma_p C \geq 0$ for all pure product states $\sigma_p := \rho_A \otimes \rho_B$.*

Proof. If we have $\text{Tr}\sigma C \geq 0 \forall \sigma \in \mathcal{S}$ then of course also $\text{Tr}\sigma_p C \geq 0$ since the pure product states σ_p are separable states as well. Consider the form (1.35) of a separable state. If $\text{Tr}\sigma_p C \geq 0$, it follows that $\text{Tr}\sigma C = \text{Tr} \sum_i p_i \sigma_p^i C = \sum_i p_i \text{Tr}\sigma_p^i C \geq 0$ since $p_i \geq 0$. \square

3. Geometric entanglement detection

At first sight Corollary 3.1 may appear redundant, but it bears the advantage that in order to check if a given operator satisfies the separability condition (3.13), we do not have to check all separable states but consider pure product states only, which implies a decrease in effort. Purity of the states is not essential, but is more convenient for parameterizations.

For an arbitrary operator basis we use the Bloch decomposition (2.55) to write a Hermitian operator $C \in \mathcal{A}^D$ as

$$\begin{aligned}
C &= \delta \left(\mu \mathbb{1}_{d_A} \otimes \mathbb{1}_{d_B} \right. \\
&\quad \left. + \sum_{i=0}^{d_A-1} \tilde{a}_i A_i \otimes \mathbb{1}_{d_B} + \sum_{j=0}^{d_B-1} \tilde{b}_j \mathbb{1}_{d_A} \otimes B_j + \sum_{i,j} \tilde{c}_{ij} A_i \otimes B_j \right), \\
\mu &:= \sqrt{\frac{(d_A-1)(d_B-1)N_A N_B}{d_A d_B}}, \quad \delta \in \mathbb{R}^+.
\end{aligned} \tag{3.14}$$

The condition of Hermiticity, $C^\dagger = C$, allows only real values for the overall coefficient δ , its value is insignificant for the forthcoming arguments, but should be positive: If a Hermitian operator C_{pre} has a negative constant δ in the decomposition (3.14), we “make” it positive by considering $C = -C_{pre}$.

For $d_A = d_B = d$ we use Eq. (2.59) to get the singular value optimized (SVO) form,

$$\begin{aligned}
C &= \delta \left(\tilde{\mu} \mathbb{1}_d \otimes \mathbb{1}_d \right. \\
&\quad \left. + \sum_{i=0}^{d-1} \tilde{r}_i D_i^A \otimes \mathbb{1}_d + \sum_{j=0}^{d-1} \tilde{t}_j \mathbb{1}_d \otimes D_j^B + \sum_i \tilde{s}_i D_i^A \otimes D_i^B \right), \\
\tilde{\mu} &:= \frac{d-1}{d} \sqrt{N_A N_B},
\end{aligned} \tag{3.15}$$

and obtain for the expectation value with product states σ_p from Eqs. (2.56) and (3.14) (we use σ_p^\dagger in order to conveniently utilize the orthogonality condition of the operator bases (see Eq. (2.7)))

$$\begin{aligned}
\text{Tr} \sigma_p^\dagger C &= \delta \mu \left(1 + \sqrt{\frac{d_B}{N_B(d_B-1)}} \sum_i \tilde{a}_i n_i^* + \sqrt{\frac{d_A}{N_A(d_A-1)}} \sum_j \tilde{b}_j m_j^* \right. \\
&\quad \left. + \sum_{i,j} \tilde{c}_{ij} n_i^* m_j^* \right),
\end{aligned} \tag{3.16}$$

which simplifies for $d_A = d_B = d$ to (using Eqs. (2.60) and (3.15))

$$\begin{aligned}
\text{Tr} \sigma_p^\dagger C &= \delta \tilde{\mu} \left(1 + \sqrt{\frac{d}{N_B(d-1)}} \sum_i \tilde{r}_i \bar{n}_i^* + \sqrt{\frac{d}{N_A(d-1)}} \sum_j \tilde{t}_j \bar{m}_j^* \right. \\
&\quad \left. + \sum_i \tilde{s}_i \bar{n}_i^* \bar{m}_i^* \right).
\end{aligned} \tag{3.17}$$

Using the above expressions for the expectation values we obtain a condition for $\text{Tr}C\sigma_p \geq 0$ (of Corollary 3.1) in terms of Bloch decompositions:

Corollary 3.2. *Given a decomposition (3.14) of an operator C into an arbitrary operator basis, the expectation value for any product state (2.56) is positive or vanishes, $\text{Tr}C\sigma_p \geq 0$, if and only if*

$$S := \sqrt{\frac{d_B}{N_B(d_B - 1)}} \sum_i \tilde{a}_i n_i^* + \sqrt{\frac{d_A}{N_A(d_A - 1)}} \sum_j \tilde{b}_j m_j^* + \sum_{i,j} \tilde{c}_{ij} n_i^* m_j^* \geq -1 \quad (3.18)$$

for all Bloch vectors \vec{n}, \vec{m} . For equal dimensions of the subsystems, $d_A = d_B = d$, the condition (3.18) can be simplified to

$$S := \sqrt{\frac{d}{N_B(d - 1)}} \sum_i \tilde{r}_i \bar{n}_i^* + \sqrt{\frac{d}{N_A(d - 1)}} \sum_j \tilde{t}_j \bar{m}_j^* + \sum_i \tilde{s}_i \bar{n}_i^* \bar{m}_i^* \geq -1, \quad (3.19)$$

where we used the SVO form (2.59) of C .

Proof. The proof is evident from the expressions for the expectation values in Eqs. (3.16) and (3.17). \square

Remark 3.2. Consider the case when there also exists at least one state ρ for which $\text{Tr}C\rho < 0$. Then C is an entanglement witness if $S \geq -1$. Note that by stating ‘‘Bloch vector’’ we mean vectors \vec{n}, \vec{m} that correspond to states (i.e. $\rho_A \geq 0$ and $\rho_B \geq 0$ in Eq. (2.10)). For arbitrary dimensions d of the Hilbert space, an arbitrary vector $\vec{n} \in \mathbb{C}^{d^2-1}$ for which ρ has real eigenvalues does not always implicate $\rho \geq 0$, this is only true for $d = 2$, where the familiar matrix basis out of the Pauli matrices or rotations thereof is used.

Remark 3.3. It directly follows from Corollaries 3.1 and 3.2 that C is an optimal entanglement witness if and only if there exists a state ρ such that $\text{Tr}C\rho < 0$ and Bloch vectors \vec{n}, \vec{m} such that $S = -1$.

Remark 3.4. For operators C (3.14) with vanishing coefficients \tilde{a}_i, \tilde{b}_i , condition (3.18) reduces to

$$\sum_{i,j} \tilde{c}_{ij} n_i^* m_j^* \geq -1, \quad (3.20)$$

and (3.19) to

$$\sum_i \tilde{s}_i \bar{n}_i^* \bar{m}_i^* \geq -1. \quad (3.21)$$

This is for example the case if we consider geometric operators (see Sec. 3.5.2) constructed with states that are *locally maximally mixed*, which means their reduced density matrices are the maximally mixed states $(1/d_A)\mathbb{1}$ and $(1/d_B)\mathbb{1}$.

Lemma 3.1. For operators C (3.14) on a Hilbert space \mathcal{H} of equal dimensional subsystems, $d_A = d_B$, with vanishing coefficients \tilde{a}_i, \tilde{b}_i , the expectation value for product states is greater than or equal to zero, $\text{Tr}\sigma_p \geq 0$, if the singular values \tilde{s}_i of the correlation coefficient matrix \tilde{c}_{ij} are smaller or equal to one, $\tilde{s}_i \leq 1$.

Proof. With vanishing coefficients \tilde{a}_i, \tilde{b}_i , the term S in Eq. (3.18) reduces to $S = \sum_{i,j} \tilde{c}_{ij} n_i m_j$. For $d_A = d_B$ we can write the operator in SVO form, which gives $S = \sum_i \tilde{s}_i \tilde{n}_i^* \tilde{m}_i^*$. With the condition $s_i \leq 1$ and the Cauchy-Schwartz inequality we get

$$|S| = \left| \sum_i \tilde{s}_i \tilde{n}_i^* \tilde{m}_i^* \right| \leq \sum_i \tilde{s}_i |\tilde{n}_i^*| |\tilde{m}_i^*| \leq \sum_i |\tilde{n}_i^*| |\tilde{m}_i^*| \leq 1, \quad (3.22)$$

and thus $S \geq -1$. □

Remark 3.5. Note that Lemma 3.1 gives only a sufficient condition for satisfying the inequality $\text{Tr}\sigma_p \geq 0$. It is necessary for dimensions 2×2 only, since in this case any vectors \vec{n} and \vec{m} (2.56) correspond to states, see Remark 3.2, and with at least one singular value $s_i > 1$ one can easily construct Bloch vectors such that $S < -1$. For higher dimensions it is possible that some $s_i > 1$, and still there exist no Bloch vectors \vec{n} and \vec{m} (that provide $\rho \geq 0$) such that $S < -1$.

3.5. Geometric entanglement witnesses

3.5.1. Definitions and general methods

A possible method to construct entanglement witnesses are *geometric entanglement witnesses*. They bear the advantage that they can be constructed directly out of two states, where one of them is detected by the witness, if it is entangled. They are called *geometric* entanglement witnesses, since they can directly be related to hyperplanes in Hilbert-Schmidt space that are orthogonal to the “vector” between the two states from which they were constructed. Thus the witnesses have a direct geometrical representation as hyperplanes in the Euclidean representation of Hilbert-Schmidt space.

Let us start with the definition of a geometric operator, from which we can continue with defining a geometric entanglement witness.

Definition 3.3. A *geometric operator* $G \in \mathcal{A}^D$ is defined as

$$G := \rho_1 - \rho_2 - \langle \rho_1, \rho_1 - \rho_2 \rangle \mathbb{1}_D, \quad (3.23)$$

where ρ_1 and ρ_2 are arbitrary states in \mathcal{A}^D and $\rho_1 \neq \rho_2$.

The definition originates from the construction of entanglement witnesses in Refs. [102, 25], with the difference that in our definition the geometric operator

(3.23) does not yet have to be an entanglement witness. The construction (3.23) provides $\text{Tr}\rho_1 G = 0$ and $\text{Tr}\rho_2 G < 0$,

$$\begin{aligned}\text{Tr}\rho_1 G &= \langle \rho_1, G \rangle = \langle \rho_1 - \rho_1, \rho_1 - \rho_2 \rangle = 0, \\ \text{Tr}\rho_2 G &= \langle \rho_2, G \rangle = \langle \rho_2 - \rho_1, \rho_1 - \rho_2 \rangle = -\|\rho_1 - \rho_2\|^2 < 0.\end{aligned}\quad (3.24)$$

A geometric operator corresponds to a hyperplane in the Hilbert-Schmidt space \mathcal{A}^D that divides the whole state space into states ρ_n for which $\text{Tr}\rho_n G < 0$ and states ρ_p for which $\text{Tr}\rho_p G \geq 0$, see Ref [19]. The hyperplane is orthogonal to $\rho_1 - \rho_2$ since for all states ρ_G on the plane, i.e. that satisfy $\text{Tr}\rho_G G = 0$, the operator $\rho_1 - \rho_2$ is orthogonal to $\rho_G - \rho_1$ because $\text{Tr}\rho_G G = \langle \rho_G - \rho_1, \rho_1 - \rho_2 \rangle = 0$.

Definition 3.4. A *geometric entanglement witness (GEW)* W_G is a geometric operator that satisfies $\text{Tr}\sigma_p W_G \geq 0$ for all pure product states σ_p .

Due to its construction, a geometric entanglement witness (see also Refs. [102, 25, 103, 19]) has to witness at least the entanglement of ρ_2 . For arbitrary states ρ_2 it is easy to construct geometric operators G (Definition 3.3) that ensure $\text{Tr}\rho_2 G < 0$, but difficult to confirm that also $\text{Tr}\sigma_p G \geq 0$ for all pure product states, which would yield $G = W_G$. Nevertheless, due to their simple geometric construction, geometric operators provide useful tools to characterize entanglement, as we will see in the further sections of this paragraph.

To detect entanglement it is sufficient to consider geometric entanglement witnesses only:

Lemma 3.2. *Any entangled state is witnessed by a geometric entanglement witness.*

Proof. If ρ is entangled, then there exists a so-called *nearest separable state* σ_0 , i.e. the separable state for which the Hilbert-Schmidt distance (1.12) from ρ to the set of separable states \mathcal{S} is minimal, because \mathcal{S} is convex and compact. The corresponding geometric operator $\sigma_0 - \rho - \langle \sigma_0, \sigma_0 - \rho \rangle \mathbb{1}_D$ is an entanglement witness, since the corresponding hyperplane includes σ_0 , is orthogonal to $\sigma_0 - \rho$ and is therefore tangent to \mathcal{S} . For more details on nearest separable states and the related Hilbert-Schmidt measure of entanglement, see Sec. 4.2 and Refs. [142, 25, 19]. \square

Geometric entanglement witnesses bear the advantage that they can be “shifted” along lines of parameterized states.

Proposition 3.1 (Shift method). *If a geometric operator*

$$G_\lambda = \rho_\lambda - \rho - \langle \rho_\lambda, \rho_\lambda - \rho \rangle \mathbb{1}_D \quad (3.25)$$

with a parameterized family of states

$$\rho_\lambda := \lambda\rho + (1 - \lambda)\tilde{\rho}, \quad 0 \leq \lambda < 1, \quad \rho, \tilde{\rho} \in \mathcal{A}^D \quad (3.26)$$

is an entanglement witness in a parameter region $\lambda \in [\lambda_i, 1)$, i.e. if it satisfies $\text{Tr}\sigma_p G_\lambda \geq 0$ for all pure product states σ_p , then ρ_λ is entangled for $\lambda \in (\lambda_i, 1]$.

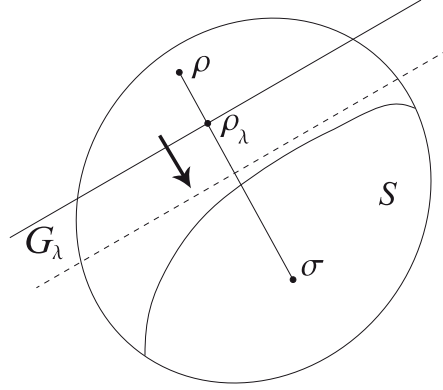


Figure 3.2.: Outside-in shift method. On the line between the entangled state ρ and the separable state σ one can detect more entangled states, e.g. bound entangled states, by shifting the geometric operator G_λ .

Proof. We consider states ρ_λ with $\lambda_i < \lambda \leq 1$ and the geometric entanglement witness $W_{\lambda_i} = \rho_{\lambda_i} - \rho - \langle \rho_{\lambda_i}, \rho_{\lambda_i} - \rho \rangle \mathbb{1}_D$. The expectation value in ρ_λ is

$$\begin{aligned} \text{Tr} \rho_\lambda W_{\lambda_i} &= \langle \rho_\lambda, W_{\lambda_i} \rangle = \langle \rho_\lambda - \rho_{\lambda_i}, \rho_{\lambda_i} - \rho \rangle \\ &= (\lambda_i - \lambda)(1 - \lambda_i) \langle \rho - \tilde{\rho}, \rho - \tilde{\rho} \rangle = (\lambda_i - \lambda)(1 - \lambda_i) \|\rho - \tilde{\rho}\|^2 < 0, \end{aligned} \quad (3.27)$$

hence the states ρ_λ with $\lambda_i < \lambda \leq 1$ are entangled. \square

An effective way to use the shift method of Proposition 3.1 is to identify $\tilde{\rho}$ in Eq. (3.26) with a separable state, and ρ with a state which is known to be entangled. There are two cases where this is of particular interest:

1. (*Outside-in shift.*) Starting from the entangled state ρ , we can detect further entangled states along the line in direction to the separable state. By proving that G_λ is an entanglement witness for a parameter region $\lambda_i \leq \lambda < 1$ (the case $\lambda = 1$ can be included with a suitable normalization of G_λ), one can infer that all states ρ_λ within this region are entangled. A reasonable choice for the separable state is the maximally mixed state $(1/D)\mathbb{1}$. In this way one can detect bound entangled states, for example if we choose a PPT entangled “starting state” ρ , then we are likely to find more bound entangled states along the parameterized line ρ_λ . The outside-in shift is illustrated in Fig. 3.2.
2. (*Inside-out shift.*) Another application of the shift method is the step-by-step construction of the convex set of separable states. Here one has to use optimal GEWs that correspond to hyperplanes tangent to the set of separable states. In the following we assume that we are given a specific convex subset of states for which we want to determine the entanglement properties, and that some separable states are known. From these we can construct a *kernel polytope* of separable states, i.e. the convex hull of the

known separable states. Then we assign geometric operators to hyperplanes tangent to the kernel polytope. For example, an operator corresponding to a plane that includes the line between two separable states can be constructed in the following way: Given two separable states σ_1 and σ_2 , the convex line between them is $\sigma_\mu = \mu\sigma_1 + (1 - \mu)\sigma_2$. Now we choose an entangled state ω , that of course lies outside the kernel polytope, such that there exists a μ_i with $\tilde{\sigma} = \sigma_{\mu_i}$ for which we have the orthogonality condition $\langle \sigma_1 - \sigma_2, \omega - \tilde{\sigma} \rangle = 0$. The geometric operator is then given by

$$G = \tilde{\sigma} - \omega - \langle \tilde{\sigma}, \tilde{\sigma} - \omega \rangle \mathbb{1}_D \quad (3.28)$$

and a shift operator G_λ between $\tilde{\sigma}$ and ω according to Eqs. (3.25) and (3.26). The construction of operators that correspond to boundary planes of the kernel polygon identified by more than two separable states is done similarly, using more orthogonality conditions and the convex hull between three states.

Once we assigned geometric operators to the boundary of the kernel polytope, we utilize Proposition 3.1 to “shift” the operators outside and survey the minimum of S in Eq. (3.18) or (3.19). At one point of the parameterized line (3.26) we obtain $S = -1$; the geometric operators become optimal geometric entanglement witnesses. In this way we can assemble the shape of the set of separable states for the considered set of states and distinguish it from the set of entangled states. It may likely be that we have an idea of the shape of the set of separable states that we got from applying necessary separability criteria. Then we can use the inside-out shift to verify or falsify that shape: The inside-out shifted geometric operators should correspond to optimal GEWs when they become tangent to the estimated shape. In this way we get vertices of a new polytope, whose boundary planes are shifted again. Thus we either verify the estimated shape of separable states, or, if a shifted plane is an optimal GEW before it is tangent to the shape, it is an enclosure of all separable states and also entangled ones. We require finite steps of this method if the estimated shape is a polygon, and (in principle) infinite steps if it is not a polygon, i.e. if it has a curved surface.

If we have no idea of a possible shape of the set of separable states, or if our estimation turned out to be wrong, we can use the inside-out shift to obtain at least a tight enclosure polytope. It is a polytope that encloses all separable states but might also contain some entangled states, it can be obtained by applying the shift to more than one kernel polytope. Both situations are sketched in Fig. 3.3.

The difficult part of Proposition 3.1 is to prove that G_λ is an entanglement witness, in particular the verification of the separability condition (3.13). To accomplish this we can efficiently use Corollary 3.2 and Lemma 3.1 derived from Bloch decompositions, which will be demonstrated by the example of the next section.

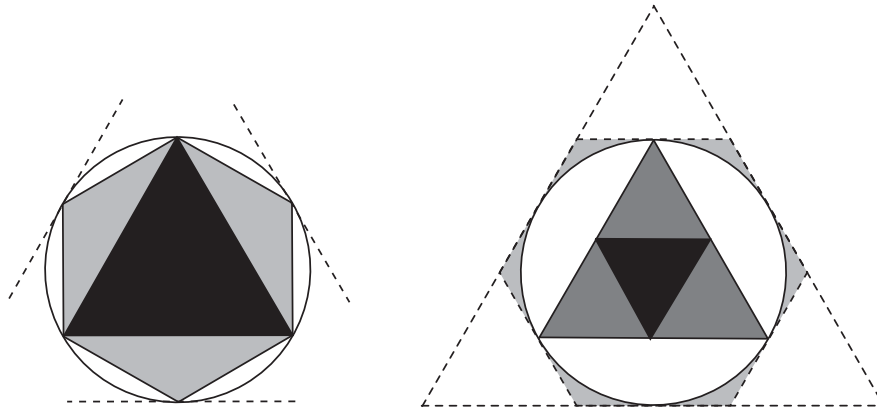


Figure 3.3.: Left: Sketch of the inside-out shift with an estimate of the shape of separable states, which in this case coincides with the true set of separable states, pictured by the circle. We start with a kernel polytope (black triangle) and shift the boundary planes outside until they become optimal GEWs, which are tangents to the circle (dashed lines). In this way we can draw a new polytope (hexagon, grey). In the next steps (not illustrated) the boundaries of the new polytope are shifted and we gain a new polytope, and so on. In this way we reconstruct the circle shape. Right: Sketch of the inside-out shift where we do not rely on an estimate of the shape of separable states. The true set of separable states is again pictured by a circle. Here we get a first enclosure polytope (biggest triangle with dashed lines), by shifting the boundaries of a first kernel polytope outside (dark grey triangle). A tighter enclosure polytope (hexagon with dashed lines) is obtained by shifting the boundaries of a second kernel polytope (small black triangle) outside. The light grey areas mark states inside the enclosure polytope that are not separable and thus account for the deviation of the enclosure polytope from the true set of separable states.

3.5.2. Entanglement properties of a family of two-qudit states

Before we show the explicit example, it is useful to give a construction method of a basis of maximally entangled vector states for two qudits, i.e. vector states of the Hilbert space $\mathcal{H}^d \otimes \mathcal{H}^d$. The method uses local unitary operations on one subsystem, in which way we can construct a basis of d^2 maximally entangled vector states $|\phi_i\rangle$ [134, 139],

$$|\phi_i\rangle = V_i \otimes \mathbb{1}_d |\phi_+^d\rangle, \quad i = 0, 1, 2, \dots, d^2 - 1, \quad (3.29)$$

where $\{V_i\}$ is a unitary and orthogonal operator basis of \mathcal{A}^d , and $V_0 = \mathbb{1}_d$. The vector state $|\phi_+^d\rangle$ is the usual maximally entangled two-qudit state given in Eq. (2.61). Note that it is crucial to use unitary operators in Eq. (3.29), since only in this case we obtain maximally entangled *and* orthogonal vector states. For the unitary operator basis $\{V_i\}$ we choose, e.g., the Weyl operator basis (see Sec. 2.6). In this way we construct the so-called *two-qudit Bell states*

$$|\phi_{nk}\rangle := (U_{nk} \otimes \mathbb{1}_d) |\phi_+^d\rangle, \quad n, k = 0, 1, \dots, d - 1, \quad (3.30)$$

which can be seen as a higher dimensional generalization of the well known two-qubit Bell states. The projectors onto these generalized Bell states are given by

$$P_{nk} := (U_{nk} \otimes \mathbb{1}_d) |\phi_+^d\rangle \langle \phi_+^d| (U_{nk}^\dagger \otimes \mathbb{1}). \quad (3.31)$$

Note that the two-qudit Bell states (3.30) have a practical importance in quantum communication: In the teleportation protocol of Ref. [13] the states (3.31) serve as the higher dimensional generalization of the two-qubit Bell states and the Weyl operators U_{nm} are the analogue of the Pauli operators, they correspond to the operators Bob has to apply at the end of the protocol in order to obtain the teleported state. A construction of the type (3.29) can in general be done with any unitary operators that form a matrix basis of the Hilbert-Schmidt space, obtaining other bases of orthogonal maximally entangled states.

An interesting set of states is the *magic simplex* of two-qudit states [10, 11, 12]. It is the set of all states that are mixtures of Bell states P_{nm} ,

$$\mathcal{W} := \left\{ \sum_{n,m=0}^{d-1} q_{nm} P_{nm} \mid q_{nm} \geq 0, \sum_{n,m} q_{nm} = 1 \right\}. \quad (3.32)$$

The reduced density operators of states that are elements of the magic simplex are the maximally mixed states $1/d \mathbb{1}_d$. Nevertheless, not all two-qudit states with maximally mixed reduced density operators are elements of the magic simplex, apart from dimension 2×2 , where all locally maximally mixed states are included in the tetrahedron of all Bell state mixtures [12]. The magic simplex has a high symmetry in the phase space of the coefficients nm , for a detailed discussion see Refs. [10, 11].

3. Geometric entanglement detection

The Bell states P_{nm} (3.31) can be expressed with Weyl operators as (where the indices have to be taken mod d)

$$P_{nk} = \frac{1}{d^2} \sum_{m,l=0}^{d-1} e^{\frac{2\pi i}{d}(kl-nm)} U_{lm} \otimes U_{-lm} = \frac{1}{d^2} \sum_{l,m=0}^{d-1} c_{lm} U_{lm} \otimes U_{-lm}. \quad (3.33)$$

Obviously the Bloch vectors corresponding to the Bell states have a diagonal but in general complex coefficient matrix (c_{ij}) , where i counts the different combinations of lm and j those of kn , and $c_{ii} := c_{lm}$.

A subset of the magic simplex of two-qutrit states (dimension 3×3) that reveals interesting entanglement characteristics is the three-parameter family

$$\rho_{\alpha,\beta,\gamma} := \frac{1 - \alpha - \beta - \gamma}{9} \mathbb{1}_9 + \alpha P_{00} + \frac{\beta}{2} (P_{10} + P_{20}) + \frac{\gamma}{3} (P_{01} + P_{11} + P_{21}), \quad (3.34)$$

where we write $\mathbb{1}_9$ for $\mathbb{1}_3 \otimes \mathbb{1}_3$ and the parameters are constrained by the positivity requirement $\rho_{\alpha,\beta,\gamma} \geq 0$,

$$\begin{aligned} \alpha &\leq \frac{7}{2}\beta + 1 - \gamma, & \alpha &\leq -\beta + 1 - \gamma, \\ \alpha &\leq -\beta + 1 + 2\gamma, & \alpha &\geq \frac{\beta}{8} - \frac{1}{8} + \frac{1}{8}\gamma. \end{aligned} \quad (3.35)$$

The family of states (3.34) contains a one-parameter family of states that have three entanglement properties; they can be separable, PPT entangled and NPT entangled. We call them Horodecki states ρ_b [68],

$$\rho_b = \frac{2}{7} |\phi_+^3\rangle \langle \phi_+^3| + \frac{b}{7} \sigma_+ + \frac{5-b}{7} \sigma_-, \quad 0 \leq b \leq 5, \quad (3.36)$$

$$\sigma_+ = \frac{1}{3} (|01\rangle \langle 01| + |12\rangle \langle 12| + |20\rangle \langle 20|), \quad (3.37)$$

$$\sigma_- = \frac{1}{3} (|10\rangle \langle 10| + |21\rangle \langle 21| + |02\rangle \langle 02|). \quad (3.38)$$

According to the parametrization of Eq. (3.34), the Horodecki states can be written as

$$\rho_b := \rho_{\alpha,\beta,\gamma} \quad \text{with} \quad \alpha = \frac{6-b}{21}, \quad \beta = -\frac{2b}{21}, \quad \gamma = \frac{5-2b}{7}. \quad (3.39)$$

Using the PPT criterion (Theorem 3.2) we find regions of PPT and NPT Horodecki states: They are NPT for $0 \leq b < 1$, PPT for $1 \leq b \leq 4$ and again NPT for $4 < b \leq 5$. In Ref. [68] it is shown that the states are separable for $2 \leq b \leq 3$ and PPT entangled for $3 < b \leq 4$.

Now let us apply the PPT criterion and the realignment criterion (Theorem 3.3) to our three-parameter family (3.34). The PPT criterion provides the following parameter constraints for PPT states $\rho_{\alpha,\beta,\gamma}$:

$$\begin{aligned} \alpha &\leq -\beta - \frac{1}{2} + \frac{1}{2}\gamma, \\ \alpha &\leq \frac{1}{16} (-2 + 11\beta + 3\Delta), \quad \alpha \geq \frac{1}{16} (-2 + 11\beta - 3\Delta), \end{aligned} \quad (3.40)$$

where $\Delta = \sqrt{4 + 9\beta^2 + 4\gamma - 7\gamma^2 - 6\beta(2 + \gamma)}$. Hence all states $\rho_{\alpha,\beta,\gamma}$ with constraints (3.40) are either bound entangled or separable, whereas the others are NPT entangled.

From the realignment criterion we obtain the constraints

$$\alpha \leq \frac{1}{16} (6 + 11\beta - \gamma - \Delta_1) , \quad (3.41)$$

$$\alpha \leq \frac{1}{16} (6 + 11\beta - \gamma + \Delta_1) , \quad (3.42)$$

$$\alpha \geq \frac{1}{16} (-6 + 11\beta - \gamma - \Delta_2) , \quad (3.43)$$

$$\alpha \geq \frac{1}{16} (-6 + 11\beta - \gamma + \Delta_2) , \quad (3.44)$$

where

$$\begin{aligned} \Delta_1 &:= \sqrt{4 + 36\beta + 81\beta^2 - 12\gamma - 54\beta\gamma + 33\gamma^2} \quad \text{and} \\ \Delta_2 &:= \sqrt{4 - 36\beta + 81\beta^2 + 12\gamma - 54\beta\gamma + 33\gamma^2}. \end{aligned} \quad (3.45)$$

Only constraint (3.41) is violated by some PPT states, which thus have to be bound entangled. The PPT entangled states exposed by the realignment criterion are therefore concentrated in the region confined by the constraints

$$\alpha \leq \frac{7}{2}\beta + 1 - \gamma, \quad \alpha \leq \frac{1}{16} (-2 + 11\beta + 3\Delta), \quad \alpha \geq \frac{1}{16} (6 + 11\beta - \gamma - \Delta_1) . \quad (3.46)$$

Remark 3.6. The three-parameter family (3.34) also bears the advantage that it can be nicely illustrated by the Euclidean geometry. To do this, note that the orthogonality conditions of the Hilbert-Schmidt space $\mathcal{A}^9 = \mathcal{A}^3 \otimes \mathcal{A}^3$ have to be transferred correctly, which is achieved by choosing a nonorthogonal and differently scaled coordinate system of parameter axes α , β , and γ . They are chosen such that they each become orthogonal to one of the boundary planes of the set of the three-parameter family of states, given by the positivity constraints (3.35). If the Hilbert-Schmidt inner product $\langle \rho_1 - \rho_2 | \rho_3 - \rho_4 \rangle$ vanishes for four states of the family, in the geometrical picture this would correspond to two orthogonal lines, where one line is drawn between the points corresponding to the states ρ_1 and ρ_2 and the other line between the points corresponding to ρ_3 and ρ_4 . See also Remark 4.2.

In order to calculate quantities well known in an Euclidean space spanned by an orthogonal equally scaled coordinate system, we have to transform points of the non-orthogonal coordinates (α, β, γ) into points of orthogonal coordinates (a, b, c) and vice versa by

$$a = \alpha - \frac{1}{8}\beta - \frac{1}{8}\gamma, \quad b = \frac{\sqrt{3}}{8} (3\beta - \gamma), \quad c = \frac{\sqrt{3}}{4}\gamma. \quad (3.47)$$

In Fig. 3.4 the three-parameter family of states $\rho_{\alpha,\beta,\gamma}$ (3.34) including NPT entangled, PPT entangled (bound entangled) and further PPT states is illustrated in the Euclidean geometry picture.

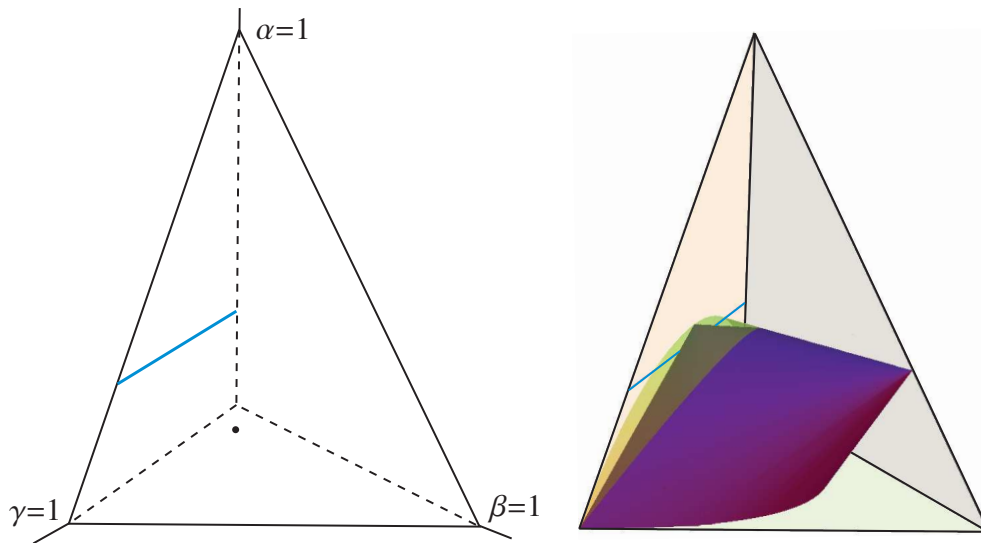


Figure 3.4.: Illustration of the family of states $\rho_{\alpha,\beta,\gamma}$ (3.34) by Euclidean geometry. Left: All states $\rho_{\alpha,\beta,\gamma}$ lie within a pyramid due to the positivity constraints (3.35). The dot represents the origin of the coordinate axes, which is the maximally mixed state $(1/9)\mathbb{1}$. The line (blue) on the left boundary plane represents the Horodecki states (3.36). Right: Illustration of the PPT and realignment criteria. The cone with tip on the right vertex line of the pyramid contains the PPT states, which is intersected by a cone (tip on the left boundary plane) of states that satisfy the realignment criterion, and hence PPT entangled states can be revealed (translucent yellow region). All other states of the pyramid are NPT entangled.

3.5.2.1. Applying the outside-in shift

We can apply the outside-in shift method to detect most of the bound entangled states (3.46), which we want to show in the following. The idea is to choose PPT starting points on the boundary plane $\alpha = \frac{7}{2}\beta + 1 - \gamma$ of the positivity pyramid, on the Horodecki line and in a region close to this line, and shift the operators G_λ along the parameterized lines that connect the starting points with the maximally mixed states. If we can show that G_λ is an entanglement witness until a certain λ_{min} , all states ρ_λ (3.26) with $1 \leq \lambda < \lambda_{min}$ are PPT entangled.

We parameterize our “starting states” on the boundary plane by

$$\rho_{\text{plane}} \equiv \rho_{\alpha,\beta,\gamma} \quad \text{with} \quad \left(\alpha = \frac{1 + \gamma + \epsilon}{6}, \beta = \frac{-5 + 7\gamma + \epsilon}{21}, \gamma \right), \quad \epsilon \in \mathbb{R}, \quad (3.48)$$

where we introduced an additional parameter ϵ to account for the deviation from the line within the boundary plane.

Depending on γ and ϵ the shifting operator $G_{\gamma,\epsilon,\lambda}$ (3.25) has the following form:

$$\begin{aligned} G_{\gamma,\epsilon,\lambda} &= \rho_\lambda - \rho_{pl} - \langle \rho_\lambda, \rho_\lambda - \rho_{pl} \rangle \mathbb{1} = a(2\mathbb{1} + c_1 U_1 + c_2 U_2^I + c_2^* U_2^{II}), \\ \text{with } a &= \frac{d}{36} \lambda(1 - \lambda), \quad d = 1 + 3\gamma^2 + 3\epsilon(2 + \epsilon)/7, \\ c_1 &= -\frac{4(2 + \epsilon)}{7d\lambda}, \quad c_2 = \frac{2(1 - 7\sqrt{3}\gamma i - 3\epsilon)}{7d\lambda}. \end{aligned} \quad (3.49)$$

The operators U_1, U_2^I, U_2^{II} are defined by

$$\begin{aligned} U_1 &:= U_{01} \otimes U_{01} + U_{02} \otimes U_{02} + U_{11} \otimes U_{-11} + U_{12} \otimes U_{-12} \\ &\quad + U_{21} \otimes U_{-21} + U_{22} \otimes U_{-22}, \\ U_2 &:= U_2^I + U_2^{II} \quad \text{with } U_2^I := U_{10} \otimes U_{-10}, \quad U_2^{II} := U_{20} \otimes U_{-20}, \end{aligned} \quad (3.50)$$

and the singular values of the correlation coefficient matrix are given by $s_i = |c_i|$. The family of states ρ_λ is the parameterized line between our starting states (3.48) and the maximally mixed state,

$$\rho_\lambda = \lambda \rho_{\text{plane}} + \frac{1 - \lambda}{9} \mathbb{1}. \quad (3.51)$$

We want to find the minimal λ , denoted by λ_{min} , depending on the parameters γ and ϵ , such that all states on the line (3.51) are bound entangled for $\lambda_{min} < \lambda \leq 1$. To accomplish this we define the functions

$$g_1(\gamma, \epsilon, \lambda) := |c_1| \quad \text{and} \quad g_2(\gamma, \epsilon, \lambda) := |c_2|, \quad (3.52)$$

then λ_{min} is attained at $\max\{g_1(\gamma, \epsilon, \lambda), g_2(\gamma, \epsilon, \lambda)\} = 1$ (see Lemma 3.1). Bound entanglement can be found in a region where $\lambda_{min} < 1$ and the starting points of the lines (3.51) are PPT states. That means, ϵ and γ are chosen such that the starting points are PPT states and the corresponding line allows a $\lambda_{min} < 1$. The

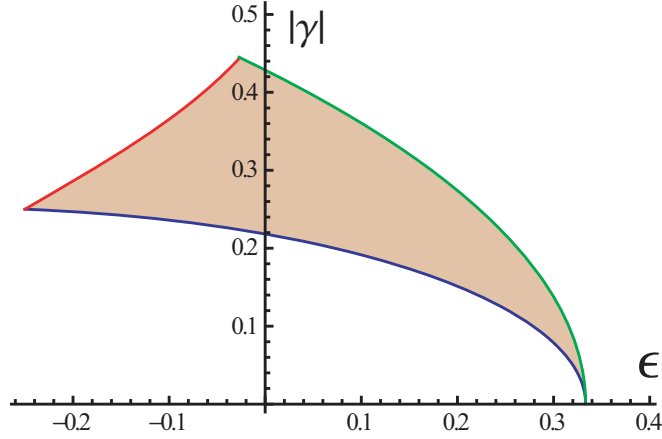


Figure 3.5.: Plot of the parameter range γ versus ϵ of starting points of the lines (3.51) such that bound entangled states can be detected.

parameter ϵ is bounded by $-1/4 < \epsilon < 1/3$, where the lower bound is reached for $\lambda_{\min} \rightarrow 1$ at $|\gamma| = 1/4$ and the upper bound arises from the boundary of the PPT states at $\gamma = 0$. For every ϵ in this interval we have an interval of $|\gamma|$ where bound entangled states are located.

More precisely, in the interval for the ϵ parameter $-1/4 < \epsilon < \epsilon_0$ with $\epsilon_0 = (8 - 7(2/(-5 + \sqrt{29}))^{1/3} + 7(2/(-5 + \sqrt{29}))^{-1/3})/3 \simeq -0.03$ the parameter γ is confined by $\sqrt{1 - 2\epsilon + 3\epsilon^2}/\sqrt{21} < |\gamma| < \sqrt{7 - 6\epsilon - 3\epsilon^2 - 2(1 - 48\epsilon - 12\epsilon^2)^{1/2}}/\sqrt{21}$, under the constraint $\lambda_{\min} < 1$. For the remaining interval $\epsilon_0 < \epsilon < 1/3$ we get the bounds $\sqrt{1 - 2\epsilon + 3\epsilon^2}/\sqrt{21} < |\gamma| < \sqrt{9 - 26\epsilon - 3\epsilon^2}/7$, where the lower bound is again constrained by $\lambda_{\min} < 1$ and the upper one by the PPT condition. A plot of the allowed values of ϵ and γ for the starting points on the boundary plane is depicted in Fig. 3.5. We have equality of the coefficient functions $g_1 = g_2$ for $|\gamma| = \sqrt{15 + 22\epsilon - 5\epsilon^2}/7\sqrt{3} =: \gamma_0$, $g_1 > g_2$ for $|\gamma| < \gamma_0$ and $g_1 < g_2$ for $|\gamma| > \gamma_0$, where $|\gamma|$ is always restricted to the allowed range described above. As mentioned, λ_{\min} is gained from the condition $\max\{g_1(\gamma, \epsilon, \lambda), g_2(\gamma, \epsilon, \lambda)\} = 1$ for particular values of γ and ϵ . The total minimum $\lambda_{\min}^{\text{tot}}$ is finally reached at

$$\lambda_{\min}^{\text{tot}} = \frac{1}{8} (3 + \sqrt{13}) \simeq 0.826, \quad (3.53)$$

which is significantly below the value 1. The total minimum (3.53) is attained at $\epsilon = (7\sqrt{13} - 25)/2 \simeq 0.12$ and $|\gamma| = \sqrt{5 + 11\gamma_0/3 - 5\gamma_0^2/12}/7 \simeq 0.35$ where $\gamma_0 = -25 + 7(13)^{1/2}$. The whole line of states ρ_λ (3.51) within the interval $\lambda_{\min}^{\text{tot}} < \lambda \leq 1$ is found to be bound entangled. The volume of the detected bound entangled states is illustrated in Fig. 3.6. For $\gamma = 0$ no bound entanglement is detected (cf. the two-parameter case in Sec. 4.4.2), which is represented in Fig. 3.6 at the meeting point of the two bound entangled regions.

Actually all PPT entangled states of Eq. (3.46), Fig. 3.4, can be detected using Lemma 3.1. To see this, we construct tangent planes onto the surface of the

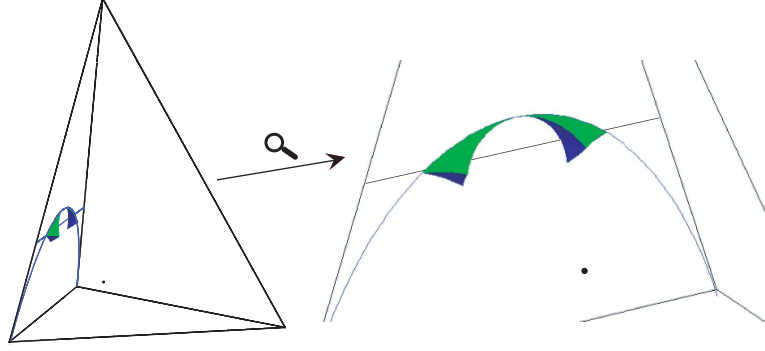


Figure 3.6.: Regions of detected bound entangled states within the pyramid represented by the three-parameter states $\rho_{\alpha,\beta,\gamma}$ (3.34). The dot represents the maximally mixed state, the Horodecki states are represented by the line through the boundary plane from which the regions of bound entanglement emerge. In the magnified picture on the right hand side the viewpoint is altered a bit to gain a better visibility.

function

$$\alpha = \frac{1}{16} (6 + 11\beta - \gamma - \Delta_1) \quad (3.54)$$

from the realignment criterion (3.41), where we use orthogonal coordinates (3.47). In this way we can assign geometric operators to the tangential planes by choosing points \vec{a} inside the planes and points \vec{b} outside the planes such that $\vec{a} - \vec{b}$ is orthogonal to the planes. Since the Euclidean geometry of our picture is isomorphic to the Hilbert-Schmidt geometry, the points \vec{a} and \vec{b} correspond to states ρ_a and ρ_b and we can construct the geometric operator accordingly,

$$G_{\text{re}} = \rho_a - \rho_b - \langle \rho_a, \rho_a - \rho_b \rangle \mathbb{1}_9. \quad (3.55)$$

These operators (3.55) are linear combinations of the three-parameter states $\rho_{\alpha,\beta,\gamma}$ which are linear combinations of the Bell states P_{nm} (3.31) and can be written as a Bloch decomposition using Eq. (3.33).

The geometric operators (3.55) corresponding to tangent planes in points $(\alpha_t, \beta_t, \gamma_t)$, where α_t is a function of β_t and γ_t , given by the realignment function (3.54), are

$$\begin{aligned} G_{\text{re}} &= a (2 \mathbb{1} - U_1 + c U_2^I + c^* U_2^{II}), \quad \text{with} \\ a &= \frac{1}{36} (-2 - 9\beta_t + 3\gamma_t + 3\Delta_c), \\ c &= \frac{9\gamma_t^2 + (-2 - 9\beta_t + 3\gamma_t)\Delta_c + \sqrt{3}\gamma_t (2 + 9\beta_t - 3\gamma_t + 3\Delta_c) i}{(2 + 9\beta_t)^2 - 6(2 + 9\beta_t)\gamma_t + 36\gamma_t^2}, \\ \Delta_c &:= \sqrt{4 + 36 + 81\beta_t^2 - 12\gamma_t - 54\beta_t\gamma_t + 33\gamma_t^2}. \end{aligned} \quad (3.56)$$

The singular values of the correlation coefficient matrix are the absolute values of the coefficients -1 , c and c^* in Eq. (3.56), which are all one,

$$\{s_i\} = \{1, 1, 1, 1, 1, 1, 1, 1\}, \quad (3.57)$$

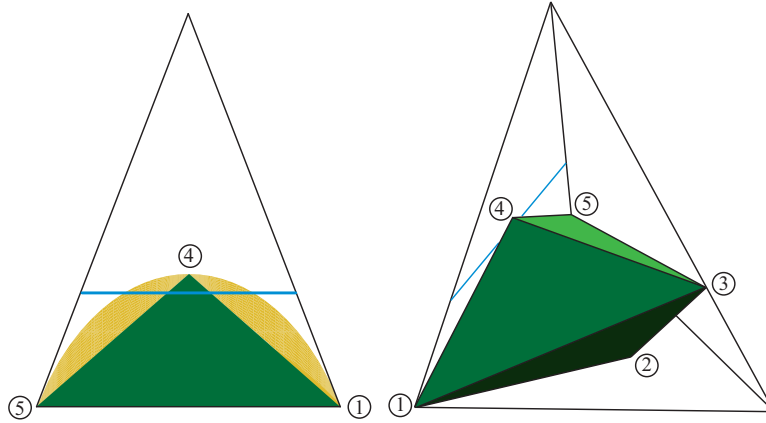


Figure 3.7.: Left: The entanglement properties of the three-parameter family on the boundary plane (3.58) where the Horodecki states are located. The triangular region (green) contains the separable states, the bound entangled states are located in the parabolic region (yellow), and the remaining states are NPT entangled. Right: The kernel polytope is a polygon (green) that includes states that are necessarily separable.

and therefore, according to Lemma 3.1, the geometric operators G_{re} are entanglement witnesses that detect the entanglement of all states “above” the corresponding planes, thus also the bound entangled states in the region of Eq. (3.46).

3.5.2.2. Applying the inside-out shift

We might ask ourselves if the PPT entanglement of Eq. (3.46), revealed by the realignment criterion and also by GEWs, is all there is for the three-parameter family (3.34). Or, to put it differently, are all the three-parameter states that satisfy *both* the PPT and the realignment criterion separable? We can answer this question by using GEWs and the inside-out shift method. The entanglement properties of the states on the boundary plane

$$\alpha = \frac{7}{2}\beta + 1 - \gamma \quad (3.58)$$

of the positivity pyramid are already fixed. The realignment function (3.54) and also the GEWs G_{re} (3.56) draw a triangle on this plane, whose vertices are separable states. The tip of the triangle is a separable state since it is PPT and $\gamma = 0$ (all PPT states of the two-parameter subset $\gamma = 0$ are separable, shown in Ref. [10]), the other two, at $\gamma = 1$ and $\gamma = -1$, are simple mixtures of Bell states P_{nm} that are also shown to be separable in Ref. [10]. So the triangle is the convex hull of the three separable states and thus has to be separable. For an illustration of the entanglement properties on the boundary plane (3.58) see Fig. 3.7. But what about all the three-parameter states (3.34)? First, we construct a kernel polytope of those states that are necessarily separable. This can be done by identifying five separable states that serve as vertices for the kernel

polytope. Three arise from the two-parameter subset $\gamma = 0$, where all PPT states are separable, the remaining two vertices are the separable states with $\gamma = 1$ and $\gamma = -1$ on the boundary plane (3.58). The resulting kernel polytope is a polygon with five vertices, see Fig. 3.7. Alternatively, one can also use sufficient criteria for separability to construct a kernel polytope of separable states. In Ref. [36] a sufficient separability criterion is presented that is shown to be applicable for states of the magic simplex.

The question is if this polygon contains all separable states of the three-parameter family (3.34), which would imply much greater regions of bound entanglement than detected before. In the following we want to show that this is not the case.

We can assign geometric operators to four boundary planes of the kernel polygon, in the same way as we did for the planes on the realignment surface, see Eq. (3.55), where we use the geometric isomorphism again. We call the four geometric operators G_{\pm}^u, G_{\pm}^d , which correspond to the following planes given by three vertex points (see Fig. 3.7): G_+^u to 1, 3, 4, G_-^u to 3, 4, 5, G_+^d to 1, 2, 3, and G_-^d to 2, 3, 5. The plus and minus sign indicates the side with positive or negative values of the parameter γ . The operators are

$$\begin{aligned} G_{\pm}^u &= a(2\mathbb{1} - U_1 + cU_2^I + c^*U_2^{II}), \quad \text{with } a = \frac{1}{63}, \quad c = -1 \pm \sqrt{3}i, \\ G_{\pm}^d &= a(2\mathbb{1} + U_1 + cU_2^I + c^*U_2^{II}), \quad \text{with } a = \frac{1}{63}, \quad c = -1 \pm \sqrt{3}i. \end{aligned} \quad (3.59)$$

The boundary planes can be easily shifted along parameterized lines through their normal vectors, and so can the assigned geometric operators (3.59). Note that we have a simplified picture of locally maximally mixed states, see Remark 3.4. The operators G_{\pm}^u, G_{\pm}^d themselves are not entanglement witnesses, since the condition (3.20) can be numerically shown to be violated (see Corollary 3.2). The singular values are again the absolute values of the correlation coefficients, $\{s_i\} = \{1, 1, 1, 1, 1, 1, 2, 2\}$, hence Lemma 3.1 does not give an answer. It is difficult to show a violation analytically because of the complex Bloch vector geometry of qutrits, see Remarks 3.2 and 3.5. In order to check the condition (3.20) we minimize the left-hand term numerically by varying the possible Bloch vectors \vec{n}^*, \vec{m}^* , restricted by the condition $\rho \geq 0$ with ρ of Eq. (2.47). Shifting the operators outside, we find a minimum $S = -1$ of condition (3.20) when the planes become tangent to the shape enclosed by the PPT and realignment criterion³, achieving new vertices at the touch points. Employing the inside-out shift method, see Sec. 3.5 and Fig. 3.3, we construct a new polygon with the new vertices, and assign new geometric operators corresponding to the new boundary planes. Shifting the new operators outside, we again find the minimum $S = -1$ at planes tangent to the PPT and realignment shape. Therefore there is a very strong implication that the PPT and realignment shape, seen as the two-cone

³Standard numerical procedures suffice (e.g. with Mathematica), since due to the convexity of the set of separable states, the achieved minimum has to be a global minimum.

shape in Fig. 3.4, is the shape of the separable states. Fig. 3.4 thus is a picture of all entanglement properties of the three-parameter family.

3.6. Decomposition of entanglement witnesses for experimental application

Entanglement witnesses are Hermitian operators and therefore observables that should be measurable in a given experimental setup. According to the entanglement witness criterion (Theorem 3.4) one can reliably detect entangled states by measuring the expectation value of the witness. In this way one is in principle able to detect entanglement in experiments without performing a full tomography of the density matrix. The advantage of using entanglement witnesses for entanglement detection over Bell inequalities (see Refs. [39, 78, 51, 128] for Bell inequalities in higher dimensional systems) is that witnesses usually detect more entangled states than Bell inequalities, especially if they are optimal. Bell inequalities correspond to non-optimal entanglement witnesses [119, 72] and detect states for which certain measurement outcomes are not compatible with local realistic theories (so-called *non-local* states). The expectation value of the witness W is given by

$$\langle W \rangle = \text{Tr} \rho W \quad (3.60)$$

for some state ρ . If $\langle W \rangle < 0$ then the state ρ is entangled. But which measurements have to be performed? Even if it is theoretically known that the witness is an observable, it is not trivial to find the concrete measurements that have to be performed in experiments.

Obviously it is appropriate to express the entanglement witness in terms of generalized Gell-Mann matrices (2.13) - (2.15), since they are Hermitian. For $d = 3$ – the qutrit case – the Gell-Mann matrices (2.17) - (2.19) can be expressed in terms of eight “physical” operators, the observables $S_x, S_y, S_z, S_x^2, S_y^2, \{S_x, S_y\}, \{S_y, S_z\}, \{S_z, S_x\}$ of a spin-1 system, where $\vec{S} = (S_x, S_y, S_z)$ is the spin operator and $\{S_i, S_j\} = S_i S_j + S_j S_i$ (with $i, j = x, y, z$) denotes the corresponding anti-commutator. We can decompose the Gell-Mann matrices into spin-1 operators as follows (for a similar expansion, see Ref. [92]):

$$\begin{aligned} \lambda_s^{12} &= \frac{1}{\sqrt{2}\hbar^2} (\hbar S_x + \{S_z, S_x\}), & \lambda_s^{13} &= \frac{1}{\hbar^2} (S_x^2 - S_y^2), \\ \lambda_s^{23} &= \frac{1}{\sqrt{2}\hbar^2} (\hbar S_x - \{S_z, S_x\}), & \lambda_a^{12} &= \frac{1}{\sqrt{2}\hbar^2} (\hbar S_y + \{S_y, S_z\}), \\ \lambda_a^{13} &= \frac{1}{\hbar^2} \{S_x, S_y\}, & \lambda_a^{23} &= \frac{1}{\sqrt{2}\hbar^2} (\hbar S_y - \{S_y, S_z\}), \\ \lambda^1 &= 2 \mathbb{1} + \frac{1}{2\hbar^2} (\hbar S_z - 3S_x^2 - 3S_y^2), & \lambda^2 &= \frac{1}{\sqrt{3}} \left(-2 \mathbb{1} + \frac{3}{2\hbar^2} (\hbar S_z + S_x^2 + S_y^2) \right). \end{aligned} \quad (3.61)$$

All operators can be represented by the following matrices:

$$\begin{aligned}
 S_x &= \frac{\hbar}{\sqrt{2}} \begin{pmatrix} 0 & 1 & 0 \\ 1 & 0 & 1 \\ 0 & 1 & 0 \end{pmatrix}, & S_y &= \frac{\hbar}{\sqrt{2}} \begin{pmatrix} 0 & -i & 0 \\ i & 0 & -i \\ 0 & i & 0 \end{pmatrix}, & S_z &= \hbar \begin{pmatrix} 1 & 0 & 0 \\ 0 & 0 & 0 \\ 0 & 0 & -1 \end{pmatrix}, \\
 S_x^2 &= \frac{\hbar^2}{2} \begin{pmatrix} 1 & 0 & 1 \\ 0 & 2 & 0 \\ 1 & 0 & 1 \end{pmatrix}, & S_y^2 &= \frac{\hbar^2}{2} \begin{pmatrix} 1 & 0 & -1 \\ 0 & 2 & 0 \\ -1 & 0 & 1 \end{pmatrix}, \\
 \{S_x, S_y\} &= \hbar^2 \begin{pmatrix} 0 & 0 & -i \\ 0 & 0 & 0 \\ i & 0 & 0 \end{pmatrix}, & \{S_y, S_z\} &= \frac{\hbar^2}{\sqrt{2}} \begin{pmatrix} 0 & -i & 0 \\ i & 0 & i \\ 0 & -i & 0 \end{pmatrix}, \\
 \{S_z, S_x\} &= \frac{\hbar^2}{\sqrt{2}} \begin{pmatrix} 0 & 1 & 0 \\ 1 & 0 & -1 \\ 0 & -1 & 0 \end{pmatrix}.
 \end{aligned} \tag{3.62}$$

Thus we can express any observable on a n -qutrit Hilbert space - a composite system of n particles with three degrees of freedom - in terms of the spin operators (3.62).

As an example we want to study the entanglement witness for the isotropic two-qutrit state, i.e. state (4.4) for $d = 3$ (a detailed study of entanglement witnesses and entanglement quantification of the isotropic two-qutrit state follows in Sec. 4.3). In this case we obtain for the optimal entanglement witness

$$W_{\text{iso}} = \frac{1}{4\sqrt{2}} \left(\frac{4}{3} \mathbb{1} \otimes \mathbb{1} - \Lambda \right), \tag{3.63}$$

(i.e. Eq. (4.10) for $d = 3$) where the operator Λ is defined in Eq. (2.69).

Expressing the Gell-Mann matrices in Λ by the spin operator decomposition (3.61) the expectation value of the entanglement witness W_{iso} is given by

$$\langle W_{\text{iso}} \rangle = \frac{1}{3\sqrt{2}} - \frac{1}{4\sqrt{2}} \langle \Lambda \rangle, \tag{3.64}$$

where

$$\begin{aligned}
 \langle \Lambda \rangle &= \frac{1}{\hbar^2} \left(\langle S_x \otimes S_x \rangle - \langle S_y \otimes S_y \rangle + \langle S_z \otimes S_z \rangle \right) + \frac{16}{3} \langle \mathbb{1} \otimes \mathbb{1} \rangle \\
 &\quad - \frac{4}{\hbar^2} \left(\langle \mathbb{1} \otimes S_x^2 \rangle + \langle \mathbb{1} \otimes S_y^2 \rangle + \langle S_x^2 \otimes \mathbb{1} \rangle + \langle S_y^2 \otimes \mathbb{1} \rangle \right) \\
 &\quad + \frac{4}{\hbar^4} \left(\langle S_x^2 \otimes S_x^2 \rangle + \langle S_y^2 \otimes S_y^2 \rangle \right) + \frac{2}{\hbar^4} \left(\langle S_x^2 \otimes S_y^2 \rangle + \langle S_y^2 \otimes S_x^2 \rangle \right) \\
 &\quad + \frac{1}{\hbar^4} \left(\langle \{S_z, S_x\} \otimes \{S_z, S_x\} \rangle - \langle \{S_y, S_z\} \otimes \{S_y, S_z\} \rangle - \langle \{S_x, S_y\} \otimes \{S_x, S_y\} \rangle \right).
 \end{aligned} \tag{3.65}$$

In principle it should be possible to determine the various expectation values in (3.65) experimentally, possible procedures to measure expectation values of the observables in Eq. (3.62) are given in Ref. [6].

3.7. Summary and conclusion

In this chapter we first review entanglement criteria for vector states and density operators. We combine the concept of Bloch vector decompositions for operators and states (previously discussed in Chapter 2) with entanglement witnesses and derive conditions that can be used to identify operators as entanglement witnesses. Furthermore, we give the definition of geometric entanglement witnesses and present methods to “shift” them along parameterized lines of states to detect entanglement and identify separable states. This is illustrated on a three-parameter family of two-qutrit states for which we determine regions of NPT entangled, PPT entangled and separable states. Finally we present a decomposition of entanglement witnesses via measurable spin-1 operators.

Our approach to entanglement detection is guided by the geometrically intuitive way of using entanglement witnesses. The construction of geometric entanglement witnesses directly uses the fact that entanglement witnesses correspond to hyperplanes in the Hilbert-Schmidt geometry. In this way it becomes easier to apply geometric operations like the shifting of planes, and representations in Euclidean geometry are easy to perform. By employing the convenient parametrization of the Bloch vector decompositions of operators and states, the conditions for identifying geometric entanglement witnesses can be simplified. The construction of geometric entanglement witnesses does not rely on special properties of the states, i.e. it can be done for NPT or PPT entangled states likewise.

The presented example is relevant in many aspects. First of all, the states of the magic simplex are a higher dimensional analogy of Bell-state mixtures of the two-qubit case that are relevant for quantum communication tasks; they are used for a higher dimensional teleportation protocol, as explained in Sec. 3.5.2. Furthermore it is interesting and surprising that this particular three-parameter family includes the Horodecki states that were among the first examples of bound entangled states and are an example of a family of states that include all entanglement properties. Thus the three-parameter family can be viewed as a more-parameter extension of the Horodecki states that includes significantly more bound entangled states. Finally, the presented family of states allows a nice three-dimensional Euclidean illustration that makes the regions of entangled, bound entangled and separable states visible.

In this chapter only bipartite systems are investigated. Of course a multipartite extension is trivially possible if we only want to distinguish between states that contain entanglement between any of the subsystems and states that are fully separable into all subsystems. The definition of separable states just has to be extended with additional tensor products, respectively (see Sec. 5.2). The distinction of states that are separable with respect to a certain number of subsystems, is, however, not trivial [69, 58, 59]. In this respect a generalization of the used Bloch decompositions of product states seems to be non-trivial. In the case of multipartite states one can distinguish between the distillability of states into entangled states of a fixed number of particles [57], and the notion of bound en-

tanglement becomes more involved. Entangled multipartite states can themselves be classified in different ways, see, e.g., Refs. [46, 1, 132] and Chapter 5.

4. Geometric quantification of entanglement

4.1. Introduction

In the last chapter we discussed the concept of geometric entanglement witnesses and how to use them for entanglement detection. In this chapter we show that geometric entanglement witnesses are also applicable in the context of entanglement quantification by giving concrete examples for families of two-qubit, two-qutrit and two-qudit states.

Entanglement quantification is a mathematical task in which one seeks for continuous functions that “measure” the amount of entanglement of a given vector state or density operator. Of course, since the separability problem has not yet been solved, neither is the problem of entanglement quantification of states of arbitrary dimensional Hilbert spaces and arbitrary many subsystems. For lower dimensions, in particular for two-qubit states, entanglement measures exist that can be computed for all density operators of this dimensions, which matches the fact that in this case we can also always determine if a density operator is entangled or separable.

For vector states of bipartite systems a computable and convenient entanglement measure is provided by the entropy measure of entanglement [17, 14]; it is defined as the von-Neumann entropy of the reduced density operators. A generalization of this concept is given by the *entanglement of formation* [17]. Here a standard method to generalize an entanglement measure for pure states to mixed states is used: It is defined as the mean value of the entropy measure for the pure states that the mixed states can be decomposed into, and takes the infimum over all possible decompositions. This method is in general not computable. For two qubits, however, entanglement of formation can be related to the *concurrence* [17], which can be computed [60, 143]. For bipartite systems of arbitrary dimension the concurrence can be generalized [126, 112, 4, 94, 95], for mixed states only lower bounds are calculable [94]. The generalized concurrence can, however, detect PPT entangled states [94, 5]. A computable entanglement measure for bipartite systems of arbitrary dimension is the *negativity* [133], which, however, vanishes not only for separable states but also for PPT entangled states. So far no universally computable entanglement measure for PPT entangled states is known. In the case of multipartite systems, various approaches to entanglement quantification exist [38, 18, 93, 108, 9, 95, 40, 90, 85, 73], but even for pure states there is no uniquely approved entanglement measure. The reason is that the

purpose of what entanglement to quantify can vary, e.g. if one wants to measure the amount of entanglement present in the whole composite system, or between various subsystems. An approach that embraces both aspects is presented in Ref. [59].

A geometric approach to entanglement quantification is provided by so-called *geometric entanglement measures* that are defined as the minimal distance of a state to the set of separable states¹ [130, 129]. This distance can be defined in multiple ways, e.g. by distances induced by the Hilbert-Schmidt metric [142, 98, 25, 19] or the Bures metric [129] of the operator space. Also the relative entropy of entanglement [130, 129] is widely used, which is not a distance in the usual sense as it is not defined via a metric.

The chapter is organized as follows: In Sec. 4.2 we start with the definition of the Hilbert-Schmidt measure of entanglement and explain how geometric entanglement witnesses can be used in this respect. In Sec. 4.3 we determine the Hilbert-Schmidt measure for the isotropic two-qudit states using geometric entanglement witnesses and Bloch decompositions into the three bases discussed in Chapter 2. In Sec. 4.4 we calculate the Hilbert-Schmidt measure for two-parameter families of two-qubit and two-qutrit states. We draw conclusions in Sec. 4.5.

The chapter is based on Refs. [20, 23, 24]:

- Reinhold A. Bertlmann and Philipp Krammer
Bloch vectors for qudits and geometry of entanglement
e-print arXiv:0706.1743
- Reinhold A. Bertlmann and Philipp Krammer
Geometric entanglement witnesses and bound entanglement
Phys. Rev. A **77**, 024303 (2008)
- Reinhold A. Bertlmann and Philipp Krammer
Entanglement witnesses and geometry of entanglement of two-qutrit states
Ann. Phys. **324**, 1388 (2009)

4.2. The Hilbert-Schmidt measure and geometric entanglement witnesses

Geometric entanglement measures have a simple geometric approach to the quantification of entanglement: A state has as much entanglement as its minimal distance to the set of separable states. This concept was initiated in Refs. [130, 129], where also the properties that the measure should satisfy were listed:

¹Note that the definition of geometric entanglement measures given here is different to the measure introduced in [137].

- (G1) It should vanish for separable states, which is trivially satisfied,
- (G2) it should be invariant under local unitary transformations, and
- (G3) it should not increase on average under local operations and classical communication.

A concrete realization is the Hilbert-Schmidt measure of entanglement, introduced in Ref. [142]. It uses the Hilbert-Schmidt distance (1.12) to define the measure of a state ρ as

$$D_{\text{HS}}(\rho) := \min_{\sigma \in S} d(\rho, \sigma) = \|\rho - \sigma_0\|, \quad (4.1)$$

where σ_0 is the separable state for which $d(\rho, \sigma)$ takes the minimum. Such a state always exists since the set of separable states is convex and compact. It is called the *nearest separable state* to the state ρ , and $D_{\text{HS}}(\rho)$ is called the *Hilbert-Schmidt measure* of entanglement. This geometric measure induced by the Hilbert-Schmidt measure is believed to be a proper entanglement measure, it satisfies the properties G1 (of course the nearest separable state to a separable state is the state itself, yielding a zero Hilbert-Schmidt measure for separable states) and G2 [142]. However, a proof of property G3 is still outstanding [98], but since no counterexample has been found yet that would prove a violation, it can be reasonably conjectured that the property is satisfied. Clearly the greatest difficulty in the evaluation of the Hilbert-Schmidt measure is to find the nearest separable state to a given entangled state. This cannot be achieved operationally. In Ref. [87], e.g., an algorithm for a detection of the nearest separable state is presented that gives a solution or good approximation in many cases. Another method, introduced in Ref. [19], tests if a good guess is indeed equal to the nearest separable state, given in the following lemma.

Lemma 4.1 ([19]). *Let $\rho \in \mathcal{A}^D$ be an arbitrary entangled state on a bipartite Hilbert space $\mathcal{H}_A \otimes \mathcal{H}_B$. A state $\tilde{\sigma} \in \mathcal{A}^D$ is equal to the nearest separable state σ_0 , $\tilde{\sigma} = \sigma_0$, if and only if the geometric operator*

$$\tilde{G} := \tilde{\sigma} - \rho - \langle \tilde{\sigma}, \tilde{\sigma} - \rho \rangle \mathbb{1} \quad (4.2)$$

is an entanglement witness.

Proof. The detailed proof can be found in Ref. [19]. The idea is the following: If $\tilde{\sigma}$ is the nearest separable state, then the hyperplane corresponding to \tilde{G} is tangent to the set of separable states due to its convexity and thus is an optimal entanglement witness. It remains to prove that if $\tilde{\sigma}$ is not the nearest separable state, then \tilde{G} is not an entanglement witness. This is easy to see, since if $\tilde{\sigma}$ is not the nearest separable state, \tilde{G} is no longer tangent to the set of separable states and hence cannot be an entanglement witness, see Fig. 4.1. \square

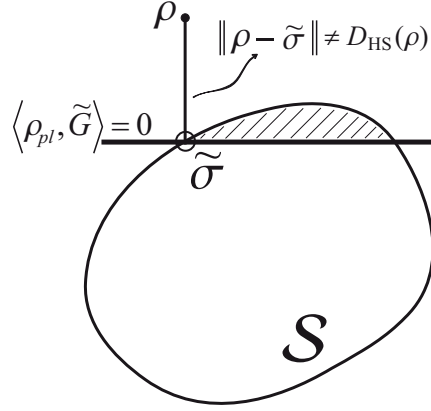


Figure 4.1.: Illustration of the proof of Lemma 4.1. As usual, the geometric operator \tilde{G} is represented by the hyperplane $\langle \rho_{pl}, \tilde{G} \rangle = 0$.

Remark 4.1. Once the nearest separable state σ_0 to an entangled state ρ has been found, an optimal geometric entanglement witness that detects the entanglement of ρ is given by [102, 25, 19] (see also Lemma 3.2)

$$W_{\text{opt}} := \sigma_0 - \rho - \langle \sigma_0, \sigma_0 - \rho \rangle \mathbb{1}. \quad (4.3)$$

The method of Lemma 4.1 is non-operational, since in general it is not straightforward to see whether the geometric operator (4.2) is an entanglement witness or not. Corollary 3.2 and Lemma 3.1, which are derived using Bloch decompositions, however, often help to decide this.

4.3. Hilbert-Schmidt measure for the isotropic two-qudit states

The isotropic two-qudit states are defined as the one-parameter family of states [61, 105, 65]

$$\rho_{\alpha}^{(d)} = \alpha |\phi_+^d\rangle \langle \phi_+^d| + \frac{1-\alpha}{d^2} \mathbb{1}_{d^2}, \quad \alpha \in \mathbb{R}, \quad -\frac{1}{d^2-1} \leq \alpha \leq 1, \quad (4.4)$$

i.e. the maximally entangled state (2.61) subjected to white noise. We shortly write $\mathbb{1}_{d^2}$ for $\mathbb{1}_d \otimes \mathbb{1}_d$. It is shown in Ref. [61] that these states are separable for $-1/(d^2-1) \leq \alpha \leq 1/(d+1)$, and entangled for $1/(d+1) < \alpha \leq 1$. Using the decompositions of the maximally entangled state $|\phi_+^d\rangle \langle \phi_+^d|$ into the generalized Gell-Mann matrices basis (GGB), the polarization operator basis (POB), and the

Weyl operator basis (WOB), we can decompose the isotropic two-qudit states as

$$\rho_\alpha^{(d)} = \frac{1}{d^2} \mathbb{1}_{d^2} + \frac{\alpha}{2d} \Lambda, \quad (4.5)$$

$$= \frac{1}{d^2} \mathbb{1}_{d^2} + \frac{\alpha}{d} T, \quad (4.6)$$

$$= \frac{1}{d^2} \mathbb{1}_{d^2} + \frac{\alpha}{d^2} U, \quad (4.7)$$

where Λ , T , and U are defined in Eqs. (2.69), (2.73), and (2.76), respectively. To calculate the Hilbert-Schmidt measure, we have to determine the nearest separable states $\sigma_0^{(d)}$ to the entangled isotropic states of Eq. (4.4). A reasonable guess $\tilde{\sigma}^{(d)}$ is the isotropic state with $\alpha = 1/(d+1)$, i.e. the isotropic state that lies on the boundary of the set of separable states. Using the decomposition of the isotropic states into the GGB (4.5), this state has the form

$$\tilde{\sigma}^{(d)} = \rho_{\alpha=\frac{1}{d+1}}^{(d)} = \frac{1}{d^2} \mathbb{1}_{d^2} + \frac{1}{2d(d+1)} \Lambda, \quad (4.8)$$

and we can set up the operator (4.2) and bring it in the form of Eq. (3.14),

$$\tilde{G}(\rho_{\alpha,\text{ent}}^{(d)}) = \frac{1}{2\sqrt{d^2-1}} \left(\frac{2(d-1)}{d} \mathbb{1}_{d^2} - \Lambda \right). \quad (4.9)$$

To apply Lemma (3.1) we have to calculate the singular values of the correlation coefficient matrix. These are the absolute values of the coefficients of the terms of Λ , which are ± 1 , and thus for the singular values we have $s_i = 1 \forall i$. Hence (see Lemma 3.1) $\tilde{G}(\rho_{\alpha,\text{ent}}^{(d)})$ is an optimal entanglement witness and we can write

$$W_{\text{opt}}(\rho_{\alpha,\text{ent}}^{(d)}) = \frac{1}{2\sqrt{d^2-1}} \left(\frac{2(d-1)}{d} \mathbb{1}_{d^2} - \Lambda \right). \quad (4.10)$$

According to Lemma 4.1, $\tilde{\sigma}^{(d)}$ is the nearest separable state $\sigma_0^{(d)}$ for all possible values of α of the entangled isotropic two-qudit state. Of course the above quantities can be decomposed into the POB and the WOB likewise. Comparing the three forms for the isotropic qudit states (4.5), (4.6) and (4.7) we find the relations

$$\Lambda = 2T \quad \text{and} \quad T = \frac{1}{d} U, \quad (4.11)$$

and obtain for the nearest separable states and the optimal entanglement witnesses

$$\begin{aligned} \sigma_0^{(d)} = \rho_{\alpha=\frac{1}{d+1}}^{(d)} &= \frac{1}{d^2} \mathbb{1}_{d^2} + \frac{1}{d(d+1)} T, \\ &= \frac{1}{d^2} \mathbb{1}_{d^2} + \frac{1}{d^2(d+1)} U, \end{aligned} \quad (4.12)$$

$$\begin{aligned} W_{\text{opt}}(\rho_{\alpha, \text{ent}}^{(d)}) &= \frac{1}{\sqrt{d^2 - 1}} \left(\frac{d-1}{d} \mathbb{1}_{d^2} - T \right), \\ &= \frac{1}{d\sqrt{d^2 - 1}} ((d-1)\mathbb{1}_{d^2} - U), \end{aligned} \quad (4.13)$$

where we used Lemma 3.1 and Lemma 4.1 in the same way as for the GGB.

The Hilbert-Schmidt measure is of course independent of the choice of basis for the operator decompositions and is given by

$$D(\rho_{\alpha, \text{ent}}^{(d)}) = \left\| \sigma_0^{(d)} - \rho_{\alpha, \text{ent}}^{(d)} \right\| = \frac{\sqrt{d^2 - 1}}{d} \left(\alpha - \frac{1}{d+1} \right). \quad (4.14)$$

4.4. Hilbert-Schmidt measure for two-parameter families of states

To further demonstrate the methods for a geometrical quantification of entanglement given in the previous section, we want to determine the Hilbert-Schmidt measure for particular two-parameter families of states that are mixtures of maximally entangled vector states.

4.4.1. Two-qubit states

As a first example we consider the following family of two-parameter two-qubit states:

$$\rho_{\alpha, \beta} = \frac{1 - \alpha - \beta}{4} \mathbb{1}_4 + \alpha |\phi^+\rangle\langle\phi^+| + \frac{\beta}{2} (|\psi^+\rangle\langle\psi^+| + |\psi^-\rangle\langle\psi^-|), \quad (4.15)$$

where $\mathbb{1}_4 = \mathbb{1}_2 \otimes \mathbb{1}_2$ and the used states are projectors onto the vector states

$$|\phi^+\rangle = \frac{1}{\sqrt{2}} (|00\rangle + |11\rangle), \quad (4.16)$$

$$|\phi^-\rangle = \frac{1}{\sqrt{2}} (|00\rangle - |11\rangle), \quad (4.17)$$

$$|\psi^+\rangle = \frac{1}{\sqrt{2}} (|01\rangle + |10\rangle), \quad (4.18)$$

$$|\psi^-\rangle = \frac{1}{\sqrt{2}} (|01\rangle - |10\rangle), \quad (4.19)$$

which are called *Bell states* and form an orthogonal basis of the 2×2 dimensional Hilbert space. The convex set \mathcal{B} of all mixtures of the four Bell states is given by (we write P_{ϕ^+} for $|\phi^+\rangle\langle\phi^+|$ (the projector onto $|\phi^+\rangle$), and equivalently for the other states)

$$\mathcal{B} := \left\{ p_1 P_{\phi^+} + p_2 P_{\phi^-} + p_3 P_{\psi^+} + p_4 P_{\psi^-}; p_i \geq 0, \sum_i p_i = 1 \right\}. \quad (4.20)$$

To get an Euclidean geometric analogue of \mathcal{B} we first notice that the four parameters of Eq. (4.20) can be reduced to three by using the completeness relation

$$P_{\phi_+} + P_{\phi_-} + P_{\psi_+} + P_{\psi_-} = \mathbb{1}_4 \quad (4.21)$$

and expressing one Bell state in terms of the others. This reduces the parameter space to three dimensions, which can be illustrated. All Bell states (in their density operator form) are equidistant from each other with respect to the Hilbert-Schmidt distance, thus the Euclidean representation is a three-dimensional tetrahedron with the four Bell states as vertices [66, 135, 25], see Fig. 4.3.

The two-parameter family (4.15) is a subset of the whole set \mathcal{B} . The requirement of positivity, $\rho_{\alpha,\beta} \geq 0$, constrains the possible parameter values:

$$\alpha \leq -\beta + 1, \quad \alpha \geq \frac{1}{3}\beta - \frac{1}{3}, \quad \alpha \leq \beta + 1, \quad (4.22)$$

and the PPT criterion (Theorem 3.2) gives parameter constraints for the positive partial transpose²:

$$\alpha \geq \beta - 1, \quad \alpha \leq \frac{1}{3}\beta + \frac{1}{3}, \quad \alpha \geq -\beta - 1, \quad (4.23)$$

The two-dimensional geometric illustration of the positivity and the PPT regions of the two-parameter states (4.15) is shown in Fig. 4.2.

Remark 4.2. Note that the Bell state $|\phi^-\rangle\langle\phi^-|$ is also included in this family for $\alpha = -1$ and $\beta = -2$. The coordinate axes according to the parameters α and β are chosen non-orthogonal and differently scaled, such that orthogonality relations in Hilbert-Schmidt space are reflected in the Euclidean geometry (see also Remark (3.6)). Of course the maximally mixed state $1/4 \mathbb{1}_4$ lies in the origin. Both parameter axes thus have to be orthogonal to a boundary line of the positivity condition, since in Hilbert-Schmidt space we have the orthogonality relations

$$\left\langle \frac{1}{2}(P_{\psi_+} + P_{\psi_-}) - P_{\phi_-}, \frac{1}{4}\mathbb{1} - P_{\phi_+} \right\rangle = \frac{1}{8}\text{Tr}P_{\psi_+} + \frac{1}{8}\text{Tr}P_{\psi_-} - \frac{1}{4}\text{Tr}P_{\phi_-} = 0, \quad (4.24)$$

$$\left\langle \frac{1}{4}\mathbb{1} - \frac{1}{2}(P_{\psi_+} + P_{\psi_-}), P_{\phi_+} - P_{\phi_-} \right\rangle = \frac{1}{4}\text{Tr}P_{\phi_+} - \frac{1}{4}\text{Tr}P_{\phi_-} = 0. \quad (4.25)$$

The location of the plane of the two-parameter states in the simplex \mathcal{B} is shown in Fig. 4.3. In order to determine the Hilbert-Schmidt measure, we need to find the nearest separable states to the entangled states of the two-parameter family. For that purpose we pursue the following idea: We calculate the ‘‘points’’ in the separable region that are nearest to the entangled states in the Euclidean two-dimensional picture (see Fig. 4.2), and then use Lemma 4.1 to check if the found nearest point indeed corresponds to the nearest separable state (with respect to

²the constraints give the region of operators (4.15) that are positive under partial transposition, they include also non-positive operators that nevertheless become positive under PT

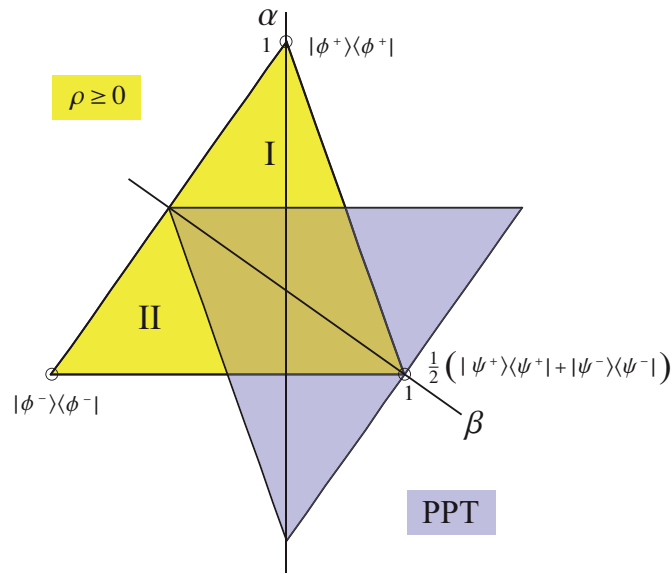


Figure 4.2.: Euclidean geometric representation of the family of two-parameter two-qubit states $\rho_{\alpha,\beta}$. The darker (purple) triangle includes all “points” (α, β) that correspond to a positive operator after partial transposition, it intersects the lighter (yellow) triangle of all states ($\rho \geq 0$). The PPT and separable states thus lie in the intersection region, the NPT entangled states in the triangular regions I and II.

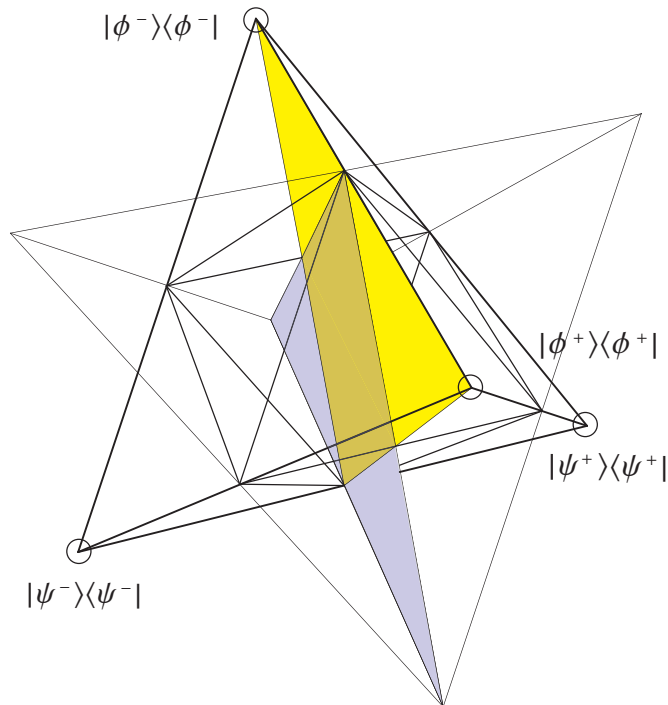


Figure 4.3.: The plane of the states $\rho_{\alpha,\beta}$ (4.15) is located in the tetrahedron of all Bell state mixtures, the set \mathcal{B} (4.20).

the whole state space). This task is further simplified if we introduce orthogonal and equally scaled coordinates a and b that depend on the original coordinates α and β ,

$$a = \alpha - \frac{1}{3}\beta, \quad b = \frac{\sqrt{2}}{3}\beta. \quad (4.26)$$

The concrete operator of the form (4.2) can then be decomposed in terms of Pauli matrices in order to apply Lemma 3.1. It is therefore convenient to express the whole family as

$$\rho_{\alpha,\beta} = \frac{1}{4} (\mathbb{1}_4 + \alpha (\sigma^x \otimes \sigma^x - \sigma^y \otimes \sigma^y) + (\alpha - \beta) \sigma^z \otimes \sigma^z), \quad (4.27)$$

where we used the decomposition of the Bell states

$$|\phi^+\rangle\langle\phi^+| = \frac{1}{4} (\mathbb{1}_4 + \sigma^x \otimes \sigma^x - \sigma^y \otimes \sigma^y + \sigma^z \otimes \sigma^z), \quad (4.28)$$

$$|\phi^-\rangle\langle\phi^-| = \frac{1}{4} (\mathbb{1}_4 - \sigma^x \otimes \sigma^x + \sigma^y \otimes \sigma^y + \sigma^z \otimes \sigma^z), \quad (4.29)$$

$$|\psi^+\rangle\langle\psi^+| = \frac{1}{4} (\mathbb{1}_4 + \sigma^x \otimes \sigma^x + \sigma^y \otimes \sigma^y - \sigma^z \otimes \sigma^z), \quad (4.30)$$

$$|\psi^-\rangle\langle\psi^-| = \frac{1}{4} (\mathbb{1}_4 - \sigma^x \otimes \sigma^x - \sigma^y \otimes \sigma^y - \sigma^z \otimes \sigma^z). \quad (4.31)$$

4.4.1.1. Region I

Let us consider the entangled states in region I (see Fig. 4.2) first, which is given by

$$\alpha \leq \beta + 1, \quad \alpha \leq -\beta + 1, \quad \alpha > \frac{\beta}{3} + \frac{1}{3}. \quad (4.32)$$

The points in the separable region that are nearest to points in region I, i.e. to points (α, β) that satisfy the constraints (4.32), can be found by applying a standard point-to-line distance calculation (using the orthogonal coordinates (4.26)). These are the points $(1/3 + \beta/3, \beta)$ that do not depend on α anymore and correspond to the states (where we insert the parameter values into Eq. (4.27))

$$\tilde{\sigma}_\beta = \frac{1}{4} \left(\mathbb{1}_4 + \frac{1+\beta}{3} (\sigma^x \otimes \sigma^x - \sigma^y \otimes \sigma^y) + \frac{1-2\beta}{3} \sigma^z \otimes \sigma^z \right). \quad (4.33)$$

To find out if the reasonable candidate $\tilde{\sigma}_\beta$ is indeed the nearest separable state, according to Lemma 4.1 we have to check if the operator

$$\tilde{C}_{pre}^I = \tilde{\sigma}_\beta - \rho_{\alpha,\beta}^I - \langle \tilde{\sigma}_\beta, \tilde{\sigma}_\beta - \rho_{\alpha,\beta}^I \rangle \mathbb{1}_4, \quad (4.34)$$

where we denote $\rho_{\alpha,\beta}^I$ as the states that lie in region I, is an entanglement witness. The decomposition into Pauli operators yields

$$\tilde{C}_{pre}^I = \frac{1}{4} \left(\alpha - \frac{\beta}{3} - \frac{1}{3} \right) (\mathbb{1}_4 - \sigma^x \otimes \sigma^x + \sigma^y \otimes \sigma^y - \sigma^z \otimes \sigma^z). \quad (4.35)$$

To get an easier expression, the operator (4.35) can be multiplied by any positive scalar, since this only changes the value but not the sign of expectation values. In our region of interest (4.32) the term $1/4(\alpha - \beta/3 - 1/3)$ is always positive and we can multiply \tilde{C}_{pre} with $[1/4(\alpha - \beta/3 - 1/3)]^{-1}$ to obtain

$$\tilde{C}^I = \mathbb{1}_4 - \sigma^x \otimes \sigma^x + \sigma^y \otimes \sigma^y - \sigma^z \otimes \sigma^z, \quad (4.36)$$

which is independent of the parameters α and β . Let us now check the properties (3.12) and (3.13). For the entangled states in Region I we obtain

$$\langle \rho_{\alpha,\beta}^I, \tilde{C}^I \rangle = -3 \left(\alpha - \frac{1}{3} - \frac{\beta}{3} \right) < 0, \quad (4.37)$$

which is negative due to the last inequality in Eq. (4.32), but which has to be negative anyway due to the definition of a geometric operator (see Definition 3.3). The crucial point is to show that property (3.13) is satisfied. But this can be quickly accomplished using Lemma 3.1: The singular values of the correlation coefficient matrix are the absolute values of the coefficients of the $\sigma^i \otimes \sigma^i$ terms: $s_1 = s_2 = s_3 = 1$, and thus according to Lemma 3.1 we have $\text{Tr} \sigma_p \tilde{C}^I \geq 0$ for all product states σ_p and hence also $\text{Tr} \sigma \tilde{C}^I \geq 0$ for all separable states (see Corollary 3.1). Thus \tilde{C}^I is an entanglement witness and therefore (Lemma 4.1) the states $\tilde{\sigma}_\beta$ are the nearest separable states $\sigma_{0,\beta}$ to the entangled states $\rho_{\alpha,\beta}^I$ of region I. Finally for the Hilbert-Schmidt measure we obtain

$$D(\rho_{\alpha,\beta}^I) = \|\sigma_{0,\beta} - \rho_{\alpha,\beta}^I\| = \frac{\sqrt{3}}{2} \left(\alpha - \frac{1}{3} - \frac{\beta}{3} \right). \quad (4.38)$$

4.4.1.2. Region II

The second region of entangled states in the three-parameter family is given by the constraints

$$\alpha \leq \beta + 1, \quad \alpha \geq \frac{1}{3}\beta - \frac{1}{3}, \quad \alpha < -\beta - 1, \quad (4.39)$$

illustrated as Region II in Fig. (4.32). The nearest separable points to the points (α, β) are

$$\begin{pmatrix} \tilde{\alpha} \\ \tilde{\beta} \end{pmatrix} = \begin{pmatrix} 1/3 (-1 + 2\alpha - \beta) \\ 1/3 (-2 - 2\alpha + \beta) \end{pmatrix}, \quad (4.40)$$

they correspond to the states $\tilde{\sigma}_{\alpha,\beta}$ that now depend on both parameters α and β . The geometric operator is then given by

$$\begin{aligned} \tilde{C}_{pre}^{II} &= \tilde{\sigma}_{\alpha,\beta} - \rho_{\alpha,\beta}^{II} - \langle \tilde{\sigma}_{\alpha,\beta}, \tilde{\sigma}_{\alpha,\beta} - \rho_{\alpha,\beta}^{II} \rangle \mathbb{1}_4 \\ &= \frac{1}{12} (-\alpha - \beta - 1) (\mathbb{1} + \sigma^x \otimes \sigma^x - \sigma^y \otimes \sigma^y - \sigma^z \otimes \sigma^z) \end{aligned} \quad (4.41)$$

which is proportional to the simplified form

$$\tilde{C}^{II} = \mathbb{1} + \sigma^x \otimes \sigma^x - \sigma^y \otimes \sigma^y - \sigma^z \otimes \sigma^z. \quad (4.42)$$

We have (cf. the last term in Eq. (4.39))

$$\langle \rho_{\alpha,\beta}^{II}, \tilde{C}^{II} \rangle = \alpha + \beta + 1 < 0, \quad (4.43)$$

and, according to Lemma 3.1, the operator \tilde{C}^{II} (4.42) is an entanglement witness, since the singular values of the correlation coefficient matrix are again $s_1 = s_2 = s_3 = 1$. Therefore, according to Lemma 4.1, the states $\tilde{\sigma}_{\alpha,\beta}$ are the nearest separable states $\sigma_{0;\alpha,\beta}$ and the Hilbert-Schmidt measure of the entangled states in Region II evaluates to

$$D(\rho_{\alpha,\beta}^{II}) = \|\sigma_{0;\alpha,\beta} - \rho_{\alpha,\beta}^{II}\| = \frac{1}{2\sqrt{3}}(-\alpha - \beta - 1). \quad (4.44)$$

4.4.2. Two-qutrit states

The procedure of determining the Hilbert-Schmidt measure, as discussed in the last subsection for the two-parameter family of two-qubit states (4.15), can also be applied to two-qutrits, i.e. 3×3 dimensional systems.

We are interested in the following two-parameter states of two qutrits as a generalization of the qubit case (4.15),

$$\rho_{\alpha,\beta} = \frac{1 - \alpha - \beta}{9} \mathbb{1}_9 + \alpha P_{00} + \frac{\beta}{2} (P_{10} + P_{20}). \quad (4.45)$$

These states are elements of the magic simplex (3.32), and is the two-parameter case of the family of states (3.34), where $\gamma = 0$. The indices n, k can be interpreted as “quantized” phase space coordinates. The Bell states P_{00}, P_{10} and P_{20} lie on a line in this phase space picture of the maximally entangled states and exhibit the same geometry as other lines, see Refs. [10, 11, 12] for details.

Inserting the Bloch vector form of P_{00}, P_{10} and P_{20} (3.33) we find the Bloch decomposition into the Weyl operator basis (see Sec. 2.6) of the two-parameter states (4.45),

$$\rho_{\alpha,\beta} = \frac{1}{9} \left(\mathbb{1}_9 + \left(\alpha - \frac{\beta}{2} \right) U_1 + (\alpha + \beta) U_2 \right), \quad (4.46)$$

where U_1 and U_2 are defined in Eq. (3.50).

The constraints for the positivity requirement ($\rho_{\alpha,\beta} \geq 0$) are

$$\alpha \leq \frac{7}{2}\beta + 1, \quad \alpha \leq -\beta + 1, \quad \alpha \geq \frac{\beta}{8} - \frac{1}{8}, \quad (4.47)$$

and those for positivity under partial transposition are

$$\alpha \leq -\beta - \frac{1}{2}, \quad \alpha \geq \frac{5}{4}\beta - \frac{1}{2}, \quad \alpha \leq \frac{\beta}{8} + \frac{1}{4}. \quad (4.48)$$

The Euclidean picture representing the Hilbert-Schmidt space geometry of the states (4.45) is shown in Fig. 4.4. The parameter coordinate axes are again

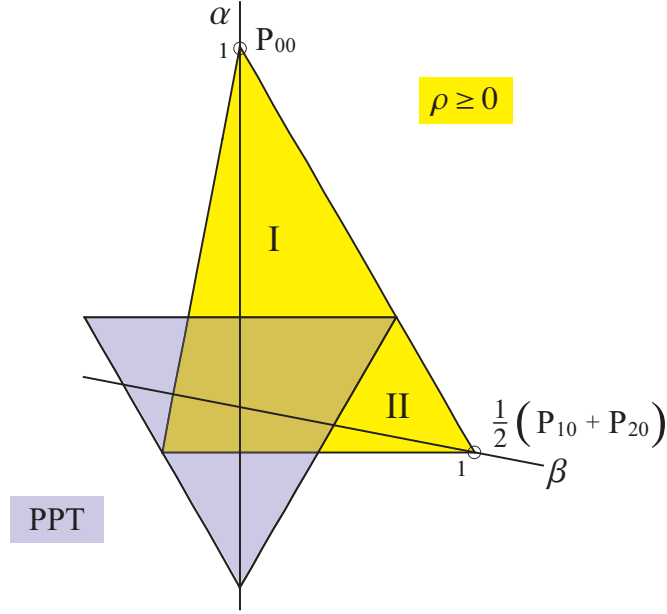


Figure 4.4.: Illustration of the two-qutrit states $\rho_{\alpha,\beta}$ (4.45) and their partial transposition. The regions I and II label the regions where the states are NPT entangled, they are PPT and separable in the overlap with the region of PPT points.

chosen non-orthogonal and not equally scaled to mirror the correct orthogonality conditions in Hilbert-Schmidt space (see Remarks 3.6 and 4.2). We saw in Sec. 3.5.2 that the three-parameter family of states (3.34) does not contain PPT entangled states if it is reduced to the two-parameter case $\gamma = 0$. It is also shown in Ref. [10] that the PPT states $\rho_{\alpha,\beta}$ (4.45) are all separable.

To determine the Hilbert-Schmidt measure for the entangled two-parameter two-qutrit states we apply the same procedure as in Sec. 4.4.1: We determine the states that are the nearest separable ones in the Euclidean sense of Fig. 4.4 and use Lemma 4.1 to check whether these are indeed the nearest separable ones with respect to the whole state space.

4.4.2.1. Region I

First we consider Region I in Fig. 4.4, i.e., the triangle region of entangled states $\rho_{\alpha,\beta}^I$ around the α -axis, constrained by the parameter values

$$\alpha \leq \frac{7}{2}\beta + 1, \quad \alpha \leq -\beta + 1, \quad \alpha > \frac{\beta}{8} + \frac{1}{4}. \quad (4.49)$$

In the Euclidean picture the point that is nearest to a point (α, β) in this region is given by $(\frac{1}{4} + \frac{1}{8}\beta, \beta)$, which corresponds to the separable two-qutrit state

$$\tilde{\sigma}_\beta = \frac{1}{9} \left(\mathbb{1}_9 + \left(\frac{1}{4} - \frac{3}{8}\beta \right) U_1 + \left(\frac{1}{4} + \frac{9}{8}\beta \right) U_2 \right), \quad (4.50)$$

with U_1 and U_2 defined in Eq. (3.50).

For the difference of this state and the entangled states we find

$$\tilde{\sigma}_\beta - \rho_{\alpha,\beta}^I = \frac{1}{9} \left(\frac{1}{4} + \frac{1}{8}\beta - \alpha \right) U, \quad (4.51)$$

where $U = U_1 + U_2$. Using the norm $\|U\| = 3\sqrt{8} = 6\sqrt{2}$ we gain the Hilbert-Schmidt distance

$$\|\tilde{\sigma}_\beta - \rho_{\alpha,\beta}^I\| = \frac{2\sqrt{2}}{3} \left(\alpha - \frac{1}{4} - \frac{1}{8}\beta \right). \quad (4.52)$$

It remains to calculate

$$\langle \tilde{\sigma}_\beta, \tilde{\sigma}_\beta - \rho_{\alpha,\beta}^I \rangle = \text{Tr} \tilde{\sigma}_\beta (\tilde{\sigma}_\beta - \rho_{\alpha,\beta}^I) = -\frac{2}{9} \left(\alpha - \frac{1}{4} - \frac{1}{8}\beta \right) \quad (4.53)$$

to set up the operator

$$\tilde{C}_{pre}^I = \tilde{\sigma}_\beta - \rho_{\alpha,\beta}^I - \langle \tilde{\sigma}_\beta, \tilde{\sigma}_\beta - \rho_{\alpha,\beta}^I \rangle \mathbb{1}_9 = \frac{1}{9} \left(\alpha - \frac{1}{4} - \frac{1}{8}\beta \right) (2\mathbb{1} - U), \quad (4.54)$$

which can be simplified to the parameter-independent operator

$$\tilde{C}^I = 2\mathbb{1} - U. \quad (4.55)$$

To test whether \tilde{C}^I (4.55) represents an entanglement witness we have to check if the operator satisfies the inequalities (3.12) and (3.13). For the first condition we find, as expected (it is already provided by the construction)

$$\langle \rho_{\alpha,\beta}^I, \tilde{C}^I \rangle = -8 \left(\alpha - \frac{1}{4} - \frac{1}{8}\beta \right) < 0. \quad (4.56)$$

To check the second condition (3.13) we use Lemma 3.1. The singular values of the correlation coefficient matrix of \tilde{C}^I are $s_i = |c_{nm}|$, where c_{nm} are the coefficients of the $U_{nm} \otimes U_{nm}$ terms. Since $c_{nm} = 1 \forall n, m$, we have $s_i = 1 \forall i$ and hence $\langle \sigma, \tilde{C} \rangle \geq 0 \forall \sigma \in S$. Thus \tilde{C}^I (4.55) is indeed an entanglement witness and $\tilde{\sigma}_\beta$ is the nearest separable state $\tilde{\sigma}_\beta = \sigma_{0;\beta}$ for the entangled states $\rho_{\alpha,\beta}^{\text{ent}}$ in Region I.

For the Hilbert-Schmidt measure of the entangled two-parameter two-qutrit states (4.45) we find

$$D(\rho_{\alpha,\beta}^I) = \|\sigma_{0;\beta} - \rho_{\alpha,\beta}^I\| = \frac{2\sqrt{2}}{3} \left(\alpha - \frac{1}{4} - \frac{1}{8}\beta \right). \quad (4.57)$$

4.4.2.2. Region II

In Region II of Fig. 4.4 the entangled two-parameter two-qutrit states $\rho_{\alpha,\beta}^{II}$ are constrained by

$$\alpha < \frac{5}{4}\beta - \frac{1}{2}, \quad \alpha \geq \frac{1}{8}\beta - \frac{1}{8}, \quad \alpha \leq -\beta + 1. \quad (4.58)$$

The points that have minimal Euclidean distance to the points (α, β) located in this region are

$$\begin{pmatrix} \tilde{\alpha} \\ \tilde{\beta} \end{pmatrix} = \begin{pmatrix} 1/24 (-2 + 20\alpha + 5\beta) \\ 1/6 (2 + 4\alpha + \beta) \end{pmatrix}, \quad (4.59)$$

and correspond to the states $\tilde{\sigma}_{\alpha,\beta}$. The quantities needed for calculating \tilde{C}^{II} are

$$\tilde{\sigma}_{\alpha,\beta} - \rho_{\alpha,\beta}^{II} = -\frac{1}{72} (4\alpha + 2 - 5\beta) (U_1 - U_2), \quad (4.60)$$

$$\langle \tilde{\sigma}_{\alpha,\beta}, \tilde{\sigma}_{\alpha,\beta}^{II} - \rho_{\alpha,\beta}^{II} \rangle = \frac{1}{36} (4\alpha + 2 - 5\beta), \quad (4.61)$$

so that operator \tilde{C}_{pre}^{II} is expressed in its Weyl operator decomposition as

$$\tilde{C}_{pre}^{II} = \tilde{\sigma}_{\beta} - \rho_{\alpha,\beta}^{II} - \langle \tilde{\sigma}_{\beta}, \tilde{\sigma}_{\beta} - \rho_{\alpha,\beta}^{II} \rangle \mathbb{1}_9 = \frac{1}{72} (-4\alpha - 2 + 5\beta) (2\mathbb{1} + U_1 - U_2), \quad (4.62)$$

or, in the simplified form,

$$\tilde{C}^{II} = 2\mathbb{1} + U_1 - U_2. \quad (4.63)$$

The check of conditions (3.12) for an entanglement witness gives (this is again only a consistency check of the construction)

$$\langle \rho_{\alpha,\beta}^{II}, \tilde{C}^{II} \rangle = 4\alpha + 2 - 5\beta < 0, \quad (4.64)$$

since $4\alpha < 5\beta - 2$, see Eq. (4.58). The singular values of the correlation coefficient matrix are again $s_i = |c_{nm}| = 1 \forall n, m$ and thus, according to Lemma 3.1, we have $\langle \sigma, \tilde{C}^{II} \rangle \geq 0 \forall \sigma \in S$. Therefore \tilde{C}^{II} (4.63) is indeed an entanglement witness and the states $\tilde{\sigma}_{\alpha,\beta}$ are the nearest separable ones $\tilde{\sigma}_{\alpha,\beta} = \sigma_{0;\alpha,\beta}$ to the entangled two-parameter states (4.45) of Region II.

Finally, for the Hilbert-Schmidt measure of these states we find

$$D(\rho_{\alpha,\beta}^{II}) = \|\sigma_{0;\alpha,\beta} - \rho_{\alpha,\beta}^{II}\| = \frac{1}{6\sqrt{2}} (-4\alpha - 2 + 5\beta). \quad (4.65)$$

Another way to derive the nearest separable states for the two-parameter states is to calculate the nearest PPT states with the method of Ref. [131] first and then check if the gained states are separable. If we do so we obtain for the nearest PPT states the same states that we found with the ‘‘guess method’’, and since for the considered cases of two qubits and two qutrits we know that these states are separable, they have to be the nearest separable states.

4.5. Summary and conclusion

In this chapter we extend the application of geometric entanglement witnesses to the field of entanglement quantification, where we show that they are useful to determine the nearest separable state to a given state in the Hilbert-Schmidt metric.

This outlines the fact that geometric entanglement detection and quantification are closely related to each other. We explicitly determine the Hilbert-Schmidt measure of entanglement for the isotropic two-qudit states and two-parameter families of two-qubit and two-qutrit states. To achieve this, we apply the methods derived in Chapters 2 and 3 using Bloch decompositions. In the case of the isotropic two-qudit state, either of the bases studied in Chapter 2 can be used. For the two-parameter family of two-qutrit states, the Weyl operator basis is the best choice, since these states are mixtures of maximally entangled states constructed with the Weyl operators (see Eq. 3.30), and Bloch decompositions can thus be easily obtained. Lemma 3.1 is used to identify the entanglement witnesses.

We use the Hilbert-Schmidt metric for a geometric quantification of entanglement, since it is closely related to the definition of geometric operators (see Ref. [19] for details).

5. Structural multipartite entanglement witnesses

5.1. Introduction

In this chapter we present a construction of multi-qubit entanglement witnesses with linear combinations of operators associated with static structure factors. We give an analytical proof that the operators have a non-negative expectation value for all separable states, using Bloch decompositions of full product states and show examples of genuinely multipartite entangled states that are detected by the witness. With this construction the expectation value of the entanglement witnesses can be measured locally, involving two-point correlations only, but detecting genuinely multipartite entangled states. In this way a connection between diffractive properties of many-body systems and multipartite entanglement is exhibited. The witnesses are appropriate for different physical realizations, e.g. for many-photon systems and solids. Some experiments with photons on the detection of genuine multipartite entanglement in the vicinity of Dicke states have already been performed, as reported in Refs. [79, 140, 104]. Theoretical work on numerical constructions of multi-qubit entanglement witnesses can be found in Refs. [125, 33].

The structure factor we use for the construction of the witness (5.3) is relevant in condensed matter physics in neutron scattering, when probing the magnetization properties of solids. It is related to the neutron scattering cross section and its dynamic formulation describes the “response” of the probed system [91]. Typically, the structure of particular molecules that can be described via Hamiltonians of spin chains, are the interest of experiments [118, 70]. Also much theoretical work on determining the structure factor and the related spectral weights of particular spin chain models has been done, numerically and analytically [8, 56, 55, 99]. Moreover, the structure factor plays an important role in the physics of ultracold atoms in optical lattices since it is related to the visibility of the interference pattern [50]. One-particle spectral functions that are related to the structure factor are investigated for various materials in [77, 117, 82].

For constructions of inequalities for multipartite entanglement detection with collective spin measurements (so-called spin-squeezing inequalities), see Refs. [121, 124, 123, 54]. A macroscopic entanglement witness that also uses two-point correlations is provided by the magnetic susceptibility, see Ref. [141].

The chapter is organized as follows: In Sec. 5.2 we shortly generalize the definition of entanglement to multipartite systems. In Sec. 5.3 we introduce the

construction of multi-qubit entanglement witnesses, which we call *structural entanglement witnesses* and give an analytical proof that they have a positive expectation value for all fully separable states. Moreover, we show that the entanglement witnesses detect so-called *Dicke states* and *Dicke-like* states with changed phases of the constituting terms and give relations to the robustness of the witnesses if these states are subjected to white noise. Dicke states are useful in applications of quantum networking protocols [104]. In Sec. 5.3.2 we provide an alternative construction for particular structural entanglement witnesses via symmetric two-qubit Bell states, for the case of three qubits, which is investigated in detail, and for the general case of N qubits. We close the chapter with summary and conclusion in Sec. 5.4.

The chapter is based on Ref. [84]:

- Philipp Krammer, Hermann Kampermann, Dagmar Bruß, Reinhold A. Bertlmann, Leong C. Kwek, and Chiara Macchiavello
Multipartite entanglement witnesses via structure factors
e-print arXiv:0904.3860 (submitted)

5.2. Multipartite generalization of the entanglement definition

In order to study entanglement properties of multipartite systems, we have to generalize the definitions of entanglement and separability given in Sec. 1.3 for bipartite systems to multipartite systems. A multipartite vector state of a quantum system consisting of N parties is an element of the Hilbert-Schmidt space $\mathcal{H}^D = \mathcal{H}^{d_1} \otimes \mathcal{H}^{d_2} \otimes \dots \otimes \mathcal{H}^{d_N}$ with $D = d_1 d_2 \dots d_N$. A *full product vector state* is defined as

$$|\psi_p\rangle = |\psi_1\rangle \otimes |\psi_2\rangle \otimes \dots \otimes |\psi_N\rangle. \quad (5.1)$$

Definition 5.1. A vector state $|\psi\rangle \in \mathcal{H}^D$ that is not a full product vector state, i.e. that cannot be written in the form of Eq. (5.1), is called *entangled*.

This definition of entanglement is the obvious generalization of the bipartite case. There are, however, different notions of entanglement for multipartite systems of more than two parties. This is intuitively clear, since the entanglement can manifest itself between two, three, \dots , N subsystems. Thus one can define the entanglement of vector states as the entanglement between those subsystems that cannot be written as a product vector state. If we cannot write a state $|\psi\rangle$ as any product between any of the subsystems, it is called *genuinely multipartite entangled* (GME). Even the genuinely multipartite entangled states can be classified according to possible *statistical local operations and classical communication* (SLOCC). For vector states of three particles this leads to two different classes of GME states, called *W* class and *Greenberger-Horne-Zeilinger* (GHZ) class [46]

(see also Sec. 5.3.2.1). According to the same classification, four particles can be entangled in nine inequivalent ways, as shown in Ref. [132].

For density operators a *fully separable state* is defined as

$$\sigma = \sum_i p_i \rho_i^1 \otimes \rho_i^2 \otimes \dots \otimes \rho_i^N, \quad p_i \geq 0, \quad \sum_i p_i = 1, \quad (5.2)$$

and we can accordingly define entangled density operators.

Definition 5.2. A state $\rho \in \mathcal{A}^D$ that is not a separable state, i.e. that cannot be written in the form of Eq. (5.2), is called *entangled*.

For density operators, the notion of entanglement between a given number of particles is more involved than for vector states. A density operator is usually defined as separable with respect to a fixed number k of subsystems if it can be written as a mixture of product states between k subsystems [69]. Thus, there is entanglement between $N - k$ subsystems. This notion of multipartite entanglement is however not completely satisfactory, since it is not clear which particular subsystems share the entanglement. A definition of separability and entanglement for density operators that distinguishes between concrete subsystems is given in Ref. [59]. Nevertheless, in the literature one calls a density operator GME if it cannot be decomposed into vector states that contain tensor products between any subsystems.

In the case of three particles, the classification into classes according to SLOCC operations for vector states can be generalized to density operators, as done in Ref. [1].

5.3. A construction of multi-qubit entanglement witnesses

5.3.1. Construction with structure factors

We consider a multi-qubit quantum system, i.e. a system consisting of N two-level subsystems, which is described by N -qubit states on the Hilbert space $\mathcal{H}_1 \otimes \mathcal{H}_2 \otimes \dots \otimes \mathcal{H}_N$ of dimension $2 \times 2 \times \dots \times 2$. The physical realization of the system can be manifold, e.g. photons in horizontal or vertical polarization, or chains of spin-1/2 particles.

To construct an entanglement witness, we use a quantity known in condensed matter physics as the static structure factor (apart from a different summation and normalization, this form appears in, e.g., Ref. [55]),

$$S^{\alpha\beta}(k) = \sum_{i < j} e^{ik(r_j - r_i)} \langle \sigma_i^\alpha \sigma_j^\beta \rangle, \quad (5.3)$$

where i, j denote the i -th and j -th spins on the one-dimensional chain, r_i, r_j their positions, and $\alpha, \beta = x, y, z$ (the usual Pauli spin-1/2 operators). The structure

factor operator is defined as

$$\hat{S}^{\alpha\beta}(k) := \sum_{i<j} e^{ik(r_i-r_j)} \sigma_i^\alpha \sigma_j^\beta, \quad (5.4)$$

i.e. the static structure factor without considering the expectation value. For periodic systems such as, e.g., spin chains, k is the wave-vector transfer in scattering experiments, and the structure factor can be determined as a function of k . The distance between spins is either defined via the periodic structure, where for two neighboring spins we normalize it to 1, or - in a non-periodic situation, like e.g. for entangled photons - via the labels of the spins. The two-qubit correlation term $\sigma_i^\alpha \sigma_j^\beta$ denotes the tensor product of the σ_α operator at the i -th position, the σ_β operator at the j -th position, and of the identity operators at the other positions. Note that for $\alpha = \beta$ and $k = 0$ we can also express the structure factor operator with the collective spin operator,

$$J_\alpha := 1/2 \sum_{k=1}^N \sigma_k^\alpha. \quad (5.5)$$

The relation to the structure factor operator is

$$\hat{S}^{\alpha\alpha}(0) = (4J_\alpha^2 - N\mathbb{1}_N)/2, \quad (5.6)$$

where $\mathbb{1}_N$ is the identity operator on the 2^N -dimensional Hilbert space.

Definition 5.3. We define a *structural entanglement witness* using the structure factor operator as

$$W(k) := \mathbb{1}_N - \Sigma(k), \quad (5.7)$$

where

$$\begin{aligned} \Sigma(k) &= \frac{1}{B(N,2)} \left(c_x \hat{S}^{xx}(k) + c_y \hat{S}^{yy}(k) + c_z \hat{S}^{zz}(k) \right), \\ c_i &\in \mathbb{R}, \quad |c_i| \leq 1, \quad k = n\pi, \quad n \in \mathbb{N}^0. \end{aligned} \quad (5.8)$$

Here the restriction to real coefficients c_i and integers n ensures that the operator is Hermitian, and $B(N,2)$ is the binomial coefficient, with $B(N,2) = N(N-1)/2$. Non-integer values of n would in general lead to non-Hermitian operators $\Sigma(k)$ and would thus be not appropriate to use as entanglement witnesses. In principle, one could also construct the witness with arbitrary real values of c_i , but this would have to be considered in an additional factor $1/\max(|c_x|, |c_y|, |c_z|)$ of $\Sigma(k)$, which leads to the same expression as normalizing the coefficients beforehand. The meaning of the parameter k depends on the physical system: For the detection of entanglement for states of multiple photons, it just fixes a sign rule for the two-point correlation terms of the witness and has no further physical meaning. For spin chains, as mentioned, k is the wave vector transfer in scattering experiments. Here the entanglement witness can be determined via a readout of values of the structure factor for various k .

The expectation value of the witness (5.7) is

$$\langle W(k) \rangle = 1 - \langle \Sigma(k) \rangle. \quad (5.9)$$

It remains to show that $W(k)$ is an entanglement witness.

Proof. The crucial point is to show that for all full product states

$$\sigma_p^N := \rho_1 \otimes \rho_2 \otimes \dots \otimes \rho_N \quad (5.10)$$

we have $\langle W(k) \rangle_{\sigma_p^N} \geq 0$, or, equivalently, $\langle \Sigma(k) \rangle_{\sigma_p^N} \leq 1$ (cf. Corollary 3.1 which is easily generalized for multipartite full product states). It is helpful to remember the Bloch decomposition for a qubit density operator (2.2), and use it for any of the terms of the product state σ_p^N ,

$$\rho_i = \frac{1}{2} \left(\mathbb{1} + \sum_{\alpha} n_{\alpha}^i \sigma^{\alpha} \right), \quad (n_x^i)^2 + (n_y^i)^2 + (n_z^i)^2 \leq 1. \quad (5.11)$$

The product state σ_p^N should then be regarded as a product of Bloch decompositions (5.11). In this way we obtain the following bound on the expectation value of $\Sigma(k)$ for product states:

$$\begin{aligned} |\langle \Sigma(k) \rangle_{\rho_p^N}| &= \\ &= \frac{1}{B(N, 2)} \left| \sum_{i < j} \left(c_x e^{ikm_{ij}} \langle \sigma_i^x \sigma_j^x \rangle + c_y e^{ikm_{ij}} \langle \sigma_i^y \sigma_j^y \rangle + c_z e^{ikm_{ij}} \langle \sigma_i^z \sigma_j^z \rangle \right) \right| \\ &= \frac{1}{B(N, 2)} \left| \sum_{i < j} \left(c_x e^{ikm_{ij}} n_x^i n_x^j + c_y e^{ikm_{ij}} n_y^i n_y^j + c_z e^{ikm_{ij}} n_z^i n_z^j \right) \right| \\ &\leq \frac{1}{B(N, 2)} \sum_{i < j} (|n_x^i| |n_x^j| + |n_y^i| |n_y^j| + |n_z^i| |n_z^j|) \leq 1, \end{aligned} \quad (5.12)$$

where $m_{ij} = r_j - r_i \in \mathbb{N}$.

Thus, for full product states we have

$$\langle W_{gen} \rangle_{\rho_p^N} \geq 0. \quad (5.13)$$

□

Remark 5.1. Note that one could construct the structural witness (5.7) in an even more general way, where the argumentation of Eq. (5.12) would be still valid: the two-point correlation terms of $\hat{S}^{\alpha\beta}$ could be summed up with arbitrary signs, and/or one could construct $W(k)$ with cyclic permutations of x, y , and z , e.g. \hat{S}^{xy} , \hat{S}^{yz} , and \hat{S}^{zx} . At the moment it is open if this would lead to advantages, the structure of the obtained witnesses would be, however, less easy to investigate.

5.3.1.1. Detecting entanglement with $W(0)$

Which states can be detected by $W(k)$? For $k = 0$ symmetric states like the Dicke states can be detected. These states are defined as pure states that are a superposition of all possible permutations of l excitations (states $|1\rangle$) in N particles [116] and denoted as $|N, l\rangle$. Examples are the W state

$$|W\rangle = |3, 1\rangle = 1/\sqrt{3}(|001\rangle + |010\rangle + |100\rangle) \quad (5.14)$$

or the four-particle Dicke state

$$|4, 2\rangle = 1/\sqrt{6}(|0011\rangle + |0110\rangle + |1100\rangle + |1001\rangle + |1010\rangle + |0101\rangle). \quad (5.15)$$

Dicke states are detected by the witness (5.7) with $c_x = c_y = 1, c_z = -1$. To see this, we calculate the expectation value $\langle \Sigma(0) \rangle$ of Eq. (5.8) for the Dicke states $|N, l\rangle$. Entanglement is detected if $\langle N, l | \Sigma(0) | N, l \rangle > 1$. For the term $S^{zz}(0)$ we get

$$\langle N, l | \hat{S}^{zz}(0) | N, l \rangle = (4\langle J_z^2 \rangle - N)/2 = ((N - 2l)^2 - N)/2, \quad (5.16)$$

where we just count the excitations of each term in $|N, l\rangle$ with a negative sign in the collective spin expectation value $\langle J_z \rangle$. To obtain $\langle N, l | \hat{S}^{xx}(0) | N, l \rangle$, remember that σ^x flips spins and that the terms in the expectation value only give a nonzero contribution if a $|0\rangle$ spin and a $|1\rangle$ spin are flipped. With l excitations this can happen $l(N - l)$ times, thus

$$\langle N, l | \hat{S}^{xx}(0) | N, l \rangle = l(N - l). \quad (5.17)$$

For $\langle N, l | \hat{S}^{yy}(0) | N, l \rangle$ we also get $l(N - l)$ since with two σ^y operators acting on $|0\rangle$ and $|1\rangle$ the additional phases after the flip cancel out. In total we have

$$\begin{aligned} \langle N, l | \Sigma(0) | N, l \rangle &= \frac{2}{N(N - 1)} \left(c_x l(N - l) \right. \\ &\quad \left. + c_y l(N - l) + c_z \frac{(N - 2l)^2 - N}{2} \right). \end{aligned} \quad (5.18)$$

For $c_x = c_y = 1, c_z = -1$ we write $\tilde{\Sigma}(0)$ and get

$$\langle N, l | \tilde{\Sigma}(0) | N, l \rangle = \frac{4l(N - l) - (N - 2l)^2 + N}{N(N - 1)}. \quad (5.19)$$

In particular, for an even particle number N and $l = N/2$ the expectation value (5.19) becomes

$$\langle \tilde{\Sigma}(0) \rangle_{\text{even}} = (N + 1)/(N - 1) > 1 \quad (5.20)$$

and for odd N and $l = (N - 1)/2$ or $l = (N + 1)/2$ we get

$$\langle \tilde{\Sigma}(0) \rangle_{\text{odd}} = (N(N + 1) - 2)/N(N - 1) > 1, \quad (5.21)$$

and thus these states are always detected. It can be seen, however, that for $N \rightarrow \infty$ we have $\langle \tilde{\Sigma}(0) \rangle \rightarrow 1$ and thus with increasing particle number it gets

more and more difficult to detect the entanglement of these Dicke states. Also other Dicke states are detected, e.g. $|6, 2\rangle$ where $\langle 6, 2 | \tilde{\Sigma}(0) | 6, 2 \rangle = 17/15 \geq 1$.

Choosing different coefficients in the construction of the witness (5.7), states different from Dicke states can be detected. An interesting example for four particles is the superposition between two Greenberger-Horne-Zeilinger (GHZ) states,

$$\frac{\cos \theta}{2}(|0011\rangle + |1100\rangle) \pm \frac{\sin \theta}{2}(|0000\rangle + |1111\rangle). \quad (5.22)$$

This state is detected for $\pi/4 < \theta < \pi/2$ if we choose $c_x = -1, c_y = c_z = 1$ (minus sign) or $c_x = 1, c_y = -1, c_z = 1$ (plus sign). In Ref. [136] an experimental preparation of a four-qubit cluster state is reported, and from the presented method it seems likely that also the above GHZ superposition states can be prepared with this setup. Other detected symmetric states are superpositions of Dicke and GHZ states, e.g., for four particles

$$\cos \theta |4, 2\rangle \pm \frac{\sin \theta}{\sqrt{2}}(|0000\rangle + |1111\rangle) \quad (5.23)$$

is detected for $\arccos 3\sqrt{2/19} < \theta < \pi/2$ with the witness coefficients $c_x = -1, c_y = c_z = 1$ (minus sign) and $c_x = 1, c_y = -1, c_z = 1$ (plus sign).

5.3.1.2. Detecting entanglement with $W(\pi)$

So far we have considered the case $k = 0$ only. If we choose $k = \pi$ in the construction of the witness $W(k)$ (5.7), still more entangled states can be detected. Note that in this case the witness is no longer symmetric under particle exchange. An example of detected states are non-symmetric Dicke states with additional phases. Choosing $W(\pi)$ with $c_x = c_y = c_z = 1$ we can detect the four-particle entangled state

$$|D_4^{ph}\rangle = \frac{1}{\sqrt{6}}(|0011\rangle + |1100\rangle + |0110\rangle + |1001\rangle - |0101\rangle - |1010\rangle). \quad (5.24)$$

For six particles and $W(\pi)$ with $c_x = c_y = c_z = 1$ again, the state

$$\begin{aligned} |D_6^{ph}\rangle = & \\ & \frac{1}{\sqrt{20}} (|111000\rangle + |001110\rangle + |010101\rangle + |011010\rangle \\ & + |100011\rangle + |100110\rangle + |101001\rangle + |101100\rangle \\ & + |110010\rangle + |001011\rangle - |000111\rangle - |110001\rangle \\ & - |101010\rangle - |100101\rangle - |011100\rangle - |011001\rangle \\ & - |010110\rangle - |010011\rangle - |001101\rangle - |110100\rangle) \end{aligned} \quad (5.25)$$

is detected. In general, all ‘‘phased’’ Dicke states $|N, l^{ph}\rangle$, i.e. Dicke states with different signs before terms that correspond to even and odd permutations of 0s

and 1s, and with $l = N/2$ for even N and $l = (N + 1)/2$ or $l = (N - 1)/2$ for odd N , are detected. Consider, e.g., the state $|6, 3^{ph}\rangle = |D_6^{ph}\rangle$ (5.25). Starting with the state $|111000\rangle$, all even permutations, i.e. an even number of transpositions of neighboring spins, have a positive sign, and all odd permutations have a negative sign. This scheme can be generalized to construct the general phased Dicke states $|N, l^{ph}\rangle$ of N particles and l excitations. The states $|N, l^{ph}\rangle$ for the mentioned particular values of l are already detected by the witness $W(\pi)$ with $c_x = c_y = 1, c_z = 0$. This can be seen as follows:

To determine $\langle N, l^{ph} | \hat{S}^{xx}(\pi) | N, l^{ph} \rangle$ we note that again we only get a nonzero contribution of each of the $\sigma_i^x \sigma_j^x$ terms if a $|0\rangle$ and a $|1\rangle$ spin are flipped. If this is the case, let us furthermore distinguish two different cases. First, if the spin flip acts on a term with positive (negative) sign and results in a term with positive (negative) sign in the state $|N, l^{ph}\rangle$, then the resulting state could be obtained with an even number of transpositions, which is equivalent to an even distance $r_j - r_i$, and thus $\sigma_i^x \sigma_j^x$ in $\hat{S}^{xx}(\pi)$ has a positive sign. Thus we get a positive overall sign for this particular term. Second, if the spin flip acts on a term with positive (negative) sign and results in a term with negative (positive) sign in the state $|N, l^{ph}\rangle$, then the resulting state could be obtained with an odd number of transpositions, which is equivalent to an odd distance $r_j - r_i$, and thus the sign of the resulting state is changed, yielding again an overall positive sign for this term. Thus, thanks to the changing signs in the terms of $\hat{S}^{xx}(\pi)$ and $\hat{S}^{yy}(\pi)$, all the negative signs cancel out, and we obtain

$$\langle N, l^{ph} | \hat{S}^{xx}(\pi) | N, l^{ph} \rangle = \langle N, l^{ph} | \hat{S}^{yy}(\pi) | N, l^{ph} \rangle = l(N - l), \quad (5.26)$$

just as for the Dicke states $|N, l\rangle$ in the previous paragraph. For phased Dicke states with even N and $l = N/2$ and for $\Sigma(\pi)$ with $c_x = c_y = 1, c_z = 0$ we get

$$\langle \Sigma(\pi) \rangle = 2\langle \hat{S}^{xx}(\pi) \rangle = N/(N - 1) > 1, \quad (5.27)$$

and for odd N with $l = (N + 1)/2$ or $l = (N - 1)/2$ we obtain

$$\langle \Sigma(\pi) \rangle = (N + 1)/N > 1. \quad (5.28)$$

Therefore these states are always detected. Note that an additional term $\hat{S}^{zz}(\pi)$ in $\Sigma(\pi)$, now with a positive sign, i.e. $c_z = 1$, can again improve the amount of violation of $\langle \Sigma(\pi) \rangle \leq 1$. This is the case for the state $|D_4^{ph}\rangle$, for which $\langle \hat{S}^{zz}(\pi) \rangle = 2/3$ and thus $\langle \Sigma(\pi) \rangle = 13/9 > 4/3$, and also for $|D_6^{ph}\rangle$, where $\langle \hat{S}^{zz}(\pi) \rangle = 3/5$ and $\langle \Sigma(\pi) \rangle = 31/25 > 6/5$.

The general phased Dicke states $|N, l^{ph}\rangle$ that include the states (5.24) and (5.25) are not detected by $W(0)$ for any choice of the coefficients c_x, c_y , and c_z , and $W(\pi)$ does not detect the ‘‘usual’’ Dicke states.

5.3.1.3. Robustness against noise

Furthermore, we want to study the robustness of the witness in Eq. (5.7) under the influence of noise. In particular, we consider two depolarizing channels, one

that acts collectively on all qubits, which efficiently results in the addition of white noise to the multipartite state, and one that affects the single qubits *independently*, i.e. that adds white noise to a single qubit ρ_s ; $\rho_{s,dp} = (1-q)\rho_s + q\mathbb{1}/2$.

We study the collective depolarizing channel first. The Dicke states $|N, N/2\rangle$ then change accordingly to

$$p\mathbb{1}_{N/2^N} + (1-p)|N, N/2\rangle\langle N, N/2|. \quad (5.29)$$

The witness $W(0)$ with $c_x = c_y = 1, c_z = -1$ detects entanglement of this state for $0 \leq p < 2/(N+1)$. The robustness decreases with a growing number of qubits N . In Ref. [122], the robustness of certain witnesses against the collective depolarizing channel, corresponding to $c_z = 0$, has been studied. These witnesses, that can detect Dicke states of the form $|N, N/2\rangle$, allow noise with $p < 1/N$. Thus, adding the z -direction measurement to the witness improves its robustness against white noise. For the general ‘‘phased’’ Dicke states and using the witness $W(\pi)$ with $c_x = c_y = 1$ and $c_z = 0$, we obtain $0 \leq p < 1/N$ for entanglement detection. Again, a greater robustness can be achieved when an additional z -direction term, $c_z = 1$, is introduced. For the noisy ‘‘phased’’ Dicke state (cf. Eq. (5.24)), i.e.

$$p\mathbb{1}/16 + (1-p)|D_4^{ph}\rangle\langle D_4^{ph}|, \quad (5.30)$$

the witness $W(\pi)$ with $c_x = c_y = c_z = 1$ detects entanglement of this state for $0 \leq p < 4/13$. In the case of six particles, it detects entanglement of the noisy state

$$p\mathbb{1}/2^6 + (1-p)|D_6^{ph}\rangle\langle D_6^{ph}| \quad (5.31)$$

(cf. Eq. (5.25)) for a parameter interval $0 \leq p < 6/31$. The maximal values of p are in both cases bigger than $1/N$.

In the following we investigate the robustness for the individual depolarizing channel, where the noise affects each qubit independently. Since we are interested in expectation values only, it is convenient to shift the influence of the Kraus operators K_i characterizing the noise model (see Ref. [97]) to the observable and leave the initial state unchanged. This is possible, because in the operator sum representation of the channel we have (where the subscript dp denotes affection by the channel)

$$\mathrm{Tr}(O\rho_{dp}) = \sum_i \mathrm{Tr}(OK_i\rho K_i^\dagger) = \sum_i \mathrm{Tr}(K_i^\dagger OK_i\rho) = \mathrm{Tr}(O_{dp}\rho). \quad (5.32)$$

Since the individual depolarizing channel transforms the Pauli operators as [33]

$$\sigma_{dp}^\alpha = (1-q)\sigma^\alpha, \quad \alpha = x, y, z, \quad (5.33)$$

the two-point correlation terms of the structure factor simply change to

$$(\sigma_i^\alpha \sigma_j^\beta)_{dp} = (1-q)^2 \sigma_i^\alpha \sigma_j^\beta. \quad (5.34)$$

Thus the observable $\Sigma(k)$ in Eq. (5.8) is influenced by the channel according to $\Sigma(k)_{dp} = (1 - q)^2 \Sigma(k)$, and for the expectation value we have

$$\langle \Sigma(k)_{dp} \rangle = (1 - q)^2 \langle \Sigma(k) \rangle. \quad (5.35)$$

Thus we can determine the robustness of $W(k)$, i.e. the region of q for which $\langle \Sigma(k)_{dp} \rangle > 1$, where entanglement is detected. For the Dicke states $|N, N/2\rangle$ and $c_x = c_y = 1, c_z = -1$ for $W(0)$ we obtain a robustness region $0 \leq q < 1 - \sqrt{(n-1)/(n+1)}$. For the phased Dicke states $|N, N/2^{ph}\rangle$ and $c_x = c_y = 1, c_z = 0$ for $W(\pi)$ we find $0 \leq q < 1 - \sqrt{(n-1)/n}$. For $c_x = c_y = c_z = 1$ and the four and six particle case (see Eqs. (5.24) and (5.25)) we obtain $0 \leq q < 1 - 3/\sqrt{13} \simeq 0.168$ for $|D_4^{ph}\rangle$ and $0 \leq q < 1 - 5/\sqrt{31} \simeq 0.102$ for $|D_6^{ph}\rangle$. Both states exhibit a robustness region that is larger for $c_z = 1$ than for the $c_z = 0$ case, it therefore seems favorable to add the z-direction measurement setting also in the case of the individual depolarizing channel. A detailed noise study for witnesses of Dicke states that includes the amplitude and phase damping channels, in connection with the numerical detection of genuine multipartite entanglement, can be found in Ref. [33].

5.3.2. Construction with symmetric Bell states

Particular structural entanglement witnesses (5.7) for $k = 0$ can be also constructed differently, using mixtures of states where two pairs of spins are in a symmetric Bell state. For simplicity reasons we show this construction method for the case of three qubits first.

5.3.2.1. Bell-state construction for three qubits

Vector states of three qubits can be classified according to the number of particles that are entangled and according to properties under SLOCC transformations (see Ref. [46] for details):

Remark 5.2. Let $|\psi\rangle \in \mathcal{H}^2 \otimes \mathcal{H}^2 \otimes \mathcal{H}^2$ be an arbitrary vector state of three qubits. If the reduced density operators ρ_A, ρ_B and ρ_C of $|\psi\rangle$ are all mixed states ($\text{Tr} \rho_X^2 < 1$, $X = A, B$ or C), then $|\psi\rangle$ is genuinely tripartite entangled. If it additionally has a vanishing three-tangle τ (see Ref. [38]), it belongs to the W class, if $\tau > 0$, it belongs to the GHZ class¹. If only two reduced density operators are mixed states, $|\psi\rangle$ is biseparable (only two particles are entangled), and if all three reduced density operators are pure states ($\text{Tr} \rho_X^2 = 1$), then $|\psi\rangle$ is fully separable.

Definition 5.4. We define an entanglement witness for three qubits constructed with symmetric Bell states as

$$W^{\psi_s} := x \mathbb{1}_{ABC} - \bar{\rho}^s, \quad (5.36)$$

¹Vector states of the W class cannot be transformed into states of the GHZ class by SLOCC and vice versa.

where A , B , and C denote the three subsystems, $\mathbb{1}_{ABC}$ is the identity operator on the three-qubit Hilbert space and

$$\bar{\rho}^s := \frac{1}{6} (\mathbb{1}_A \otimes |\psi_s\rangle\langle\psi_s|_{BC} + \mathbb{1}_B \otimes |\psi_s\rangle\langle\psi_s|_{AC} + \mathbb{1}_C \otimes |\psi_s\rangle\langle\psi_s|_{AB}) . \quad (5.37)$$

The vector state $|\psi_s\rangle$ can be one of the three symmetric Bell states (4.16), (4.17), and (4.18). The quantity x is defined as

$$x = \max_{\sigma \in \mathcal{S}} \text{Tr} \sigma \bar{\rho}^s . \quad (5.38)$$

With this construction the expectation value of the witness W^{ψ_s} (5.36) has to be positive for all separable states, as desired. The value of x can be determined in the following way: We first remember (see Corollary 3.1) that in order to find the maximum in (5.38) for all separable states it is enough to check it for pure product states $\sigma_p := |\phi_p\rangle\langle\phi_p|$ with $|\phi_p\rangle := |\phi_A\rangle \otimes |\phi_B\rangle \otimes |\phi_C\rangle$. We have

$$\begin{aligned} \max_{\sigma_p} \text{Tr} \sigma_p \bar{\rho}^s &= \\ \max_{\sigma_p} \frac{1}{6} & \left(\text{Tr} |\phi_A\rangle\langle\phi_A| \text{Tr} (|\phi_B\rangle \otimes |\phi_C\rangle\langle\phi_B| \otimes \langle\phi_C|) |\psi_s\rangle\langle\psi_s| \right. \\ & + \text{Tr} |\phi_B\rangle\langle\phi_B| \text{Tr} (|\phi_A\rangle \otimes |\phi_C\rangle\langle\phi_A| \otimes \langle\phi_C|) |\psi_s\rangle\langle\psi_s| \\ & \left. + \text{Tr} |\phi_C\rangle\langle\phi_C| \text{Tr} (|\phi_A\rangle \otimes |\phi_B\rangle\langle\phi_A| \otimes \langle\phi_B|) |\psi_s\rangle\langle\psi_s| \right) . \end{aligned} \quad (5.39)$$

Now when calculating the maximum of Eq. (5.39) for a given σ_p we first notice that $\text{Tr} |\phi_A\rangle\langle\phi_A| = 1$ and likewise for the subsystems B and C , so that we are only interested in the overlaps $\text{Tr} (|\phi_B\rangle \otimes |\phi_C\rangle\langle\phi_B| \otimes \langle\phi_C|) |\psi_s\rangle\langle\psi_s| = |(\langle\phi_B| \otimes \langle\phi_C|) |\psi_s\rangle|^2$ (and an equivalent expression for permutations of the subsystems). Then, for a particular σ_p we first spot one of the three overlaps that gives the maximal value, without loss of generalization, let us assume it is the first term. Now if $|\phi_B\rangle \neq |\phi_C\rangle$, due to the symmetry of the states $|\psi_s\rangle$, we can always find a product state $|\phi\rangle \otimes |\phi\rangle$, i.e. with the same states of the subsystems, that has the same overlap with $|\psi_s\rangle$ as $|\phi_B\rangle \otimes |\phi_C\rangle$. That means that with the state $|\phi\rangle \otimes |\phi\rangle \otimes |\phi\rangle$ we have the same maximal overlap in all three terms. Thus the maximization procedure reduces to

$$\max_{\sigma_p} \text{Tr} \sigma_p \bar{\rho}^s = \frac{1}{2} \max_{\phi} |(\langle\phi| \otimes \langle\phi|) |\psi_s\rangle|^2 . \quad (5.40)$$

Choosing a general $|\phi\rangle = \alpha|0\rangle + \beta|1\rangle$, $\alpha, \beta \in \mathbb{C}$, we obtain a maximum value

$$x = \max_{\sigma_p} \text{Tr} \sigma_p \bar{\rho}^s = \frac{1}{4} \quad (5.41)$$

for all the three symmetric Bell states $|\psi_s\rangle$, since $\max_{\phi} |(\langle\phi| \otimes \langle\phi|) |\psi_s\rangle|^2 = 1/2$.

To find the entangled states that are detected by a witness W , it is useful to determine its eigensystem, since an entanglement witness always detects the eigenstates $|\lambda_{neg}\rangle$ corresponding to its negative eigenvalues $\lambda_{neg} < 0$, as

$$\langle\lambda_{neg}| W |\lambda_{neg}\rangle = \lambda_{neg} < 0 . \quad (5.42)$$

All states of the subspace spanned by these eigenvectors are also detected, since with $|\psi_{neg}\rangle = \alpha_i|\lambda_{neg}^i\rangle$ we have

$$\langle\psi_{neg}|W|\psi_{neg}\rangle = \sum_i |\alpha_i|^2 \lambda_{neg}^i < 0. \quad (5.43)$$

Also mixtures of eigenvectors to negative eigenvalues,

$$\rho_{neg} = \sum_i p_i |\lambda_{neg}^i\rangle\langle\lambda_{neg}^i|, \quad p_i \geq 0, \sum_i p_i = 1, \quad (5.44)$$

are detected, since

$$\text{Tr}\rho_{neg}W = \sum_i p_i \lambda_{neg}^i < 0. \quad (5.45)$$

In the next paragraphs we want to study which states are detected by the structural witness (5.36) constructed with the three symmetric Bell states by investigating their eigensystems.

The witness $W^{\phi+}$. The witness $W^{\phi+}$, i.e. the witness of Eq. (5.36) with $\psi_s = \phi^+$, has two negative eigenvalues, $\lambda_7^{\phi+} = \lambda_8^{\phi+} = -1/12$. The eigenstates are the two (naturally orthogonal) vector states

$$|\lambda_7^{\phi+}\rangle = \frac{1}{2}|W\rangle + \frac{\sqrt{3}}{2}|111\rangle, \quad (5.46)$$

$$|\lambda_8^{\phi+}\rangle = |\lambda_7^{\phi+}\rangle_{flip} \quad (5.47)$$

where $|W\rangle$ is defined in Eq. (5.14) and *flip* denotes a spin flip in all subsystems. For these two vector states the expectation values of the witness are given by the negative eigenvalues, $\langle\lambda_7^{\phi+}|W|\lambda_7^{\phi+}\rangle = \langle\lambda_8^{\phi+}|W|\lambda_8^{\phi+}\rangle = -1/12$. As mentioned above, superpositions and mixtures of $|\lambda_7^{\phi+}\rangle$ and $|\lambda_8^{\phi+}\rangle$ are also detected and are thus entangled states. The reduced density operators $\rho_X^{\lambda_{7,8}^{\phi+}}$ (with $X = A, B$, or C) of $|\lambda_{7,8}^{\phi+}\rangle\langle\lambda_{7,8}^{\phi+}|$ for the three subsystems all correspond to (the same) mixed states,

$$\begin{aligned} \rho_X^{\lambda_7^{\phi+}} &= \frac{1}{12} (2|0\rangle\langle 0| + 10|1\rangle\langle 1|), \\ \rho_X^{\lambda_8^{\phi+}} &= \frac{1}{12} (10|0\rangle\langle 0| + 2|1\rangle\langle 1|), \end{aligned} \quad (5.48)$$

with $\text{Tr}\rho_X^2 = 13/18 < 1$, and therefore the states $|\lambda_7^{\phi+}\rangle$ and $|\lambda_8^{\phi+}\rangle$ have to be genuinely tripartite entangled. To check if these states and their superpositions belong to the GHZ or W class of genuinely tripartite entangled states, we have to calculate the three-tangle τ [38]. We obtain $\tau > 0$ for $|\lambda_7^{\phi+}\rangle$ and $|\lambda_8^{\phi+}\rangle$ and their superpositions $a|\lambda_7^{\phi+}\rangle + b e^{i\phi}|\lambda_8^{\phi+}\rangle$, $a, b, \phi \in \mathbb{R}$, which thus belong to the GHZ class, except for the state

$$|\psi_W\rangle = \frac{1}{\sqrt{2}}|\lambda_7^{\phi+}\rangle - \frac{1}{\sqrt{2}}e^{i\pi/4}|\lambda_8^{\phi+}\rangle \quad (5.49)$$

which has a vanishing three-tangle $\tau = 0$ and therefore belongs to the W class.

We can also calculate the expectation value of the witness for the more general one-parameter superposition states

$$|\psi_7\rangle = \sqrt{1 - \beta^2}|W\rangle + \beta|111\rangle, \quad \beta \in \mathbb{R}, \quad (5.50)$$

for which we obtain

$$\langle \psi_7 | W^{\phi^+} | \psi_7 \rangle = \frac{1}{6} \left(1 - \beta^2 - \beta \sqrt{3(1 - \beta^2)} \right). \quad (5.51)$$

It is negative for $1/2 < \beta < 1$ and hence detects the entanglement of $|\psi_7\rangle$ for this parameter interval.

Does the witness W^{ϕ^+} also detect biseparable states? It does not detect the biseparable states

$$|\psi_{A-BC}\rangle = (\alpha|0\rangle + \beta|1\rangle) \otimes |\phi^+\rangle, \quad \alpha, \beta \in \mathbb{C}, \quad |\alpha|^2 + |\beta|^2 = 1, \quad (5.52)$$

since we have

$$\langle \psi_{A-BC} | \bar{\rho}^{\phi^+} | \psi_{A-BC} \rangle = \frac{1}{4} (|\alpha|^2 + |\beta|^2) = \frac{1}{4} \quad (5.53)$$

and thus $\langle \psi_{A-BC} | W^{\phi^+} | \psi_{A-BC} \rangle = 0$. But it does detect, e.g., the entanglement of the states

$$\begin{aligned} |\phi_{A-BC}\rangle &= |0\rangle \otimes (a|00\rangle + be^{i\varphi}|11\rangle), \\ a, b, \varphi &\in \mathbb{R}^+, \quad a^2 + b^2 = 1, \quad -\pi \leq \varphi \leq \pi \end{aligned} \quad (5.54)$$

for the parameter intervals $1/\sqrt{1 - \cos^2\varphi} < a < 1$ and $0 \leq |\varphi| < \pi/2$, since here we have

$$\langle \phi_{A-BC} | \bar{\rho}^{\phi^+} | \phi_{A-BC} \rangle = \frac{1}{12} \left(1 + 2a^2 + 2a\sqrt{1 - a^2} \cos\varphi \right) > 1/4 \quad (5.55)$$

and thus $\langle \psi_{A-BC} | W^{\phi^+} | \psi_{A-BC} \rangle < 0$.

The witness W^{ϕ^-} . The witness W^{ϕ^-} , i.e. the witness of Eq. (5.36) with $\psi_s = \phi^-$, also has two negative eigenvalues, $\lambda_7^{\phi^-} = \lambda_8^{\phi^-} = -1/12$. The eigenstates are similar to the ones of W^{ϕ^+} , but have a changed sign before the $|111\rangle$ ($|\lambda_7^{\phi^-}\rangle$) or $|000\rangle$ ($|\lambda_8^{\phi^-}\rangle$) term:

$$|\lambda_7^{\phi^-}\rangle = \frac{1}{2}|W\rangle - \frac{\sqrt{3}}{2}|111\rangle, \quad (5.56)$$

$$|\lambda_8^{\phi^-}\rangle = |\lambda_7^{\phi^+}\rangle_{flip}. \quad (5.57)$$

Again superpositions and mixtures of these states are also detected, the superpositions exhibit the same GHZ or W class properties as for W^{ϕ^+} , where of course $|\lambda_7^{\phi^+}\rangle$ and $|\lambda_8^{\phi^+}\rangle$ are replaced by $|\lambda_7^{\phi^-}\rangle$ and $|\lambda_8^{\phi^-}\rangle$. Then the equivalent states to (5.50) are detected for $-1 < \beta < -1/2$.

The biseparable states

$$|\psi_{A-BC}\rangle = (\alpha|0\rangle + \beta|1\rangle) \otimes |\phi^-\rangle, \quad \alpha, \beta \in \mathbb{C}, \quad |\alpha|^2 + |\beta|^2 = 1, \quad (5.58)$$

are not detected, but the states

$$\begin{aligned} |\phi_{A-BC}\rangle &= |1\rangle \otimes (a|00\rangle - be^{i\varphi}|11\rangle), \\ a, b, \varphi &\in \mathbb{R}^+, \quad a^2 + b^2 = 1, \quad -\pi \leq \varphi \leq \pi \end{aligned} \quad (5.59)$$

are detected for the same parameter intervals of a and φ as in the case of $W^{\phi+}$ (i.e. $1/\sqrt{1 - \cos^2 \varphi} < a < 1$ and $0 \leq |\varphi| < \pi/2$).

The witness $W^{\psi+}$. The witness $W^{\psi+}$, i.e. the witness of Eq. (5.36) with $\psi_s = \psi^+$, has the two negative eigenvalues $\lambda_7^{\psi+} = \lambda_8^{\psi+} = -1/12$ with the eigenstates

$$|\lambda_7^{\psi+}\rangle = |W\rangle, \quad (5.60)$$

$$|\lambda_8^{\psi+}\rangle = |W\rangle_{flip}. \quad (5.61)$$

Of course again superpositions and mixtures of $|\lambda_7^{\psi+}\rangle$ and $|\lambda_8^{\psi+}\rangle$, i.e. superpositions and mixtures of $|W\rangle$ and $|W\rangle_{flip}$ are also detected. Superpositions $\alpha|W\rangle + \beta|W\rangle_{flip}$ always belong to the GHZ class (here the states have a non-vanishing three-tangle) if $\alpha \neq 0$ and $\beta \neq 0$.

$W^{\psi+}$ does not detect the entanglement of the biseparable states

$$|\psi_{A-BC}\rangle = (\alpha|0\rangle + \beta|1\rangle) \otimes |\psi_+\rangle, \quad \alpha, \beta \in \mathbb{C}, \quad |\alpha|^2 + |\beta|^2 = 1, \quad (5.62)$$

but the entanglement of the states

$$\begin{aligned} |\phi_{A-BC}\rangle &= |+\rangle \otimes (a|++\rangle - be^{i\phi}|--\rangle), \\ a, b, \phi &\in \mathbb{R}^+, \quad a^2 + b^2 = 1, \quad -\pi \leq \phi \leq \pi \end{aligned} \quad (5.63)$$

is detected for the parameter intervals $1/\sqrt{1 - \cos^2 \phi} < a < 1$ and $0 \leq |\phi| < \pi/2$. We defined $|+\rangle := 1/\sqrt{2}(|0\rangle + |1\rangle)$ and $|-\rangle := 1/\sqrt{2}(|0\rangle - |1\rangle)$.

5.3.2.2. Bell-state construction for N qubits

The construction of the previous section can be generalized to N qubits.

Definition 5.5. We define the entanglement witness for N qubits as

$$W_N^{\psi_s} := x_N \mathbb{1}_N - \bar{\rho}_N^s, \quad (5.64)$$

where the mixed state $\bar{\rho}_N^s$ is defined as

$$\bar{\rho}_N^s = \frac{1}{2^{N-2} B(N, 2)} \sum_T \mathbb{1}^{\setminus \{i_{N-1}, i_N\}} \otimes |\psi_s\rangle \langle \psi_s|_{i_{N-1} i_N}, \quad (5.65)$$

with $\mathbb{1}^{\setminus i_{N-1}, i_N} = \mathbb{1}_{i_1} \otimes \mathbb{1}_{i_2} \otimes \dots \otimes \mathbb{1}_{i_{N-2}}$. The indices i_1, \dots, i_N denote the position of the spin (i.e. the number of the subsystem) in the chain and are all different, and the sum is taken over all two-party transpositions, i.e. all possible different combinations of the indices $\{i_{N-1}, i_N\}$ for the bipartite symmetric Bell state $|\psi_s\rangle\langle\psi_s|$. The indices are ordered according to $i_1 < i_2 < \dots < i_{N-2}$ and $i_{N-1} < i_N$. The quantity x_N is again defined as

$$x_N = \max_{\sigma \in \mathcal{S}} \text{Tr} \sigma \bar{\rho}_N^s, \quad (5.66)$$

which guarantees that $\text{Tr} W_N^{\psi_s} \geq 0$ for all separable states.

We determine x_N in quite the same way as in the case of three qubits (see Eq. (5.39)). It is again enough to check the condition for product vector states $|\phi_p^N\rangle := |\phi_1\rangle \otimes |\phi_2\rangle \otimes \dots \otimes |\phi_N\rangle$, where we have, with $\sigma_p^N = |\phi_p^N\rangle\langle\phi_p^N|$,

$$\begin{aligned} \max_{\sigma_p^N} \text{Tr} \sigma_p^N \bar{\rho}_N^s &= \\ \max_{\sigma_p^N} \frac{1}{2^{N-2} B(N, 2)} \sum_T & \left(\text{Tr} |\phi_{i_1}\rangle\langle\phi_{i_1}| \text{Tr} |\phi_{i_2}\rangle\langle\phi_{i_2}| \cdots \text{Tr} |\phi_{i_{N-3}}\rangle\langle\phi_{i_{N-3}}| \right. \\ & \left. \cdot \text{Tr} (|\phi_{i_{N-1}}\rangle \otimes |\phi_{i_N}\rangle\langle\phi_{i_{N-1}}| \otimes \langle\phi_{i_N}|) |\psi_s\rangle\langle\psi_s|_{i_{N-1}i_N} \right), \end{aligned} \quad (5.67)$$

which leads to

$$x_N = \max_{\sigma_p} \text{Tr} \sigma_p \bar{\rho}_N^s = \frac{1}{2^{N-2} B(N, 2)} \cdot B(N, 2) \max_{\phi} |(\langle\phi| \otimes \langle\phi|) |\psi_s\rangle|^2 = \frac{1}{2^{N-1}}, \quad (5.68)$$

where we used $\max_{\phi} |(\langle\phi| \otimes \langle\phi|) |\psi_s\rangle|^2 = \frac{1}{2}$.

The three witnesses (5.64) constructed with the three symmetric Bell states are special cases of the structural witness (5.7). In particular, the relations

$$\begin{aligned} W^{\phi^-} &= \frac{1}{2^N} W(0) \quad \text{with } c_x = -1, c_y = 1, c_z = 1, \\ W^{\phi^+} &= \frac{1}{2^N} W(0) \quad \text{with } c_x = 1, c_y = -1, c_z = 1, \\ W^{\psi^+} &= \frac{1}{2^N} W(0) \quad \text{with } c_x = 1, c_y = 1, c_z = -1 \end{aligned} \quad (5.69)$$

hold. Note that the operator W^{ψ^-} would correspond to the case $W(0)$ with $c_x = c_y = c_z = 1$, but it is not an entanglement witness since it is a positive operator and thus does not detect any entangled state.

5.4. Summary and conclusion

In this chapter we consider composite systems of N qubits and construct entanglement witnesses using two-point correlations only, via static structure factors.

We give an analytical proof for identifying the constructed operators as entanglement witnesses, using Bloch decompositions of the full product states. Examples of genuinely multipartite entangled states that are detected by the structural witnesses are presented. We also give relations to the robustness of the witnesses against noise and provide an alternative construction with symmetric two-qubit Bell states. For the case of three particles, we analyze the eigensystems of these alternatively constructed witnesses, and in this way give a detailed description of the detected states.

The presented results for $k = 0$ can be compared with those of Ref. [121], where an inequality similar to the witness $W(0)$ is derived and further reduced to the case of two measurement settings in the x - and y -direction. It is shown that these two settings are enough to detect Dicke states. However, an advantage of adding the z -direction setting is the greater robustness against noise. The general construction with structure factors offers flexible application possibilities for systems different to linear optics, which distinguishes the structural witnesses from spin-squeezing inequalities.

The witnesses are dependent on the wavevector k , and thus detect a variety of different entangled states for the cases $k = 0$ and $k = \pi$, as the Dicke states and a non-symmetric version of the Dicke states, i.e. Dicke states with different phases in the constituting terms.

For particular spin chains the structure factor can be calculated or experimentally obtained, and thus it should be possible to utilize the witness for entanglement investigations of spin chains. Since the witnesses are, however, constructed for a finite number of subsystems, it seems difficult to apply them to macroscopic systems, where one would have to consider the thermodynamical limit. This problem is still under investigation.

6. Conclusion and outlook

In this last chapter final conclusions are drawn and we take an outlook on possible future research on the discussed issues.

In this thesis we show that:

- Bloch decompositions are appropriate to shorten notations and to derive and prove statements involving states and operators, in particular they prove useful in the context of detecting entanglement with entanglement witnesses. We provide decompositions of standard operators into three different suitable operator bases, and therewith a method to decompose operators of arbitrary dimension into these operator bases. We show that particular operator bases are apt for particular intentions, such as the generalized Gell-Mann operator basis is useful with regard to experimental observations, and the Weyl operator basis for states involving generalized Bell states for arbitrary dimensions. The inequalities defining entanglement witnesses are simplified by using Bloch decompositions, where we can make analytical statements if operators of a particular kind satisfy these inequalities.
- Geometric entanglement witnesses are useful tools for detecting entanglement, in particular for detecting bound entanglement. In this respect we develop a shifting method that shifts geometric operators along parameterized lines of states. In this way we can also identify regions of separable states, where we enclose the convex region of separable states for families of states with geometric entanglement witnesses by shifting them from inside the set of separable states to the boundary. To identify the geometric operators as entanglement witnesses, we use inequalities derived with Bloch decompositions.
- Geometric entanglement witnesses are also appropriate to geometrically quantify entanglement. We show that they can be used to find the nearest separable states to entangled states in the Hilbert-Schmidt metric by giving examples for two-qubit, two-qutrit and two-qudit families of states.
- Structural entanglement witnesses are suitable operators to detect genuine multipartite entanglement, for symmetric as well as for non-symmetric states. To identify the constructed operators as entanglement witnesses, again Bloch decompositions turn out to be helpful. We claim that structural witnesses have a connection to the diffractive properties of solids, and

are thus able to detect entanglement for various physical realizations of many-body quantum systems.

What is left for future research? The main part of the thesis investigates entanglement properties of bipartite systems. Therefore it seems natural to look for multipartite extensions. In particular it would be of high interest to extend the methods developed with geometric entanglement witnesses to the case of more parties, and thus be able to characterize entanglement according to different multipartite entanglement classes. The notion of Bloch decompositions, however, does not seem to be as useful as in the bipartite case when the aim is to differentiate not only between fully separable and entangled multipartite states, but also between states that are separable with respect to a certain number of subsystems only. It seems likely that one should be able to obtain bounds by using Bloch decompositions of only partly separable states, such that entanglement can be classified at least above certain thresholds. The shift method can be generalized to the multipartite case in a straightforward way, since it is independent of the number of subsystems.

The structural entanglement witnesses open new possibilities of research in different physical realizations, such as spin chains and solids. As mentioned, the problem evidently lies in the limit of infinitely many particles, as the structural witnesses and the quantities of condensed matter physics scale differently with respect to the particle number. It has to be investigated if this discrepancy can be avoided, either by constructing the witness in a modified way, or by looking at appropriate data that does not necessarily include the thermodynamical limit, but also allows to make statements for a definite number of particles.

A. Appendix

A.1. Proof of the GGB orthogonality conditions

We want to proof the orthogonality condition (2.16) for the generalized Gell-Mann operator basis. Since all generalized Gell-Mann operators are Hermitian (thus $\text{Tr}A_i^\dagger A_j = \text{Tr}A_i A_j = \text{Tr}A_j A_i$) it suffices to proof the following conditions:

$$\text{Tr} \Lambda_s^{jk} \Lambda_s^{mn} = 2 \delta^{jm} \delta^{kn}, \quad (\text{A.1})$$

$$\text{Tr} \Lambda_a^{jk} \Lambda_a^{mn} = 2 \delta^{jm} \delta^{kn}, \quad (\text{A.2})$$

$$\text{Tr} \Lambda^l \Lambda^m = 2 \delta^{lm}, \quad (\text{A.3})$$

$$\text{Tr} \Lambda_a^{jk} \Lambda_s^{mn} = 0, \quad (\text{A.4})$$

$$\text{Tr} \Lambda_s^{jk} \Lambda^m = 0, \quad (\text{A.5})$$

$$\text{Tr} \Lambda_a^{jk} \Lambda^m = 0. \quad (\text{A.6})$$

Proof. (Proof of condition (A.1).) Inserting definition (2.13) we have

$$\begin{aligned} \text{Tr} \Lambda_s^{jk} \Lambda_s^{mn} &= \sum_{l=1}^d \langle l | (|j\rangle\langle k| + |k\rangle\langle j|) (|m\rangle\langle n| + |n\rangle\langle m|) |l\rangle \\ &= \sum_l \left(\langle l|j\rangle\langle k|m\rangle\langle n|l\rangle + \langle l|j\rangle\langle k|n\rangle\langle m|l\rangle \right. \\ &\quad \left. + \langle l|k\rangle\langle j|m\rangle\langle n|l\rangle + \langle l|k\rangle\langle j|n\rangle\langle m|l\rangle \right) \\ &= \delta^{jn} \delta^{km} + \delta^{jm} \delta^{kn} + \delta^{kn} \delta^{jm} + \delta^{km} \delta^{jn} \\ &= 2 \delta^{jm} \delta^{kn}, \end{aligned} \quad (\text{A.7})$$

where we used $\delta^{jn} \delta^{km} = 0$ since we have $j < k$ and $m < n$. □

Proof. (Proof of condition (A.2).) This case is equivalent to the one before apart from changed signs that do not matter,

$$\begin{aligned} \text{Tr} \Lambda_a^{jk} \Lambda_a^{mn} &= -\delta^{jn} \delta^{km} + \delta^{jm} \delta^{kn} + \delta^{kn} \delta^{jm} - \delta^{km} \delta^{jn} \\ &= 2 \delta^{jm} \delta^{kn}. \end{aligned} \quad (\text{A.8})$$

□

Proof. (Proof of condition (A.3).) Without loss of generality we assume $l \leq m$. Using definition (2.15) and defining

$$C_l := \sqrt{\frac{2}{l(l+1)}}, \quad (\text{A.9})$$

we get

$$\begin{aligned} \text{Tr } \Lambda^l \Lambda^m &= C_l C_m \sum_{p=1}^d \left(\sum_{k=1}^l \sum_{n=1}^m \langle p|k\rangle \langle k|n\rangle \langle n|p\rangle \right. \\ &\quad + lm \langle p|l+1\rangle \langle l+1|m+1\rangle \langle m+1|p\rangle \\ &\quad \left. - m \sum_{k=1}^l \langle p|k\rangle \langle k|m+1\rangle \langle m+1|p\rangle - l \sum_{n=1}^m \langle p|l+1\rangle \langle l+1|n\rangle \langle n|p\rangle \right) \\ &= C_l C_m \left(l + lm \delta^{lm} - m \sum_{k=1}^l \delta^{k(m+1)} - l \sum_{n=1}^m \delta^{n(l+1)} \right). \end{aligned} \quad (\text{A.10})$$

Using the relation $\delta^{k(m+1)} = 0$ for $m \geq k$ and

$$l \sum_{n=1}^m \delta^{n(l+1)} = \begin{cases} 0 & \text{if } l = m \\ l & \text{if } l < m \end{cases} \quad (\text{A.11})$$

we obtain

$$\text{Tr } \Lambda^l \Lambda^m = (C_l)^2 l(l+1) \delta^{lm} = 2 \delta^{lm}. \quad (\text{A.12})$$

□

Proof. (Proof of condition (A.4).) Analogously to the proofs (A.7) and (A.8) we find

$$\text{Tr } \Lambda_a^{jk} \Lambda_s^{mn} = i (-\delta^{jn} \delta^{km} + \delta^{jm} \delta^{kn} - \delta^{jm} \delta^{kn} + \delta^{jn} \delta^{km}) = 0. \quad (\text{A.13})$$

□

Proof. (Proof of condition (A.5).) Inserting definitions (2.13) and (2.15) gives

$$\begin{aligned} \text{Tr } \Lambda_s^{jk} \Lambda^m &= C_m \sum_{p=1}^d \left(-m \langle p|k\rangle \langle j|m+1\rangle \langle m+1|p\rangle \right. \\ &\quad \left. - m \langle p|j\rangle \langle k|m+1\rangle \langle m+1|p\rangle \right. \\ &\quad \left. + \sum_{n=1}^m \langle p|j\rangle \langle k|n\rangle \langle n|p\rangle + \sum_{n=1}^m \langle p|k\rangle \langle j|n\rangle \langle n|p\rangle \right) \\ &= -2m \delta^{j(m+1)} \delta^{k(m+1)} + 2 \sum_{l=1}^m \delta^{kl} \delta^{jl} \\ &= 0, \end{aligned} \quad (\text{A.14})$$

since per definition we have $j < k$.

□

Proof. (Proof of condition (A.6).) This proof is equivalent to the previous one since constant factors in front of the terms do not matter. \square

A.2. Derivation of term B in the GGB decomposition of the maximally entangled two-qudit state

To obtain the Bloch vector notation of the term B in the generalized Gell-Mann operator basis (2.65) we insert the standard operator decomposition (2.27) for the case $j = k$. We split the tensor products in the following way:

$$B = \frac{1}{d} \left(B_1 + B_2 + B_3 + B_4 + \frac{1}{d} \mathbb{1} \otimes \mathbb{1} \right), \quad (\text{A.15})$$

where the terms B_1, \dots, B_4 are introduced by (note that $\Lambda^0 = 0$)

$$B_1 = \sum_{j=1}^d \left(\frac{j-1}{2j} \Lambda^{j-1} \otimes \Lambda^{j-1} + \sum_{n(=l)=0}^{d-j-1} \frac{1}{2(j+n)(j+n+1)} \Lambda^{j+n} \otimes \Lambda^{j+n} \right), \quad (\text{A.16})$$

$$\begin{aligned} B_2 = \sum_{j=1}^d \left(- \sum_{l=0}^{d-j-1} \sqrt{\frac{j-1}{4j(j+l)(j+l+1)}} \Lambda^{j-1} \otimes \Lambda^{j+l} \right. \\ \left. - \sum_{n=0}^{d-j-1} \sqrt{\frac{j-1}{4j(j+n)(j+n+1)}} \Lambda^{j+n} \otimes \Lambda^{j-1} \right. \\ \left. + \sum_{n \neq l, n, l=0}^{d-j-1} \frac{1}{2\sqrt{(j+n)(j+n+1)(j+l)(j+l+1)}} \Lambda^{j+n} \otimes \Lambda^{j+l} \right), \end{aligned} \quad (\text{A.17})$$

$$B_3 = \frac{1}{d} \sum_{j=1}^d \left(- \sqrt{\frac{j-1}{2j}} \Lambda^{j-1} \otimes \mathbb{1} + \sum_{n=0}^{d-j-1} \frac{1}{\sqrt{2(j+n)(j+n+1)}} \Lambda^{j+n} \otimes \mathbb{1} \right), \quad (\text{A.18})$$

$$B_4 = \frac{1}{d} \sum_{j=1}^d \left(- \sqrt{\frac{j-1}{2j}} \mathbb{1} \otimes \Lambda^{j-1} + \sum_{l=0}^{d-j-1} \frac{1}{\sqrt{2(j+l)(j+l+1)}} \mathbb{1} \otimes \Lambda^{j+l} \right). \quad (\text{A.19})$$

Only the first term B_1 (A.16) gives a contribution,

$$B_1 = \sum_{m=1}^{d-1} \left(\frac{m}{2(m+1)} + \frac{m}{2m(m+1)} \right) \Lambda^m \otimes \Lambda^m = \frac{1}{2} \sum_{m=1}^{d-1} \Lambda^m \otimes \Lambda^m, \quad (\text{A.20})$$

whereas the remaining terms vanish:

$$\begin{aligned}
B_2 &= \sum_{m < p, m, p=1}^{d-1} \left(-\sqrt{\frac{m}{4(m+1)p(p+1)}} + \frac{m}{\sqrt{4m(m+1)p(p+1)}} \right) \Lambda^m \otimes \Lambda^p \\
&+ \sum_{m > p, m, p=1}^{d-1} \left(-\sqrt{\frac{p}{4(p+1)m(m+1)}} + \frac{p}{\sqrt{4p(p+1)m(m+1)}} \right) \Lambda^m \otimes \Lambda^p \\
&= \left(\sum_{m < p} \frac{-m+m}{2\sqrt{m(m+1)p(p+1)}} + \sum_{m > p} \frac{-p+p}{2\sqrt{m(m+1)p(p+1)}} \right) \Lambda^m \otimes \Lambda^p \\
&= 0,
\end{aligned} \tag{A.21}$$

and in quite the same manner

$$\begin{aligned}
B_3 &= \frac{1}{d} \sum_{m=1}^{d-1} \frac{-m+m}{\sqrt{2m(m+1)}} \Lambda^m \otimes \mathbb{1} = 0, \\
B_4 &= \frac{1}{d} \sum_{p=1}^{d-1} \frac{-p+p}{\sqrt{2p(p+1)}} \mathbb{1} \otimes \Lambda^p = 0.
\end{aligned} \tag{A.22}$$

Thus we find the Bloch decomposition

$$B = \frac{1}{2d} \sum_{m=1}^{d-1} \Lambda^m \otimes \Lambda^m + \frac{1}{d^2} \mathbb{1} \otimes \mathbb{1}. \tag{A.23}$$

A.3. Proof of orthonormality of the WOB

We use Eq. (2.50) to proof the orthogonality (2.45) of the Weyl operators (2.44):

$$\begin{aligned}
\text{Tr } U_{nm}^\dagger U_{lj} &= \sum_{p=0}^{d-1} \sum_{k, \tilde{k}=0}^{d-1} e^{\frac{2\pi i}{d} (\tilde{k}l - kn)} \langle p | (k+m) \bmod d \rangle \langle k | \tilde{k} \rangle \langle (\tilde{k}+j) \bmod d | p \rangle \\
&= \sum_{p=0}^{d-1} \sum_{k, \tilde{k}=0}^{d-1} e^{\frac{2\pi i}{d} (\tilde{k}l - kn)} \langle p | (k+m) \bmod d \rangle \langle (\tilde{k}+j) \bmod d | p \rangle \delta_{k\tilde{k}} \\
&= \sum_{k=0}^{d-1} e^{\frac{2\pi i}{d} k(l-n)} \delta_{mj} \\
&= d \delta_{nl} \delta_{mj}.
\end{aligned} \tag{A.24}$$

Bibliography

- [1] A. Acín, D. Bruß, M. Lewenstein, and A. Sanpera, *Classification of mixed three-qubit states*, Phys. Rev. Lett. **87** (2001), 040401.
- [2] J. B. Altepeter, E. R. Jeffrey, P. G. Kwiat, S. Tanzilli, N. Gisin, and A. Acín, *Experimental methods for detecting entanglement*, Phys. Rev. Lett **95** (2005), 033601.
- [3] A. Aspect, P. Grangier, and G. Roger, *Experimental realization of Einstein-Podolsky-Rosen-Bohm gedankenexperiment: a new violation of Bell's inequalities*, Phys. Rev. Lett. **49** (1982), 91.
- [4] K. Audenaert, F. Verstraete, and B. De Moor, *Variational characterizations of separability and entanglement of formation*, Phys. Rev. A **64** (2001), 052304.
- [5] J. Bae, M. Tiersch, S. Sauer, F. de Melo, F. Mintert, B. Hiesmayr, and A. Buchleitner, *Detection and typicality of bound entangled states*, e-print arXiv:0902.4372.
- [6] L. E. Ballentine, *Quantum mechanics: a modern development*, World Scientific Publishing Co. Pte. Ltd., Singapore, 1998.
- [7] M. Barbieri, F. De Martini, G. Di Nepi, P. Mataloni, G. M. D'Ariano, and C. Macchiavello, *Detection of entanglement with polarized photons: Experimental realization of an entanglement witness*, Phys. Rev. Lett **91** (2003), 227901.
- [8] T. Barnes, J. Riera, and D. A. Tennant, *$S=1/2$ alternating chain using multiprecision methods*, Phys. Rev. B **59** (1999), 11384.
- [9] H. Barnum, E. Knill, G. Ortiz, R. Somma, and L. Viola, *A subsystem-independent generalization of entanglement*, Phys. Rev. Lett. **92** (2004), 107902.
- [10] B. Baumgartner, B. C. Hiesmayr, and H. Narnhofer, *The state space for two qutrits has a phase space structure in its core*, Phys. Rev. A **74** (2006), 032327.
- [11] _____, *A special simplex in the state space for entangled qudits*, J. Phys. A: Math. Theor. **40** (2007), 7919.

- [12] ———, *The geometry of bipartite qutrits including bound entanglement*, Phys. Lett. A **372** (2008), 2190.
- [13] C. H. Bennett, G. Brassard, C. Crépeau, R. Jozsa, A. Peres, and W. K. Wootters, *Teleporting an unknown quantum state via dual classical and Einstein-Podolsky-Rosen channels*, Phys. Rev. Lett. **70** (1993), 1895.
- [14] C. H. Bennett, G. Brassard, S. Popescu, B. Schumacher, J. A. Smolin, and W. K. Wootters, *Concentrating partial entanglement by local operations*, Phys. Rev. A **53** (1996), 2046.
- [15] ———, *Purification of noisy entanglement and faithful teleportation via noisy channels*, Phys. Rev. A **76** (1996), 722.
- [16] C. H. Bennett, D. P. DiVincenzo, T. Mor, P. W. Shor, J. A. Smolin, and B. M. Terhal, *Unextendible product bases and bound entanglement*, Phys. Rev. Lett. **82** (1998), 5385.
- [17] C. H. Bennett, D. P. DiVincenzo, J. A. Smolin, and W. K. Wootters, *Mixed-state entanglement and quantum error correction*, Phys. Rev. A **54** (1996), 3824.
- [18] C. H. Bennett, S. Popescu, D. Rohrlich, J. A. Smolin, and A. V. Thapliyal, *Exact and asymptotic measures of multipartite pure-state entanglement*, Phys. Rev. A **63** (2000), 012307.
- [19] R. A. Bertlmann, K. Durstberger, B. C. Hiesmayr, and P. Krammer, *Optimal entanglement witnesses for qubits and qutrits*, Phys. Rev. A **72** (2005), 052331.
- [20] R. A. Bertlmann and P. Krammer, *Bloch vectors for qudits and geometry of entanglement*, e-print arXiv:0706.1743.
- [21] ———, *Bloch vectors for qudits*, J. Phys. A: Math. Theor. **41** (2008), 235303.
- [22] ———, *Bound entanglement in the set of Bell-state mixtures of two qutrits*, Phys. Rev. A **78** (2008), 014303.
- [23] ———, *Geometric entanglement witnesses and bound entanglement*, Phys. Rev. A **77** (2008), 024303.
- [24] ———, *Entanglement witnesses and geometry of entanglement of two-qutrit states*, Ann. Phys. **324** (2009), 1388.
- [25] R. A. Bertlmann, H. Narnhofer, and W. Thirring, *Geometric picture of entanglement and Bell inequalities*, Phys. Rev. A **66** (2002), 032319.

-
- [26] R. A. Bertlmann and A. Zeilinger (eds.), *Quantum [un]speakables, from Bell to quantum information*, Springer, Berlin, Heidelberg, New York, 2002.
- [27] F. Bloch, *Nuclear induction*, Phys. Rev. **70** (1946), 460.
- [28] M. Bourennane, M. Eibl, C. Kurtsiefer, S. Gaertner, H. Weinfurter, O. Gühne, P. Hyllus, D. Bruß, M. Lewenstein, and A. Sanpera, *Experimental detection of multipartite entanglement using witness operators*, Phys. Rev. Lett. **92** (2004), 087902.
- [29] D. Bouwmeester, A. Ekert, and A. Zeilinger (eds.), *The physics of quantum information: quantum cryptography, quantum teleportation, quantum computation*, Springer, Berlin, Heidelberg, New York, 2000.
- [30] D. Bruß, *Characterizing entanglement*, J. Math. Phys. **43** (2002), 4237.
- [31] D. Bruß, J. I. Cirac, P. Horodecki, F. Hulpke, B. Kraus, M. Lewenstein, and A. Sanpera, *Reflections upon separability and distillability*, J. Mod. Opt. **49** (2002), 1399.
- [32] D. Bruß and Asher Peres, *Construction of quantum states with bound entanglement*, Phys. Rev. A **61** (2000), 030301.
- [33] S. Campbell, M. S. Tame, and M. Paternostro, *Characterizing multipartite symmetric Dicke states under the effects of noise*, e-print arXiv:0903.3939.
- [34] K. Chen and L.-A. Wu, *A matrix realignment method for recognizing entanglement*, Quantum Inf. Comput. **3** (2003), 193.
- [35] D. Chruscinski and A. Kossakowski, *How to construct entanglement witnesses*, J. Phys. A: Math. Theor. **41** (2008), 145301.
- [36] D. Chruscinski and A. O. Pittenger, *Generalized circulant densities and a sufficient condition for separability*, J. Phys. A: Math. Theor. **41** (2008), 385301.
- [37] J. F. Clauser, M. A. Horne, A. Shimony, and R. A. Holt, *Proposed experiment to test local hidden-variable theories*, Phys. Rev. Lett. **23** (1969), 880.
- [38] V. Coffman, J. Kundu, and W. K. Wootters, *Distributed entanglement*, Phys. Rev. A **61** (2000), 052306.
- [39] D. Collins, N. Gisin, N. Linden, S. Massar, and S. Popescu, *Bell inequalities for arbitrarily high-dimensional systems*, Phys. Rev. Lett. **88** (2002), 040404.
- [40] R. Demkowicz-Dobrzanski, A. Buchleitner, M. Kus, and F. Mintert, *Evaluable multipartite entanglement measures: Multipartite concurrences as entanglement monotones*, Phys. Rev. A **74** (2006), 052303.

- [41] D. P. DiVincenzo, T. Mor, P. W. Shor, J. A. Smolin, and B. M. Terhal, *Unextendible product bases, uncompletable product bases and bound entanglement*, Commun. Math. Phys. **238** (2003), 379.
- [42] D. P. DiVincenzo, P. W. Shor, J. A. Smolin, B. M. Terhal, and A. V. Thapliyal, *Evidence for bound entangled states with negative partial transpose*, Phys. Rev. A **61** (2000), 062312.
- [43] W. Dür and J. I. Cirac, *Classification of multiqubit mixed states: Separability and distillability properties*, Phys. Rev. A **61** (2000), 042314.
- [44] W. Dür, J. I. Cirac, M. Lewenstein, and D. Bruß, *Distillability and partial transposition in bipartite systems*, Phys. Rev. A **61** (2000), 062313.
- [45] W. Dür, J. I. Cirac, and R. Tarrach, *Separability and distillability of multi-particle quantum systems*, Phys. Rev. Lett. **83** (1999), 3562.
- [46] W. Dür, G. Vidal, and J. I. Cirac, *Three qubits can be entangled in two inequivalent ways*, Phys. Rev. A **62** (2000), 062314.
- [47] A. Einstein, B. Podolsky, and N. Rosen, *Can quantum-mechanical description of physical reality be considered complete?*, Phys. Rev. **47** (1935), 777.
- [48] U. Fano, *Pairs of two-level systems*, Rev. Mod. Phys. **55** (1983), 855.
- [49] D. I. Fivel, *Remarkable phase oscillations appearing in the lattice dynamics of Einstein-Podolsky-Rosen states*, Phys. Rev. Lett **74** (1995), 835.
- [50] F. Gerbier, A. Widera, S. Fölling, O. Mandel, T. Gericke, and I. Bloch, *Phase coherence of an atomic Mott insulator*, Phys. Rev. Lett **95** (2005), 050404.
- [51] S. Gröblacher, T. Jennewein, A. Vaziri, G. Weihs, and A. Zeilinger, *Experimental quantum cryptography with qutrits*, New J. Phys. **8** (2006), 75.
- [52] O. Guehne, P. Hyllus, D. Bruß, M. Lewenstein A. Ekert, C. Macchiavello, and A. Sanpera, *Detection of entanglement with few local measurements*, Phys. Rev. A **66** (2002), 062305.
- [53] ———, *Experimental detection of entanglement via witness operators and local measurements*, J. Mod. Opt. **50** (2003), 1079.
- [54] O. Gühne and G. Tóth, *Entanglement detection*, Phys. Rep. **474** (2009), 1.
- [55] C. J. Hamer, J. Oitmaa, W. Zheng, and R. H. McKenzie, *Critical behaviour of one-particle spectral weights in the transverse Ising model*, Phys. Rev. B **74** (2006), 060402.

-
- [56] C. J. Hamer, W. Zheng, and R. R. P. Singh, *Dynamical structure factor for the alternating heisenberg chain: A linked cluster calculation*, Phys. Rev. B **68** (2003), 214408.
- [57] B. C. Hiesmayr, F. Hipp, M. Huber, P. Krammer, and Ch. Spengler, *Simplex of bound entangled multipartite qubit states*, Phys. Rev. A **78** (2008), 042327.
- [58] B. C. Hiesmayr and M. Huber, *Multipartite entanglement measure for all discrete systems*, Phys. Rev. A **78** (2008), 012342.
- [59] B. C. Hiesmayr, M. Huber, and P. Krammer, *Two computable sets of multipartite entanglement measures*, Phys. Rev. A **79** (2009), 062308.
- [60] S. Hill and W. K. Wootters, *Entanglement of a pair of quantum bits*.
- [61] M. Horodecki and P. Horodecki, *Reduction criterion of separability and limits for a class of distillation protocols*, Phys. Rev. A **59** (1999), 4206.
- [62] M. Horodecki, P. Horodecki, and R. Horodecki, *Separability of mixed states: necessary and sufficient conditions*, Phys. Lett. A **223** (1996), 1.
- [63] ———, *Inseparable two spin-1/2 density matrices can be distilled to a singlet form*, Phys. Rev. Lett. **78** (1997), 574.
- [64] ———, *Mixed-state entanglement and distillation: Is there a “bound” entanglement in nature?*, Phys. Rev. Lett. **80** (1998), 5239.
- [65] ———, *Mixed-state entanglement and quantum communication*, Quantum Information (G. Alber et al., ed.), Springer Tracts in Modern Physics, vol. 173, Springer Verlag Berlin, 2001, p. 151.
- [66] M. Horodecki and R. Horodecki, *Information-theoretic aspects of inseparability of mixed states*, Phys. Rev. A **54** (1996), 1838.
- [67] P. Horodecki, *Separability criterion and inseparable mixed states with positive partial transposition*, Phys. Lett. A **232** (1997), 333.
- [68] P. Horodecki, M. Horodecki, and R. Horodecki, *Bound entanglement can be activated*, Phys. Rev. Lett. **82** (1999), 1056.
- [69] R. Horodecki, P. Horodecki, M. Horodecki, and K. Horodecki, *Quantum entanglement*, Rev. Mod. Phys. **81** (2009), 865.
- [70] T. Huberman, R. Coldea, R. A. Cowley, D. A. Tennant, R. L. Leheny, R. J. Christianson, and C. D. Frost, *Two-magnon excitations observed by neutron scattering in the two-dimensional spin-5/2 Heisenberg antiferromagnet Rb_2MnF_4* , Phys. Rev. B **72** (2005), 014413.

- [71] P. Hyllus, C. Moura Alves, D. Bruß, and C. Macchiavello, *Generation and detection of bound entanglement*, Phys. Rev. A **70** (2004), 032316.
- [72] P. Hyllus, O. Guehne, D. Bruß, and M. Lewenstein, *Relations between entanglement witnesses and Bell inequalities*, Phys. Rev. A **72** (2005), 012321.
- [73] T. Ichikawa, T. Sasaki, and I. Tsutsui, *Entanglement measures for intermediate separability of quantum states*, Phys. Rev. A **79** (2009), 052307.
- [74] L. M. Ioannou and B. C. Travaglione, *Quantum separability and entanglement detection via entanglement-witness search and global optimization*, Phys. Rev. A **73** (2006), 052314.
- [75] L. M. Ioannou, B. C. Travaglione, D. Cheung, and A. Ekert, *Improved algorithm for quantum separability and entanglement detection*, Phys. Rev. A **70** (2004), 060303.
- [76] L. Jak'obczyk and M. Siennicki, *Geometry of Bloch vectors in two-qubit system*, Phys. Lett. A **286** (2001), 383.
- [77] A. P. Kampf and J. R. Schrieffer, *Spectral function and photoemission spectra in antiferromagnetically correlated metals*, Phys. Rev. B **42** (1990), 7967.
- [78] D. Kaszlikowski, L. C. Kwek, J.-L. Chen, M. Żukowski, and C. H. Oh, *Cluser-horne inequality for three-state systems*, Phys. Rev. A **65** (2002), 032118.
- [79] N. Kiesel, C. Schmid, G. Tóth, E. Solano, and H. Weinfurter, *Experimental observation of four-photon entangled Dicke state with high fidelity*, Phys. Rev. Lett **98** (2007), 063604.
- [80] G. Kimura, *The Bloch vector for n-level systems*, Phys. Lett. A **314** (2003), 339.
- [81] G. Kimura and A. Kossakowski, *The Bloch-vector space for n-level systems: the spherical-coordinate point of view*, Open Sys. Information Dyn. **12** (2005), 207.
- [82] T. Kondo, R. Khasanov, T. Takeuchi, J. Schmalian, and A. Kaminski, *Competition between the pseudogap and superconductivity in the high- T_c copper oxides*, Nature **457** (2009), 296.
- [83] P. Krammer, *Characterizing entanglement with geometric entanglement witnesses*, J. Phys. A: Math. Theor. **42** (2009), 065305.
- [84] P. Krammer, H. Kampermann, D. Bruss, R. A. Bertlmann, L. C. Kwek, and C. Macchiavello, *Multipartite entanglement witnesses via structure factors*, e-print arXiv:0904.3860, submitted.

-
- [85] C. Kruszynska and B. Kraus, *Multipartite entanglement and global information*, e-print arXiv:0808.3862.
- [86] S. Kryszewski and M. Zachciał, *Alternative representation of $n \times n$ density matrix*, e-print quant-ph/0602065.
- [87] J. M. Leinaas, J. Myrheim, and E. Ovrum, *Geometrical aspects of entanglement*, e-print quant-ph/0605079.
- [88] M. Lewenstein, B. Kraus, J. I. Cirac, and P. Horodecki, *Optimization of entanglement witnesses*, Phys. Rev. A **62** (2000), 052310.
- [89] M. Lewenstein, B. Kraus, P. Horodecki, and J. I. Cirac, *Characterization of separable states and entanglement witnesses*, Phys. Rev. A **63** (2001), no. 4, 044304.
- [90] P. J. Love, A. M. van den Brink, A. Y. Smirnov, M. H. S. Amin, M. Grajcar, E. Il'ichev, A. Izmailkov, and A. M. Zagorskin, *A characterization of global entanglement*, Quant. Inf. Process. **6** (2007), 187.
- [91] W. Marshall and S. W. Lovesey, *Theory of thermal neutron scattering: the use of neutrons for the investigation of condensed matter*, Clarendon Press, Oxford, 1971.
- [92] I. P. Mendaš, *The classification of three-parameter density matrices for a qutrit*, J. Phys. A: Math. Gen. **39** (2006), 11313.
- [93] D. A. Meyer and N. R. Wallach, *Global entanglement in multiparticle systems*, J. Math. Phys. **43** (2002), 4273.
- [94] F. Mintert, M. Kuś, and A. Buchleitner, *Concurrence of mixed bipartite quantum states in arbitrary dimensions*, Phys. Rev. Lett. **92** (2004), 167902.
- [95] _____, *Concurrence of mixed multi-partite quantum states*, Phys. Rev. Lett. **95** (2005), 260502.
- [96] H. Narnhofer, *Entanglement reflected in Wigner functions*, J. Phys. A: Math. Gen. **39** (2006), 7051.
- [97] M. Nielsen and I. Chuang, *Quantum computation and quantum information*, Cambridge University Press, Cambridge, England, 2000.
- [98] M. Ozawa, *Entanglement measures and the Hilbert-Schmidt distance*, Phys. Lett. A **268** (2000), 158.
- [99] R. G. Pereira, J. Sirker, J.-S. Caux, R. Hagemans, J. M. Maillet, S. R. White, and I. Affleck, *Dynamical spin structure factor for the anisotropic spin-1/2 Heisenberg chain*, Phys. Rev. Lett **96** (2006), 257202.

- [100] A. Peres, *Separability criterion for density matrices*, Phys. Rev. Lett. **77** (1996), 1413.
- [101] A. O. Pittenger and M. H. Rubin, *Separability and Fourier representations of density matrices*, Phys. Rev. A **62** (2000), 032313.
- [102] ———, *Convexity and the separability problem of quantum mechanical density matrices*, Linear Algebr. Appl. **346** (2002), 47.
- [103] ———, *Geometry of entanglement witnesses and local detection of entanglement*, Phys. Rev. A **67** (2003), 012327.
- [104] R. Prevedel, G. Cronenberg, M. S. Tame, M. Paternostro, P. Walther, M. S. Kim, and A. Zeilinger, *Experimental realization of Dicke states of up to six qubits for multiparty quantum networking*, e-print arXiv:0903.2212.
- [105] E. M. Rains, *Bound on distillable entanglement*, Phys. Rev. A **60** (1999), 179.
- [106] C. Rakotonirina, *Expression of a tensor commutation matrix in terms of the generalized Gell-Mann matrices*, math.GM/0511451.
- [107] M. Reed and B. Simon, *Methods of modern mathematical physics I: functional analysis*, Academic Press, New York and London, 1972.
- [108] G. Rigolin, T. R. de Oliveira, and M. C. de Oliveira, *Operational classification and quantification of multipartite entangled states*, Phys. Rev. A **74** (2006), 022314.
- [109] O. Rudolph, *Further results on the cross norm criterion for separability*, e-print arXiv:quant-ph/0202121.
- [110] ———, *A separability criterion for density operators*, J. Phys. A: Math. Gen. **33** (2000), 3951.
- [111] ———, *Some properties of the computable cross norm criterion for separability*, Phys. Rev. A **67** (2003), 032312.
- [112] P. Rungta, V. Bužek, C. M. Caves, M. Hillery, and G. J. Milburn, *Universal state inversion and concurrence in arbitrary dimensions*, Phys. Rev. A **64** (2001), 042315.
- [113] E. Schrödinger, *Die gegenwärtige Situation in der Quantenmechanik*, Naturwissenschaften **23** (1935), 807, 823, 844.
- [114] P. Skwara, H. Kampermann, M. Kleinmann, and D. Bruß, *Entanglement witnesses and a loophole problem*, Phys. Rev. A **76** (2007), 012312.
- [115] J. A. Smolin, F. Verstraete, and A. Winter, *Entanglement of assistance and multipartite state distillation*, Phys. Rev. A **72** (2005), 052317.

-
- [116] J. K. Stockton, J. M. Geremia, A. C. Doherty, and H. Mabuchi, *Characterizing the entanglement of symmetric many-particle spin-1/2 systems*, Phys. Rev. A **67** (2003), 022112.
- [117] J.-B. Suck, *Inelastic neutron scattering applied to the investigation of collective excitations in topologically disordered matter*, Cond. Mat. Phys. **11** (2007), 7.
- [118] D. A. Tennant, C. Broholm, D. H. Reich, S. E. Nagler, G. E. Granroth, T. Barnes, K. Damle, G. Xu, Y. Chen, and B. C. Sales, *Neutron scattering study of two-magnon states in the quantum magnet copper nitrate*, Phys. Rev. B **67** (2003), no. 5, 054414.
- [119] B. M. Terhal, *Bell inequalities and the separability criterion*, Phys. Lett. A **271** (2000), 319.
- [120] ———, *Detecting quantum entanglement*, Theor. Comput. Sci. **287** (2002), 313.
- [121] G. Tóth, *Detection of multipartite entanglement in the vicinity of symmetric dicke states*, J. Opt. Soc. Am. B **24** (2007), 275.
- [122] G. Tóth and O. Gühne, *Entanglement detection in the stabilizer formalism*, Phys. Rev. A **72** (2005), 022340.
- [123] G. Tóth, C. Knapp, O. Gühne, and H. J. Briegel, *Spin squeezing and entanglement*, Phys. Rev. A **79** (2009), 042334.
- [124] G. Tóth, C. Knapp, O. Gühne, and H. J. Briegel, *Optimal spin squeezing inequalities detect bound entanglement in spin models*, Phys. Rev. Lett **99** (2007), 250405.
- [125] G. Tóth, W. Wieczorek, R. Krischek, N. Kiesel, P. Michelberger, and H. Weinfurter, *Practical methods for witnessing genuine multi-qubit entanglement in the vicinity of symmetric states*, e-print arXiv:0903.3910.
- [126] A. Uhlmann, *Fidelity and concurrence of conjugated states*, Phys. Rev. A **62** (2000), 032307.
- [127] D. A. Varshalovich, A. N. Moskalev, and V. K. Khersonskii, *Quantum theory of angular momentum*, World Scientific Publishing Co. Pte. Ltd., 1988.
- [128] A. Vaziri, G. Weihs, and A. Zeilinger, *Experimental two-photon, three-dimensional entanglement for quantum communication*, Phys. Rev. Lett. **89** (2002), 240401.
- [129] V. Vedral and M. B. Plenio, *Entanglement measures and purification procedures*, Phys. Rev. A **57** (1998), 1619.

- [130] V. Vedral, M. B. Plenio, M. A. Rippin, and P. L. Knight, *Quantifying entanglement*, Phys. Rev. Lett. **78** (1997), 2275.
- [131] F. Verstraete, K. Audenaert, and B. De Moor, *On the geometry of entangled states*, J. Mod. Opt. **49** (2002), 1277.
- [132] F. Verstraete, J. Dehaene, B. De Moor, and H. Verschelde, *Four qubits can be entangled in nine different ways*, Phys. Rev. A **65** (2002), 052112.
- [133] G. Vidal and R. F. Werner, *Computable measure of entanglement*, Phys. Rev. A **65** (2002), 032314.
- [134] K. G. H. Vollbrecht and R. F. Werner, *Why two qubits are special*, J. Math. Phys. **41** (2000), 6772.
- [135] ———, *Entanglement measures under symmetry*, Phys. Rev. A **64** (2001), 062307.
- [136] P. Walther, K. J. Resch, T. Rudolph, E. Schenck, H. Weinfurter, V. Vedral, M. Aspelmeyer, and A. Zeilinger, *Experimental one-way quantum computing*, Nature **434** (2005), 169.
- [137] T.-C. Wei and P. M. Goldbart, *Geometric measure of entanglement and applications to bipartite and multipartite quantum states*, Phys. Rev. A **68** (2003), 042307.
- [138] R. F. Werner, *Quantum states with Einstein-Podolsky-Rosen correlations admitting a hidden-variable model*, Phys. Rev. A **40** (1989), 4277.
- [139] ———, *All teleportation and dense coding schemes*, J. Phys. A: Math. Gen. **34** (2001), 7081.
- [140] W. Wieczorek, R. Krischek, N. Kiesel, P. Michelberger, G. Toth, and H. Weinfurter, *Experimental entanglement of a six-photon symmetric Dicke state*, e-print arXiv:0903.2213.
- [141] M. Wiesniak, V. Vedral, and Č. Brukner, *Magnetic susceptibility as a macroscopic entanglement witness*, N. J. Phys. **7** (2005), 258.
- [142] C. Witte and M. Trucks, *A new entanglement measure induced by the Hilbert-Schmidt norm*, Phys. Lett. A **257** (1999), 14.
- [143] W. K. Wootters, *Entanglement of formation of an arbitrary state of two qubits*, Phys. Rev. Lett. **80** (1998), 2245.

Abstract

Entanglement is a fascinating curiosity of quantum physics that distinguishes it considerably from classical concepts. On the one hand it implicates surprising philosophical aspects such as the incompatibility of local realistic theories with quantum physics, on the other hand it can be successfully implied in quantum information and quantum communication tasks to improve protocols with respect to classical procedures.

It is still an open mathematical problem to determine whether a quantum state is entangled or not; there is no operational procedure for a general state on an arbitrary dimensional Hilbert space. For pure states and lower dimensional bipartite systems, e.g., for two qubits, the problem is solved, since computable necessary and sufficient conditions for separability (i.e. for being not entangled) were found. Moreover, if one seeks to quantify the entanglement of a quantum state, this can be conveniently done for a system of two qubits. For higher dimensional and/or multipartite systems much has been accomplished in the context of entanglement detection and quantification, but the problem cannot be seen as solved at all, and much has still to be investigated.

The aim of this thesis is to present new methods to detect and quantify entanglement for systems beyond two qubits. States of these systems are, as usual, described by density operators that are usually put into matrix notation. For high dimensional and/or multipartite systems, these density matrices can become, however, quite unhandy. A mathematical tool to express density operators in a compact and simpler way is provided by the Bloch vector decomposition. In this notation we decompose the density operator into a complete and orthogonal basis of operators of the operator space. For qubits this notation is well known and usually one uses the Pauli spin-1/2 operators as the operator basis. For qudits, i.e. states of arbitrary dimensional systems, however, there is no unique generalization of the Pauli operator basis. We therefore present three possible choices of operator bases: the generalized Gell-Mann operator basis, the polarization operator basis, and the Weyl operator basis. We furthermore provide a method to find the decomposition of any operator (not necessarily density operators) into one of the three operator bases via the decomposition of so-called standard operators. As an application example of the method we consider the maximally entangled two-qudit state and decompose it according to each basis.

In the context of entanglement detection, entanglement witnesses are an important and frequently used tool. They are observables and detect the entanglement of a state if they reveal a negative expectation value for it, and if at the same time it is known that the expectation value has to be non-negative for all separable

states. This latter condition is, however, in general not straightforward to show. A simplification in this connection is the usage of Bloch decompositions, which offer new relations and help to prove the condition in many cases. A particular class of entanglement witnesses are geometric entanglement witnesses. These allow a direct Euclidean geometrical representation of operator space. We show the importance of these witnesses by giving shift methods that can detect entangled and in particular bound entangled states, and help to determine the set of separable states for convex subsets of states. Examples for a three-parameter family of two-qutrit states are given.

Geometric entanglement witnesses can also be applied for geometrical quantification of entanglement, in particular for determining the Hilbert-Schmidt measure of entanglement. We give examples for the isotropic two-qudit state and two-parameter families of two-qubit and two-qutrit states.

Finally, we address the problem of entanglement detection in multi-qubit systems. In this context we provide a general construction of entanglement witnesses using static structure factors. In solid state physics, structure factors describe dynamical properties of solids in scattering experiments. The structural witnesses can detect many genuinely multipartite entangled states, such as Dicke states and Dicke-like states with changed phases of the constituting terms. Moreover, they contain two-point correlations only and are apt for experimental application for various physical systems.

Zusammenfassung

Verschränkung ist eine faszinierende Eigenart der Quantenphysik, die diese beträchtlich von klassischen Konzepten unterscheidet. Einerseits impliziert Verschränkung überraschende philosophische Aspekte, wie die Unvereinbarkeit von lokal-realistischen Theorien mit der Quantenphysik, andererseits kann sie erfolgreich für Aufgaben der Quanteninformation und Quantenkommunikation verwendet werden, um Protokolle im Hinblick auf klassische Prozeduren zu verbessern.

Es ist noch immer ein offenes mathematisches Problem, herauszufinden, ob ein Quantenzustand verschränkt ist oder nicht; für einen allgemeinen Zustand auf einem beliebig dimensional Hilbertraum gibt es keine operationelle Vorgangsweise. Für reine Zustände und niedrig dimensionale Zweiteilchen-Systeme, z.B. für zwei Qubits, ist dieses Problem gelöst, da berechenbare notwendige und hinreichende Bedingungen für Separabilität (d.h. für Nicht-Verschränktheit) gefunden wurden. Außerdem kann die Verschränkung für ein Zwei-Qubit-System leicht quantifiziert werden. Für höher dimensionale und/oder Mehrteilchen-Systeme wurde in Bezug auf die Bestimmung und Quantifizierung von Verschränkung schon einiges erreicht, allerdings kann das Problem noch nicht als gelöst angesehen werden, vieles ist noch zu erforschen.

In dieser Dissertation werden neue Methoden zur Bestimmung und Quantifizierung von Verschränkung für Systeme, die über Zwei-Qubit-Systeme hinausgehen, präsentiert. Zustände solcher Systeme werden üblicherweise durch Dichteoperatoren beschrieben und in Matrix-Schreibweise verwendet. Für hochdimensionale und/oder Mehrteilchen-Systeme können diese Dichtematrizen allerdings sehr unpraktisch werden. Mit Hilfe von Bloch-Zerlegungen können Dichteoperatoren kompakter und einfacher dargestellt werden. In dieser Schreibweise werden Dichteoperatoren in eine vollständige und orthogonale Operatorenbasis des Operatorenraums zerlegt. Für Qubits ist diese Schreibweise geläufig und üblicherweise werden die Pauli-Spin-1/2 Operatoren für die Operatorenbasis verwendet. Für Qudits, das sind Zustände allgemein dimensionaler Systeme, gibt es allerdings keine eindeutige Verallgemeinerung der Pauli-Operatorenbasis. Daher untersuchen wir drei mögliche Operatorenbasen: Die verallgemeinerte Gell-Mann-Operatorenbasis, die Polarisationsoperatorenbasis, sowie die Weyloperatorenbasis. Weiters wird eine Methode präsentiert, mit welcher die Zerlegung eines beliebigen Operators in eine der drei Operatorenbasen mit Hilfe der Zerlegung von sogenannten Standardoperatoren gefunden werden kann. Als Beispiel zur Anwendung dieser Methode betrachten wir den maximal verschränkten Zwei-Qudit Zustand und zerlegen diesen in jede der Operatorenbasen.

Im Zusammenhang mit der Bestimmung von Verschränkung sind "Entangle-

ment Witnesses" ein wichtiges und oft verwendetes Hilfsmittel. Diese sind Observablen und detektieren die Verschränkung eines Zustandes, sofern sie für diesen einen negativen Erwartungswert aufweisen, und wenn gleichzeitig bekannt ist, dass der Erwartungswert für alle separablen Zustände nicht negativ werden kann. Diese letztere Bedingung ist allerdings im Allgemeinen nicht leicht zu zeigen. In diesem Zusammenhang bietet sich die Verwendung von Bloch-Zerlegungen für vereinfachte Relationen an, und somit kann die Bedingung in vielen Fällen bewiesen werden. Eine besondere Klasse von Entanglement Witnesses sind geometrische Entanglement Witnesses, welche eine direkte euklidisch-geometrische Darstellung des Operatorenraumes erlauben. Die Wichtigkeit dieser Witnesses wird durch "Shift"-Methoden verdeutlicht, welche verschränkte und im Speziellen "bound entangled" Zustände detektieren können, und außerdem helfen, die Menge der separablen Zustände von konvexen Untermengen von Zuständen zu bestimmen. Als Beispiel betrachten wir eine Drei-Parameter-Familie von Zwei-Qudit Zuständen.

Weiters können geometrische Entanglement Witnesses auch zur geometrischen Quantifizierung von Verschränkung verwendet werden, insbesondere zur Bestimmung des Hilbert-Schmidt Verschränkungsmaßes. Dies wird an den Beispielen der isotropen Zwei-Qudit Zustände und Zwei-Parameter Familien von Zwei-Qubit und Zwei-Qudit Zuständen gezeigt.

Zuletzt widmen wir uns dem Problem der Bestimmung von Verschränkung in Mehr-Qubit Systemen. In diesem Zusammenhang bieten wir eine allgemeine Konstruktion von Entanglement Witnesses unter Verwendung von statischen Strukturfaktoren an. In der Festkörperphysik beschreiben Strukturfaktoren dynamische Eigenschaften von Festkörpern in Streuexperimenten. Die strukturellen Entanglement Witnesses detektieren echte Mehrteilchen-Verschränkung, wie z.B. Dicke-Zustände und Dicke-ähnliche Zustände mit geänderten Phasen der vorkommenden Terme. Sie beinhalten außerdem nur Zwei-Punkt-Korrelationen und sind für die experimentelle Anwendung in verschiedenen physikalischen Systemen geeignet.

Curriculum Vitae

Personal Information



Name: Philipp Krammer
Academic degree: Mag. rer. nat.
Date of birth: 04/October/1980
Place of birth: Oberndorf bei Salzburg
Nationality: Austria

Education

09/1991 – 06/1999 Secondary school (AHS): Akademisches Gymnasium Salzburg
06/1999 Matura (Austrian school leaving examination), passed with distinction
10/1999 – 09/2000 Civilian service at "Lebenshilfe Salzburg"
10/2000 – 11/2005 Studies of physics at the University of Vienna
01/2002 1st diploma examination, passed with distinction
06/2004 2nd diploma examination, passed with distinction
11/2005 3rd diploma examination, passed with distinction
Diploma thesis in theoretical quantum physics, title: "Quantum Entanglement: Detection, Classification, and Quantification", Supervisor: Ao. Univ. Prof. Dr. Reinhold A. Bertlmann
11/2005 Degree: Mag. rer. nat.
since 03/2006 Doctorate studies of physics, University of Vienna
since 02/2008 Member of the "CoQus doctoral program", www.coqus.at
10/2009 Prospective degree: Dr. rer. nat.

Professional record

03/2006 – 07/2007 Tutor (assistant teaching in courses) for Theoretical Mechanics and Theoretical Quantum Physics
01/2007 – 12/2007 "Forschungsstipendium F140-N" at the University of Vienna, Institute for Theoretical Physics, funded by the University of Vienna
since 02/2008 Scientific employee at the University of Vienna, group "Quantum Optics, Quantum Nanophysics, Quantum Information" within the "CoQus doctoral program" (www.coqus.at)
01/2009 – 03/2009 Research stay abroad at the Heinrich-Heine-Universität Düsseldorf, Institut für Theoretische Physik III (group of Prof. Dagmar Bruß)

Participation at Workshops, Conferences & Seminars

10/1998	Forum "From Space Exploration to Earth Observation", in Graz, Austria
09/2003	"Triangle Summer School" in Raach, Lower Austria (topic: particle physics and quantum information)
since 10/2004	"Non-local Seminar", meetings for scientific discussion with the "Research Center for Quantum Informa- tion" of Bratislava
05/2005	Conference "Quantum Physics of Nature" in Vienna
09/2005	Annual conference of the ÖPG (Österreichische Physi- kalische Gesellschaft) in Vienna Talk: <i>Optimal entanglement witnesses for qubits and qutrits</i>
05/2006	Workshop "CEQIP 2006" (3rd Central European Quan- tum Information Processing Workshop) in Znojmo, Czech Republic Poster: <i>Optimal entanglement witnesses for qubits and qutrits</i>
05/2006	Workshop "CEWQO 2006" (13th Central European Workshop on Quantum Optics) in Vienna
06/2007	"Vienna Symposium on the Foundations of Modern Physics" in Vienna Poster: <i>Bloch vectors for qudits and geometry of en- tanglement</i>
08/2007	"European Young Scientists Conference on Quantum Information" in Vienna Talk: <i>Bloch vectors for qudits and geometry of entan- glement</i>
06/2008	"5 th CEQIP 2008" in Telc, Czech Republic Poster: <i>Geometric entanglement witnesses and bound entanglement</i>
11/2008	"Vienna-theory-lunch-club" in Vienna Talk: <i>Geometric entanglement witnesses</i>
03/2009	"73. Jahrestagung und DPG Frühjahrstagung der Sek- tion AMOP", Hamburg, Germany Talk: <i>Characterizing entanglement with geometric en- tanglement witnesses</i>
06/2009	"2 nd Vienna Symposium on the Foundations of Modern Physics" in Vienna Poster: <i>Entanglement witnesses via structure factors</i>